eCAM Evidence-Based Complementary and Alternative Medicine

Advances in Metabolic Profiling and Pharmacokinetics of Herbal Medicinal Products

Lead Guest Editor: Xinguang Liu
Guest Editors: Yong Ai and Jiang Ma

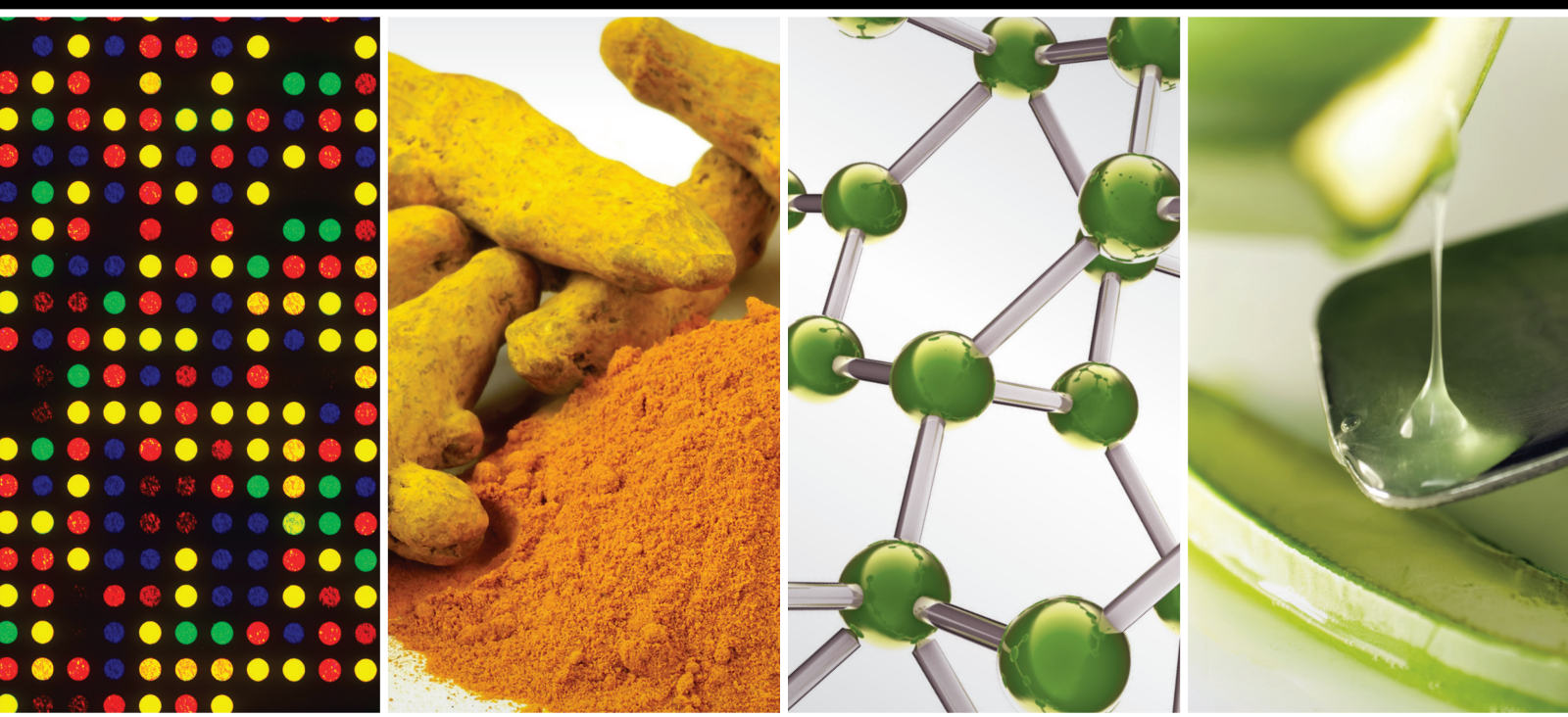

Advances in Metabolic Profiling and Pharmacokinetics of Herbal Medicinal Products

Evidence-Based Complementary and Alternative Medicine

Advances in Metabolic Profiling and Pharmacokinetics of Herbal Medicinal Products

Lead Guest Editor: Xinguang Liu
Guest Editors: Yong Ai and Jiang Ma

Editorial Board

Contents

Hindawi
Evidence-Based Complementary and Alternative Medicine
Volume 2019, Article ID 5190972, 2 pages
https://doi.org/10.1155/2019/5190972

Editorial

Advances in Metabolic Profiling and Pharmacokinetics of Herbal Medicinal Products

Xinguang Liu,[1,2] **Yong Ai**,[3] **and Jiang Ma**[4]

[1]*Collaborative Innovation Center for Respiratory Disease Diagnosis and Treatment & Chinese Medicine Development of Henan Province, Henan University of Chinese Medicine, Zhengzhou, Henan, China*
[2]*Institute of Integrative Medicine, Dalian Medical University, Dalian, Liaoning, China*
[3]*University of Maryland, Baltimore, USA*
[4]*School of Biomedical Sciences, The Chinese University of Hong Kong, Hong Kong*

Correspondence should be addressed to Xinguang Liu; lxg1987519@163.com

Received 16 April 2019; Accepted 16 April 2019; Published 6 May 2019

Herbal medicinal products (HMPs) are expected to be safe and effective. Nevertheless, evidence-based verification of the safety and efficacy of HMPs is still lacking. Understanding the metabolic profile and *in vivo* fate of HMPs has been considered an important issue to identify pharmacologically active or toxic compounds in HMPs or their metabolites for further discovery and development of new drugs or for safety monitoring. These processes include investigation of bioavailability to assess to what degree and how fast compounds are absorbed after drug administration, elucidation of metabolic pathways, and elimination routes and their kinetics, as well as the interactions of HMPs with synthetically derived drug products. Due to the complex chemical composition of HMPs, the absorption, distribution, metabolism, and excretion characteristics of the bioactive or toxic HMPs remain to be further explored. The difficulty lies primarily in the selection of appropriate biomarkers for detection, quantification of trace constituents, identification of potential drug-drug interactions, and the discovery of active constituents based on metabolic results.

In this special issue, investigators contribute original research articles and review articles that would facilitate the understanding of the basic mechanisms as well as the development of new and promising complementary and alternative strategies for the metabolic profiling and pharmacokinetics of HMPs.

Integrating pharmacokinetics is a crucial tool to identify the therapeutic agent. The research article by C. Zhang et al. elucidated the pharmacokinetic profiles and disposition kinetics of the administered and generated stereoisomers in the brain and cerebrospinal fluid (CSF) after oral administration of Isorhynchophylline (IRN) and Rhynchophylline (RN). The results demonstrated that, after oral administration, RN showed significantly higher systemic exposure and disposition in the brain and CSF than IRN, indicating that RN would be more appropriate to be developed as a potential therapeutic agent for the treatment of AD.

In technology, ultrahigh-performance liquid chromatography tandem mass spectrometry (UPLC-MS/MS) is still the most popular tool for the pharmacokinetics study of HMPs. The research article by Y. Fu et al. established a simple, sensitive, and reliable UPLC-MS/MS method for quantifying pinosylvin in rat plasma, urine, feces, and various tissues. Nine metabolites of pinosylvin were found in plasma, and glucuronidation, hydroxylation, and methylation proved to be its main metabolic pathways.

There are many factors affecting the pharmacokinetics of HMPs, among which herb-drug interaction has been frequently studied. The research article by D. Yim et al. examined the selective interaction of *Sophora flavescens* extract with cytochrome P450 (CYP) isoforms in human liver microsomes. The result showed that *S. flavescens* and its prenylated flavonoids caused significant herb-drug interactions when coadministered or incubated with substrates of CYP2B6, CYP2C8, CYP2C9, and CYP3A4. The research article by N. Temyingyong et al. determined the effect of

short-course oral ciprofloxacin on isoflavone pharmacokinetics in healthy postmenopausal women. The results showed that ciprofloxacin administration significantly reduced the absorption of the aglycones of genistein and daidzein.

Drug formulation and administration route also significantly affect the pharmacokinetics of HMPs. The research article by P. Smyk et al. elucidated the influence of propolis on ion channels, channels location in cell membrane, and electrical resistance of skin. In this work, a model skin of Ussing chamber proved to be useful for studying the effect of chemicals on transepidermal ion transport.

Finally, in addition to herb-drug interaction, the review article by S. Sun et al. summarized other important factors that affect the clinical practice of HMPs, such as herb pretreatment, herb-herb interactions, pathological status, gender, age of patients, and chemical and physical modification of certain ingredients.

Thus, this special issue included different aspects related to the recent advances in metabolic profiling and pharmacokinetics of HMPs, based on various *in vitro* and *in vivo* studies as well as the literature review related to the objective of this special issue.

Conflicts of Interest

The editors have no conflicts of interest regarding the publication of this special issue.

Xinguang Liu
Yong Ai
Jiang Ma

Hindawi
Evidence-Based Complementary and Alternative Medicine
Volume 2019, Article ID 7192326, 10 pages
https://doi.org/10.1155/2019/7192326

Research Article

Effect of Short-Course Oral Ciprofloxacin on Isoflavone Pharmacokinetics following Soy Milk Ingestion in Healthy Postmenopausal Women

Nathathai Temyingyong,[1] **Nut Koonrungsesomboon**,[2,3] **Nutthiya Hanprasertpong**,[2] **Mingkwan Na Takuathung**,[2] **and Supanimit Teekachunhatean**[2,4]

[1]*Graduate School, Chiang Mai University, Chiang Mai 50200, Thailand*
[2]*Department of Pharmacology, Faculty of Medicine, Chiang Mai University, Chiang Mai 50200, Thailand*
[3]*Musculoskeletal Science and Translational Research (MSTR), Chiang Mai University, Chiang Mai 50200, Thailand*
[4]*Center of Thai Traditional and Complementary Medicine, Faculty of Medicine, Chiang Mai University, Chiang Mai 50200, Thailand*

Correspondence should be addressed to Supanimit Teekachunhatean; supanimit.t@cmu.ac.th

Received 7 November 2018; Revised 16 March 2019; Accepted 21 March 2019; Published 11 April 2019

Guest Editor: Xinguang Liu

Soy isoflavones have several potential benefits related to postmenopausal health. Isoflavone glycosides, found predominantly in nonfermented soy products, e.g., soy milk, require conversion by gut microbiota to their respective bioavailable aglycones prior to absorption into portal circulation. Use of short-course oral ciprofloxacin for the treatment of acute uncomplicated cystitis, the incidence of which is increasing among postmenopausal women, might adversely affect gut microbiota. The objective of this one-group pre-post treatment study was to determine the effect of short-course oral ciprofloxacin on isoflavone pharmacokinetics in healthy postmenopausal women. Eleven postmenopausal subjects were assigned to consume a single oral dose of 375 mL UHT soy milk (SOY phase). Blood samples were collected immediately before soy milk ingestion and at specific times for 32 hours after soy milk ingestion. Following a washout period of at least seven days, subjects were assigned to take 250 mg oral ciprofloxacin after breakfast and dinner for three days, followed by a single oral dose of 375 mL UHT soy milk the next day (CIPRO/SOY phase). Blood samples were collected at the same time points as in the SOY phase. Plasma samples were treated with β-glucuronidase/sulfatase and plasma concentrations of aglycones (genistein and daidzein) were determined using high-performance liquid chromatography. C_{max}, $AUC_{0\text{-}t}$, and $AUC_{0\text{-}\infty}$ of both aglycones and T_{max} of genistein obtained from the CIPRO/SOY phase were significantly lower than those obtained from the SOY phase, while T_{max} of daidzein and $t_{1/2}$ of both aglycones in the two phases were not significantly different.

1. Introduction

Soy isoflavones, nonsteroidal polyphenolic compounds found in soybeans [1], are structurally similar to 17β-estradiol and have estrogen-like effects [2, 3]. Evidence suggests that soy isoflavones have several potential benefits related to women's health, such as relief of postmenopausal vasomotor symptoms [4] as well as prevention of estrogen-related cancer [5–7], cardiovascular disease [8, 9], and osteoporosis [10, 11].

Soy isoflavones occur in three aglycone structures (daidzein, genistein, and glycitein), which can enter into three β-glycoside conjugates (daidzin, genistin, and glycitin), each with its corresponding acetyl- and malonyl-glycoside conjugates. As glycitein and its glycoside conjugates account for less than 5-10% of the total isoflavones in soy-based products, most studies have focused on daidzein and genistein and their respective glycoside conjugates [12].

The popularity of soy milk consumption is increasing worldwide because soy milk is an important beverage source of isoflavones [13]. It is also the preferred alternative to cow's milk for individuals with lactose intolerance [13]. Regular consumption of isoflavone-rich soy milk alleviates climacteric symptoms (both somatic and urogenital domain symptoms) in peri- and postmenopausal women [14] and

helps prevent lumbar spine bone loss in postmenopausal women [15].

Genistin and daidzin, both β-glycoside conjugates, have been found to be the main isoflavone components in soy milk [13, 16]. Glycosides are poorly absorbed in the gastrointestinal tract, requiring gut microbiota-mediated conversion to aglycone forms prior to absorption into portal circulation [17, 18]. Thus gut microbiota plays a crucial role in isoflavone absorption and may contribute significantly to the health benefits of isoflavones [19].

Short-course ciprofloxacin (a broad-spectrum fluoroquinolone antibiotic) is one of the recommended antibiotic regimens for treatment of acute uncomplicated cystitis [20], the incidence of which is increasing among postmenopausal women [19]. However, due to its broad spectrum effect against both gram-negative and gram-positive microorganisms, oral ciprofloxacin may also affect the human gut microbiota, resulting in altered isoflavone pharmacokinetics, in particular, a reduction of isoflavone absorption [21]. For that reason, it is postulated that food-drug interaction might occur in postmenopausal women with acute uncomplicated cystitis following coadministration of soy-based products and oral ciprofloxacin. This study aimed to evaluate the effect of short-course oral ciprofloxacin on the pharmacokinetics of soy isoflavones in healthy postmenopausal women.

2. Materials and Methods

2.1. Study Design. This study was a one-group pre-post treatment study. The study was approved by the Human Research Ethics Committee, Faculty of Medicine, Chiang Mai University, and complied with the Declaration of Helsinki. This trial was registered with Thai Clinical Trials Registry (TCTR): TCTR20180118003.

2.2. Subjects. The number of subjects enrolled in this study was determined by the sample size calculation for testing two dependent means (two-tailed test) [22, 23] using the following equation, where σ is the standard deviation (SD), delta (Δ) is the difference between the two phases, alpha (α) is the significance level, and beta (β) is the type II error probability.

$$n = \frac{\left(z_{1-\alpha/2} + z_{1-\beta}\right)^2 \sigma^2}{\Delta^2} \quad (1)$$

In this study, the extent of absorbed soy isoflavone genistein (consistent with the area under the concentration-time curve, AUC) was the main criteria for comparison of isoflavone bioavailability. The mean difference in AUC (Δ) between pre- and posttreatment was estimated to be 4,800 ng.h/mL and the SD of AUC (σ) was assumed to be 5,500. The required sample size to achieved 80% power (β = 0.2) at α = 0.05 was at least 11 subjects.

Eleven Thai postmenopausal women, aged more than 45 years with a postmenopausal status of more than one year and serum follicle-stimulating hormone (FSH) concentration of greater than 40 IU/L, were enrolled in this study. Their body mass index (BMI) was between 18 and 25 kg/m^2. All subjects were in good health based on their medical history and a physical examination. Routine blood examination (10 mL from each subject), including complete blood count as well as kidney (BUN, creatinine) and liver function tests, was carried out to identify and exclude subjects with hematological diseases or impaired kidney/liver function. Subjects with known contraindications or hypersensitivity to soy isoflavones or ciprofloxacin were excluded as were women with a history of breast disease, malignancy, cardiovascular or pulmonary disorders, or musculoskeletal disease, e.g., neck or chest pain, back pain, achiness, arthralgia, joint stiffness, or flare-up of gout. Other exclusion criteria included a history of regular consumption of alcohol-containing beverages, use of antibiotics or laxatives within the previous four weeks, cigarette smoking, and substance abuse or addiction. No other medications and nutritional supplements (vitamins, minerals, fiber products, prebiotics, probiotics, synbiotics, or isoflavones) were allowed during the four weeks prior to study initiation. Details of the study were explained to all subjects and signed informed consent was obtained from all subjects prior to study participation. Withdrawal criteria from this study were adverse drug reactions during the study, inability to comply with the study protocol, and voluntary withdrawal from the study.

2.3. Soy and Ciprofloxacin Preparation. The soy-based product used in this study was the UHT soy milk (V-soy®, lot number 8851028004127, expiration date 27 March 2019, manufactured by Green Spot Co., Ltd., Bangkok, Thailand). The mean isoflavone contents of daidzin (the β-glycoside form of daidzein) and genistin (the β-glycoside form of genistein) were 86.58±0.65 and 47.57±0.36 mg/375 mL, respectively. The amounts of daidzein and genistein were negligible. The ciprofloxacin oral tablets used were CIPROBAY® (ciprofloxacin HCL, batch number BXHSB11, expiration date May 2021, manufactured by Bayer Healthcare Pharmaceuticals Inc., Germany).

2.4. Dosage and Administration. The schedule of administration of soy milk and ciprofloxacin is shown in Figure 1. Each subject was assigned to receive a single oral dose of 375 mL soy milk the morning after an overnight fast of at least eight hours (Day_0 of the SOY phase). Subjects fasted for an additional two hours after oral administration of the soy milk. Water and lunch were served two and four hours after dosing, respectively. During the first four hours after dosing, subjects were instructed to remain upright. Blood samples were collected at various time points (see below). After a washout period of at least seven days, subjects were assigned to consume 250 mg ciprofloxacin twice a day for three consecutive days (Day_{-3}–Day_{-1}), followed by a single oral dose of 375 mL soy milk the morning of the following day (Day_0 of the CIPRO/SOY phase). Administration of soy milk and collection of blood samples were performed in the same manner as in the SOY phase. Identical isoflavone-free foods and beverages were served during the two phases of the study. Subjects were instructed that the ciprofloxacin should not be taken with milk, yogurt, calcium-fortified juice, caffeine,

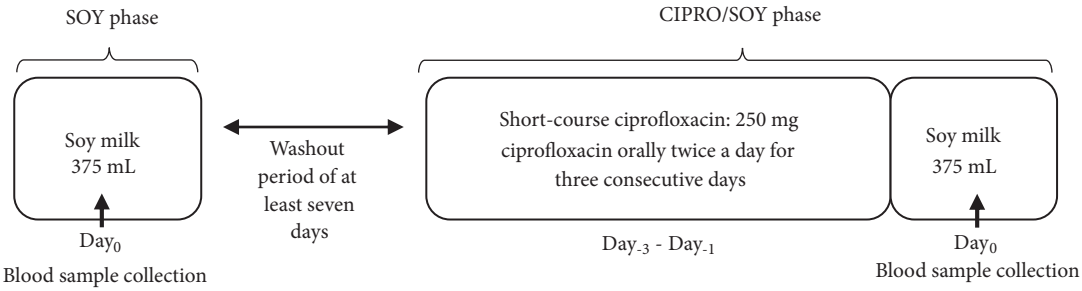

Figure 1: Schedule of administration of soy milk and ciprofloxacin in both phases of the study. The SOY phase represents a single oral administration of soy milk. The CIPRO/SOY phase represents an oral administration of short-course ciprofloxacin followed by a single oral administration of soy milk.

or food or drink containing high levels of magnesium, aluminum, iron, or zinc. Subjects were required to refrain from soy-rich products, e.g., soy milk and tofu, as well as caffeine- and alcohol-containing beverages throughout the study period.

2.5. Collection of Blood Samples. For both phases of the study, blood samples were obtained from the forearm by venipuncture through an indwelling intravenous catheter. A 5 mL blood sample for quantification of plasma isoflavones was collected immediately prior to and at 0.5, 1, 2, 4, 6, 8, 10, 12, 24, and 32 hours after oral administration of the soy milk. The blood samples were centrifuged within 30 minutes of collection to separate the plasma and were then kept at −70°C until analysis.

2.6. Determination of Plasma Concentrations of Isoflavones

2.6.1. Sample Preparation. Since absorbable aglycones are extensively further metabolized in the intestines and/or liver and are consequently present in the systemic circulation as their β-glucuronide and sulfate conjugates [17, 18], the plasma samples were treated with a mixture of β-glucuronidases/sulfatase in order to cleave the glucuronide, and sulfate conjugates to their respective aglycones prior to determination of isoflavone concentration. Thus plasma levels of isoflavones reported here are the respective aglycone concentrations. This study focused on the determination of daidzein and genistein because these aglycones and their respective glycosides are known to be the major constituents (>90%) of soy isoflavones [13].

Sample preparation and the method of determination of isoflavone concentrations in plasma were modified from the method described by Teekachunhatean et al. [18, 24–27]. Briefly, a 250 μL aliquot of plasma was treated with 0.15 mL of a mixture of β-glucuronidases:sulfatase (97600:2380 units/mL) from *Helix pomatia*, to hydrolyze the glucuronide and sulfate conjugates to aglycones. The enzyme mixture was composed of 0.01 g ethylenediaminetetraacetic acid (EDTA) and 0.1 g ascorbic acid in 10 mL of 0.1 M sodium acetate buffer mixed with 250 μL of *Helix pomatia*. Plasma samples containing the enzyme mixture were heated in a water bath at 37°C for 15 hours and then cooled at room temperature. After enzymatic hydrolysis, plasma samples were spiked with 10 μL of an internal standard (50,000 ng/mL fluorescein in 80% methanol). Fluorescein is recommended as an internal standard in order to correct for unknown losses during the High-Performance Liquid Chromatography (HPLC) analyses of phytoestrogens [28]. It is eluted separately from other UV-absorbing compounds extracted from the soy-based foods and its HPLC retention index is distinct from those of any other soy-based components [29, 30]. After adding an internal standard, plasma samples were deproteinated by adding 1,000 μL of 1% acetic acid in acetonitrile and mixing on a vortex mixer for 30 seconds. The mixture was then centrifuged at 14,000 rpm for ten minutes. An aliquot of the supernatant was isolated and vacuum-evaporated to dryness for three hours at 60°C. The residue was dissolved in 50 μL of mobile phase B (see below), and 5 μL of the sample was injected into the HPLC system. The chromatogram of isoflavone-free plasma and the chromatogram of the plasma sample containing daidzein, genistein, and the internal standard are shown in Figure 2.

2.6.2. High-Performance Liquid Chromatography (HPLC) Conditions. The assay of isoflavones was modified from the HPLC methods and conditions described by Teekachunhatean et al. [18, 24–27]. The chromatographic system consisted of a 5 μm C-18 column equipped with a guard column of the same material. The chromatographic conditions comprised mobile phases A and B. The proportions of 60 mM ammonium acetate in deionized water/acetonitrile/methanol in mobile phases A and B were 250/50/50 and 250/250/220 (v/v/v), respectively. Both mobile phases contained 30 μL of perchloric acid and 250 μL of 1.44 g sodium dodecyl sulfate. Separation was performed at 25°C. A gradient elution of 85% A with 15% B for 12.80 minutes, 33:67 with A:B for 12.81-20.00 minutes, and 85:15 for 20.01-24.00 minutes was scheduled. The mobile phase was maintained at the flow rate of 1 mL/min, and the analyses were detected by UV absorption at 259 nm.

2.6.3. Method Validation. Method validation of isoflavones was performed according to the Food and Drug Administration Guidance for Industry Bioanalytical Method Validation (2018) [31]. The isoflavone content of the samples was determined using a calibration curve of the peak height

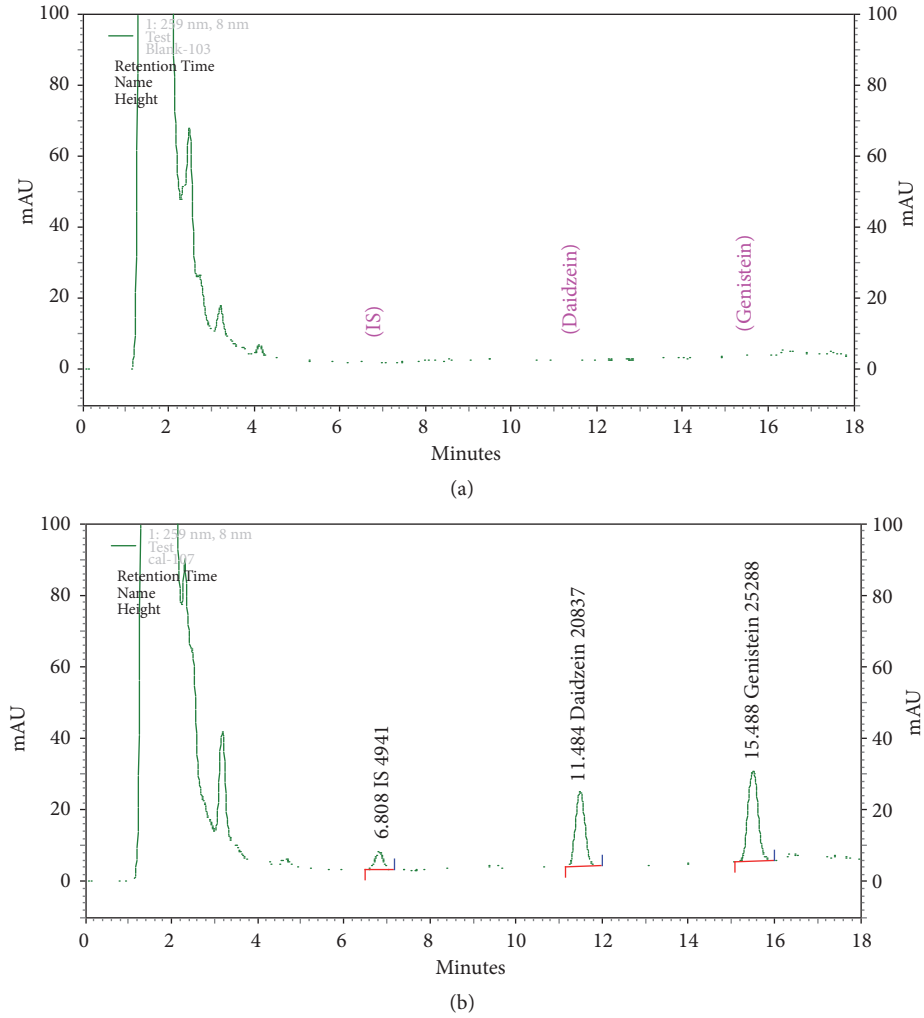

Figure 2: (a) Chromatogram of isoflavone-free plasma. (b) Chromatogram of plasma sample containing daidzein (k = 11.484 min) and genistein (k = 15.488 min) as well as internal standard (IS, k = 6.808 min).

ratios of the isoflavones and the internal standard versus their respective isoflavone concentrations (37.5, 75, 150, 300, 600, 1,200, and 2,400 ng/mL). Linear regression analysis of peak height ratios of isoflavones versus isoflavone concentrations consistently yielded coefficients of the determinant (r^2) of 0.999 or better.

The precision of the HPLC method for assay of isoflavones in plasma is reported as the percentage of coefficient of variation (%CV) which was calculated as follows (where SD is the standard deviation and $\overline{X}$ is the mean plasma concentration of the measured isoflavone).

$$\%\text{CV} = \frac{\text{SD}}{\overline{X}} \times 100 \quad (2)$$

Accuracy for the assay of isoflavones in plasma was calculated using the following equation:

$$\%\text{Accuracy} = \frac{\text{Measured concentration}}{\text{Spiked concentraion}} \times 100 \quad (3)$$

The lower limit of quantification (LLOQ) was defined as the lowest concentration on the calibration curve (37.5 ng/mL) that could be measured with acceptable precision (%CV less than 20%) and acceptable accuracy (80-120%). The LLOQ was determined by analyzing a series of five replicate samples of gradually decreasing concentrations until the lowest concentration with acceptable precision and accuracy was obtained. The mean LLOQ of daidzein and genistein were 36.67±1.20 and 37.19±0.75, respectively. The %CV and %accuracy of LLOQ for daidzein were 3.25% and 98.59%, respectively, whereas, those for genistein were 2.01% and 99.17%, respectively.

Recovery was determined by comparing the peak height of the isoflavone standard samples in the mobile phase, with the peak height of isoflavones in plasma extracted from five sets of three different concentrations of quality control samples (110, 1,100, and 2,200 ng/mL). The extraction recovery of daidzein and genistein in human plasma is shown in Table 1.

For within-day precision, five samples from each of three quality control (QC) samples (110, 1,100, and 2,200 ng/mL)

Table 1: Extraction recovery of daidzein and genistein in human plasma (n=5).

Compound	Concentration (ng/mL)	Peak height (mAU)		%Recovery
		In mobile phase (mean±SD)	In plasma (mean±SD)	
Daidzein	110	1573±11.39	1327±43.33	84.38
	1100	14531±95.16	12371±233.50	85.14
	2200	27001±498.58	24130±1453.77	89.36
Average recovery				86.29
Genistein	110	2176±49.60	1962±137.96	90.17
	1100	19789±131.30	16789±287.45	84.84
	2200	34279±634.20	31042±1910.87	90.56
Average recovery				88.52

Table 2: Precision and accuracy for assay of daidzein and genistein in human plasma.

Compound	Concentration (ng/mL)	Within-day (n=5)			Between-day (n=5)		
		Measured concentration (ng/mL), mean±SD	Precision (%CV)	Accuracy (%)	Measured concentration (ng/mL), mean±SD	Precision (%CV)	Accuracy (%)
Daidzein	110	105.54±1.20	1.14	95.95	112.01±4.41	3.94	101.83
	1100	1169.95±13.06	1.12	106.36	1106.44±57.40	5.19	100.59
	2200	2271.59±24.85	1.09	103.25	2267.39±120.66	5.32	103.06
Average			1.12	101.85		4.81	101.82
Genistein	110	108.79±1.99	1.83	98.90	113.16±8.18	7.23	102.87
	1100	1131.92±12.52	1.11	102.90	1070.99±76.98	7.19	97.36
	2200	2203.29±26.97	1.22	100.15	2199.30±125.02	5.68	99.97
Average			1.39	100.65		6.70	100.07

were evaluated with a single calibration curve. For between-day precision, five sets of three different concentrations of QC samples (110, 1,100, and 2,200 ng/mL) were studied on five different days with five concurrent calibration curves. The precision and deviation for assay of daidzein and genistein in human plasma are shown in Table 2.

Short-term stability was tested by preparing quality control samples at two different concentrations (110 and 2,200 ng/mL) in triplicate and analyzing them after remaining on the bench for eight hours at room temperature. For long-term stability evaluation, the quality control samples were stored in a freezer for three months at −70°C for comparison with freshly prepared samples. Freeze-thaw stability was assessed before storage at −70°C and again after three freeze-thaw cycles. Quality control samples after extraction with the same concentration levels in five replicates stored in an autosampler were used to evaluate postpreparative stability. The stability for assay of daidzein and genistein in human plasma is shown in Table 3.

2.7. Data Analysis and Statistical Methods

2.7.1. Pharmacokinetic Parameters. The parameters of interest were maximal plasma concentration (C_{max}), time to reach peak concentration (T_{max}), the area under the plasma concentration-time curve from time zero to the last measurable concentration ($AUC_{0\text{-}t}$) and from time zero to infinity ($AUC_{0\text{-}\infty}$), and the terminal half-life ($t_{1/2}$). The individual plasma concentration-time curves were analyzed with a noncompartmental approach using the TopFit pharmacokinetic data analysis program. C_{max} and T_{max} were obtained directly from each subject's plasma concentration-time curve. The terminal elimination rate constant (k_e) was estimated by log-linear regression of the concentration observed during the terminal phase of elimination. $t_{1/2}$ was calculated as $0.693/k_e$. The $AUC_{0\text{-}t}$ was calculated by the trapezoidal rule. The extrapolated $AUC_{t\text{-}\infty}$ was determined as C_t/k_e. Total $AUC_{0\text{-}\infty}$ was the sum of $AUC_{0\text{-}t} + AUC_{t\text{-}\infty}$.

2.7.2. Statistical Analysis. Pharmacokinetic parameters are presented as mean±SD and median (interquartile range). The mean values of pharmacokinetic parameters obtained from the CIPRO/SOY phase were compared to those of the SOY phase using the paired t-test, whereas the differences between median values of both phases were compared using Wilcoxon's signed rank test. A p value of <0.05 was considered statistically significant.

Table 3: Stability for assay of daidzein and genistein in human plasma.

Compound	Concentration (ng/mL)	Short-term stability (8 hours, n=3) %Remaining	Long-term stability (3 months, n=3) %Remaining	Freeze-thaw stability (n=3) %Remaining	Post-preparative stability (n=5) %Remaining
Daidzein	110	98.42	105.19	86.26	98.01
	2200	98.54	94.57	100.14	98.11
Average stability		98.48	99.88	93.20	98.06
Genistein	110	99.56	104.44	91.15	96.76
	2200	99.25	95.67	110.88	96.94
Average stability		99.40	100.05	101.02	96.85

Table 4: Demographic characteristics of the 11 subjects participating in this study.

Subject No.	Age (y)	Weight (kg)	Height (m)	BMI (kg/m^2)	FSH (IU/L)
1	69	56.00	1.50	24.89	63.99
2	54	51.00	1.52	22.07	85.14
3	54	49.70	1.58	19.91	56.78
4	59	50.50	1.58	20.36	98.80
5	51	56.00	1.52	24.24	53.76
6	62	52.00	1.48	23.74	80.66
7	63	52.00	1.52	22.66	70.78
8	59	60.00	1.58	24.03	82.08
9	69	47.00	1.48	21.46	48.76
10	72	61.00	1.57	24.75	62.73
11	50	49.50	1.54	20.87	89.33
Mean	60.18	53.15	1.53	22.63	72.07
SD	7.57	4.50	0.04	1.81	16.20

3. Results

Eleven postmenopausal subjects completed the study. Their mean age, weight, height, BMI, and serum FSH concentration were 60.18±7.57 years, 53.15±4.50 kg, 1.53± 0.04 m, 22.63± 1.81 kg/m^2, and 72.07±16.20 IU/L, respectively (Table 4).

The mean plasma concentration-time curves of daidzein and genistein from the 11 subjects who underwent the SOY and CIPRO/SOY phases are shown in Figures 3 and 4, respectively. The mean plasma concentration-time curves of both aglycones in both phases exhibited a biphasic pattern.

In the SOY phase, the first and second peak concentrations were attained at approximately two to four hours and at six hours, respectively. The second peak concentration of each aglycone was markedly higher than the first peak. It is noteworthy that the second peaks of both aglycones obtained from the CIPRO/SOY phase were remarkably lower than those of the SOY phase, whereas the short-course oral ciprofloxacin given in the CIPRO/SOY phase caused a slight reduction in the first peak concentrations of both aglycones in comparison to those observed in the SOY phase.

The pharmacokinetic parameters of daidzein and genistein (C_{max}, T_{max}, $AUC_{0\text{-}t}$, $AUC_{0\text{-}\infty}$, and $t_{1/2}$) after oral administration of soy milk obtained from both phases are shown in Tables 5 and 6. The mean/median values of C_{max}, $AUC_{0\text{-}t}$, and $AUC_{0\text{-}\infty}$ of both daidzein and genistein, as well as the T_{max} of genistein obtained from the CIPRO/SOY phase, were significantly lower than those of the SOY phase. However, the mean/median values of T_{max} of daidzein, as well as $t_{1/2}$ of both

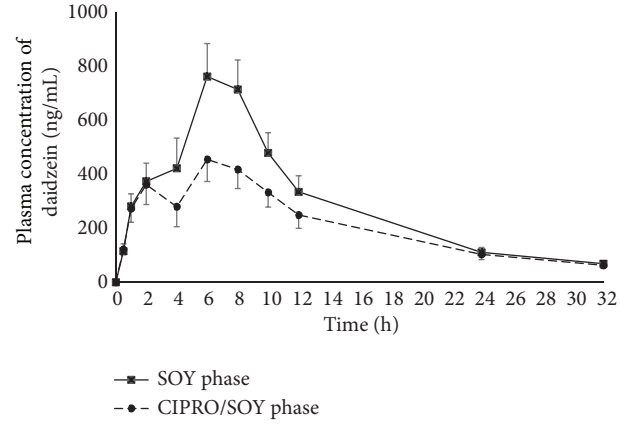

Figure 3: Mean plasma daidzein concentration-time curves from 11 subjects receiving a single oral administration of soy milk (SOY phase) and a short-course oral administration of ciprofloxacin followed by a single oral administration of soy milk (CIPRO/SOY phase). Error bars represent standard error of the mean (SEM).

Table 5: Pharmacokinetic parameters of daidzein obtained from 11 subjects receiving a single oral administration of soy milk (SOY Phase) and a short-course oral ciprofloxacin followed by a single oral administration of soy milk (CIPRO/SOY phase).

Pharmacokinetic parameters	Daidzein			
	SOY phase		CIPRO/SOY phase	
	Mean±SD	Median (IQR)	Mean±SD	Median (IQR)
C_{max} (ng/mL)	833.12±351.17	752.60 (298.52)	511.17±243.74*	497.19 (323.01)**
T_{max} (h)	6.36±1.21	6.00 (1.00)	6.55±1.29	6.00 (2.00)
$AUC_{0\text{-}t}$ (ng.h/mL)	8553.84±5424.86	6826.87 (5759.28)	5977.10±4256.78*	5599.80 (4391.67)**
$AUC_{0\text{-}\infty}$ (ng.h/mL)	9431.94±5411.69	7254.24 (4777.05)	6746.22±4403.37*	6003.36 (4164.71)**
$t_{1/2}$ (h)	6.52±1.89	6.23 (1.64)	6.42±2.07	6.36 (1.45)

Data represent mean±SD and median (interquartile range, IQR). * p <0.05 versus SOY phase using a paired t-test. ** p <0.05 versus SOY phase using Wilcoxon's signed-rank test.

Table 6: Pharmacokinetic parameters of genistein obtained from 11 subjects receiving a single oral administration of soy milk (SOY Phase) and a short-course oral ciprofloxacin followed by a single oral administration of soy milk (CIPRO/SOY phase).

Pharmacokinetic parameters	Genistein			
	SOY phase		CIPRO/SOY phase	
	Mean±SD	Median (IQR)	Mean±SD	Median (IQR)
C_{max} (ng/mL)	826.64±462.97	731.95 (521.01)	434.75±276.24*	306.17 (214.37)**
T_{max} (h)	6.00±1.55	6.00 (0.00)	3.27±2.24*	2.00 (2.00)**
$AUC_{0\text{-}t}$ (ng.h/mL)	9583.48±6482.03	8911.53 (7711.23)	4956.98±4263.76*	3834.93 (4106.07)**
$AUC_{0\text{-}\infty}$ (ng.h/mL)	10540.60±7024.65	9284.07 (7789.07)	5791.53±4567.84*	4366.76 (3976.55)**
$t_{1/2}$ (h)	7.40±1.20	7.26 (1.57)	7.54±1.69	7.16 (1.69)

Data represent mean±SD and median (interquartile range, IQR). * p <0.05 versus SOY phase using a paired t-test. ** p <0.05 versus SOY phase using Wilcoxon's signed-rank test.

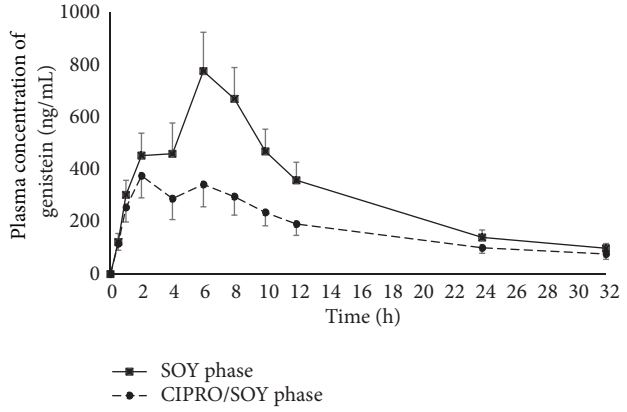

Figure 4: Mean plasma genistein concentration-time curves from 11 subjects receiving a single oral administration of soy milk (SOY phase) and a short-course oral administration of ciprofloxacin followed by a single oral administration of soy milk (CIPRO/SOY phase). Error bars represent standard error of the mean (SEM).

daidzein and genistein, did not differ significantly between the two phases.

4. Discussion

In this one-group pre-post treatment study, the dependent variables of interest (pharmacokinetic parameters of isoflavones) were measured in a single group of 11 participants and then measured again in the same group after exposure to an intervention (a short-course of oral ciprofloxacin) to determine the difference between the initial (pretreatment, SOY phase) and second (posttreatment, CIPRO/SOY phase) measurements. With this within-subjects design, the conditions in pre- and posttreatment phases were assumed to be equivalent with regard to individual difference variables because the same participants participated in both conditions. In addition, a washout period between the SOY and the CIPRO/SOY phases of at least seven days is considered sufficient to avoid carryover effects as that period is >4-5 times $t_{1/2}$ of isoflavones, ensuring that any isoflavones absorbed during the SOY phase were entirely eliminated before initiation of the CIPRO/SOY phase. As it is difficult to estimate carryover effects on the restoration of gut microbiota after taking antibiotics, this study was conducted in a fixed sequence: the SOY phase followed by the CIPRO/SOY phase.

The biphasic pattern of plasma concentration-time curves of the isoflavones obtained from the SOY phase was consistent with findings previously reported in studies of postmenopausal Thai women [18, 24–27]. The first and second peaks are due to absorption of isoflavones in the small and the large intestine, respectively [32]. In the upper small intestine, conversion of isoflavone glycosides (the predominant forms in soy milk) to aglycones facilitates rapid absorption via passive diffusion across the intestinal brush border [33]. This conversion involves the action of intestinal lactase

phlorizin hydrolase [34], enterocytic β-glucosidase [35], and microbial β-glucosidases [36, 37]. The remaining isoflavone glycosides that are not absorbed in the upper intestinal tract would pass through to the lower intestinal tract, where gut microbial β-glycosidases further cleave them into aglycones prior to absorption [38]. Additionally, the metabolites of isoflavones (glucuronide and sulfate conjugates), which are excreted into the intestinal tract via the biliary tract, can be deconjugated by gut microbial β-glycosidases and can undergo enterohepatic recycling. This phenomenon also contributes to the appearance of a second peak [39]. Since the lower intestinal tract (especially the colon) is the major site of isoflavone absorption [32], it was not surprising that the second peak concentration of each aglycone obtained from the SOY phase was markedly higher than the first peak. There are various types of microbiota involved in the conversion of isoflavone glycosides to readily absorbable aglycones, e.g., streptococcus, lactobacillus, bifidobacterium, bacteroides, enterobacteria, eubacteria, and enterococcus [3, 38, 40].

Although ciprofloxacin (250 mg, orally, twice daily for three consecutive days) is considered to be an alternative or second-line antimicrobial agent for treatment of acute uncomplicated cystitis in otherwise healthy women according to international guidelines on urological infections [20], this regimen is commonly used in medical practice in Thailand due to the high prevalence of pathogens resistant to first-line regimens. This regimen may also be indicated when beta-lactam agents are contraindicated. Investigation of the impact of a three-day regimen on gut microbiota ecology has found a significant reduction in enterobacteria and a slight increase in the amount of bifidobacteria and anaerobic cocci [41]; furthermore, a higher dose (500 mg orally twice daily for five consecutive days) has been reported to cause a reduction in the amount of enterobacteria and enterococci [42]. The potential impact of ciprofloxacin on gut microbiota ecology could possibly affect the oral bioavailability of ingested isoflavone glycosides.

In this study, short-course oral ciprofloxacin caused a marked decrease in the second peak concentrations, but only a slight decrease in the first peak concentrations of both aglycones. These findings presumably reflect the impact of ciprofloxacin on the quantities of microbiota which are responsible for the conversion of isoflavone glycosides to readily absorbable aglycones. Since the microbiota plays a crucial role in the absorption of isoflavone glycosides in the lower intestinal tract but partly contributes to an absorption in the upper small intestine, it was not surprising that oral ciprofloxacin caused a greater impact on the second peak than the first peak observed in the CIPRO/SOY phase. The findings of this study are consistent with previous studies demonstrating that use of oral antibiotics (erythromycin and neomycin) together with mechanical bowel preparation (in order to radically reduce gut microbiota) negatively affect the second peak [32]. On the other hand, either prebiotic or synbiotic supplementation (which can facilitate the growth of gut microbiota) results in an enhancement of the second peak in postmenopausal women [25, 26].

The presumed decrease in the amount of gut microbiota appears to be the likely cause of the significant reduction in the mean/median values of C_{max}, $AUC_{0\text{-}t}$, and $AUC_{0\text{-}\infty}$ of both daidzein and genistein obtained from the CIPRO/SOY phase compared to those of the SOY phase. With T_{max} obtained from the CIPRO/SOY phase, ciprofloxacin reduced the second peak of genistein concentration below that of the first peak, significantly shifting T_{max} of genistein toward the first peak. In contrast, the second peak of daidzein concentration was not lower than the first peak. As a result, T_{max} of daidzein was not altered from that observed in the SOY phase. In addition, $t_{1/2}$ of both daidzein and genistein did not differ significantly between the two phases, suggesting that ciprofloxacin has a negligible impact on isoflavone elimination.

The findings of this study suggest that a three-day oral ciprofloxacin reduces the oral bioavailability of isoflavones (as evidenced by the decrease in AUC and C_{max}) following ingestion of soy milk in postmenopausal women. This food-drug interaction appears to be of clinical relevance in cases where this ciprofloxacin regimen is prescribed to treat illnesses, e.g., acute uncomplicated cystitis, in postmenopausal women receiving oral isoflavones (especially glycoside forms) or nonfermented soy-based products. However, it is still unclear how long the carryover effect of ciprofloxacin on isoflavone pharmacokinetic lasts after treatment discontinuation. A previous study suggested that gut microbiota ecology might return to normal within two weeks [42]. Further studies addressing this issue are required.

Some limitations of this study should be addressed. First, there is a diversity of gut microbiota ecology among human populations [43–46]. This study was conducted in Thai postmenopausal women; the findings could be different in other racial and ethnic groups as well as other geographic locations. Second, the 250 mg of ciprofloxacin in this study was given twice daily for three consecutive days; the effect of ciprofloxacin might differ with a different dose and/or duration. Third, the effect of food-drug interaction also would probably differ if other fluoroquinolones and soy-based products were coadministered. Finally, the lack of direct quantification of fecal microbiota to determine the impact of oral ciprofloxacin on gut microbiota ecology was also considered a limitation.

5. Conclusions

A three-day regimen of oral ciprofloxacin followed by a single oral administration of soy milk causes a significant decrease in C_{max}, $AUC_{0\text{-}t}$, and $AUC_{0\text{-}\infty}$ of both daidzein and genistein, as well as T_{max} of genistein compared to a single oral dose of soy beverage alone. However, T_{max} of daidzein and $t_{1/2}$ of aglycones, genistein, and daidzein, are not significantly different.

Abbreviations

$AUC_{0\text{-}t}$: Area under the plasma concentration-time curve from time zero to the last measurable concentration

$AUC_{0-\infty}$: Area under the plasma concentration-time curve from time zero to infinity
C_{max}: Maximal plasma concentration
k_e: Terminal elimination rate constant
T_{max}: Time to reach peak concentration
$t_{1/2}$: Terminal half-life.

Data Availability

The data used to support the findings of this study are available from the corresponding author upon request.

Conflicts of Interest

The authors do not have any direct financial relation with any of the commercial identities mentioned in this paper and have no conflicts of interest.

Acknowledgments

The authors are grateful to Dr. G. Lamar Robert for his assistance in editing the paper. We would also like to gratefully acknowledge Ms. Sujitra Techatoei for her secretarial support. This research was financially supported by the Faculty of Medicine, Chiang Mai University (Grant no. 104/2561).

References

[1] K. Zaheer and M. Humayoun Akhtar, "An updated review of dietary isoflavones: Nutrition, processing, bioavailability and impacts on human health," *Critical Reviews in Food Science and Nutrition*, vol. 57, no. 6, pp. 1280–1293, 2017.

[2] P.-F. Cheng, J.-J. Chen, X.-Y. Zhou et al., "Do soy isoflavones improve cognitive function in postmenopausal women? A meta-analysis," *Menopause*, vol. 22, no. 2, pp. 198–206, 2015.

[3] T. Larkin, W. E. Price, and L. Astheimer, "The key importance of soy isoflavone bioavailability to understanding health benefits," *Critical Reviews in Food Science and Nutrition*, vol. 48, no. 6, pp. 538–552, 2008.

[4] K. Taku, M. K. Melby, F. Kronenberg, M. S. Kurzer, and M. Messina, "Extracted or synthesized soybean isoflavones reduce menopausal hot flash frequency and severity: systematic review and meta-analysis of randomized controlled trials," *Menopause*, vol. 19, no. 7, pp. 776–790, 2012.

[5] S. Loibl, A. Lintermans, A. S. Dieudonné, and P. Neven, "Management of menopausal symptoms in breast cancer patients," *Maturitas*, vol. 68, no. 2, pp. 148–154, 2011.

[6] P. J. Magee, H. McGlynn, and I. R. Rowland, "Differential effects of isoflavones and lignans on invasiveness of MDA-MB-231 breast cancer cells in vitro," *Cancer Letters*, vol. 208, no. 1, pp. 35–41, 2004.

[7] H. B. Patisaul and W. Jefferson, "The pros and cons of phytoestrogens," *Frontiers in Neuroendocrinology*, vol. 31, no. 4, pp. 400–419, 2010.

[8] B. E. Merz-Demlow, A. M. Duncan, K. E. Wangen et al., "Soy isoflavones improve plasma lipids in normocholesterolemic, premenopausal women," *American Journal of Clinical Nutrition*, vol. 71, no. 6, pp. 1462–1469, 2000.

[9] X. Zhang, Y.-T. Gao, G. Yang et al., "Urinary isoflavonoids and risk of coronary heart disease," *International Journal of Epidemiology*, vol. 41, no. 5, pp. 1367–1375, 2012.

[10] D.-F. Ma, L.-Q. Qin, P.-Y. Wang, and R. Katoh, "Soy isoflavone intake inhibits bone resorption and stimulates bone formation in menopausal women: meta-analysis of randomized controlled trials," *European Journal of Clinical Nutrition*, vol. 62, no. 2, pp. 155–161, 2008.

[11] P. Wei, M. Liu, Y. Chen, and D. Chen, "Systematic review of soy isoflavone supplements on osteoporosis in women," *Asian Pacific Journal of Tropical Medicine*, vol. 5, no. 3, pp. 243–248, 2012.

[12] S. Teekachunhatean, N. Hanprasertpong, and T. Teekachunhatean, "Factors affecting isoflavone content in soybean seeds grown in Thailand," *International Journal of Agronomy*, vol. 2013, Article ID 163573, 11 pages, 2013.

[13] K. Nara, N. P. Botting, P. Kachlicki et al., "Isoflavones: chemistry, analysis, function and effects," in *Food and Nutritional Components in Focus*, V. R. Preedy, Ed., vol. 5, pp. 001–683, Royal Society of Chemistry, Cambridge, UK, 2013.

[14] S. Tranche, C. Brotons, B. Pascual de la Pisa, R. Macías, E. Hevia, and M. Marzo-Castillejo, "Impact of a soy drink on climacteric symptoms: an open-label, crossover, randomized clinical trial," *Gynecological Endocrinology*, vol. 32, no. 6, pp. 477–482, 2016.

[15] E. Lydeking-Olsen, J.-E. Beck-Jensen, K. D. R. Setchell, and T. Holm-Jensen, "Soymilk or progesterone for prevention of bone loss—a 2 year randomized, placebo-controlled trial," *European Journal of Nutrition*, vol. 43, no. 4, pp. 246–257, 2004.

[16] E. Hirattanapun, N. Koonrungsesomboon, and S. Teekachunhatean, "Variability of isoflavone content in soy milk products commercially available in Thailand," *Journal of Health Science and Medical Research*, vol. 36, no. 2, pp. 117–126, 2018.

[17] C. Sabarinath and A. Annie, "Pharmacokinetics of dietary isoflavones," *Journal of Steroids and Hormonal Science*, pp. 1–8, 2013.

[18] W. Limopasmanee, S. Chansakaow, N. Rojanasthien, M. Manorot, C. Sangdee, and S. Teekachunhatean, "Effects of the Chinese herbal formulation (Liu Wei Di Huang Wan) on the pharmacokinetics of isoflavones in postmenopausal women," *BioMed Research International*, vol. 2015, Article ID 902702, 8 pages, 2015.

[19] L. P. Marques, J. T. Flores, O. d. Barros Junior, G. B. Rodrigues, C. d. Mourão, and R. M. Moreira, "Epidemiological and clinical aspects of urinary tract infection in community-dwelling elderly women," *The Brazilian Journal of Infectious Diseases*, vol. 16, no. 5, pp. 436–441, 2012.

[20] K. Gupta, T. M. Hooton, K. G. Naber et al., "International clinical practice guidelines for the treatment of acute uncomplicated cystitis and pyelonephritis in women: a 2010 update by the infectious diseases society of America and the European Society for Microbiology and Infectious Diseases," *Clinical Infectious Diseases*, vol. 52, no. 5, pp. e103–e120, 2011.

[21] C. Edlund and C. E. Nord, "Effect on the human normal microflora of oral antibiotics for treatment of urinary tract infections," *Journal of Antimicrobial Chemotherapy*, vol. 46, no. 1, pp. 41–48; discussion 63-45, 2000.

[22] D. H. Glueck, "Sample size calculations in clinical research 2nd edition by S.-C. CHOW, J. SHAO, and H. WANG," *Biometrics*, vol. 64, no. 4, pp. 1307-1308, 2008.

[23] C. Ngamjarus and C. Virasakdi, "n4Studies: sample size calculation for an epidemiological study on a smart device," *Siriraj Medical Journal*, vol. 68, pp. 160–170, 2016.

[24] E. Anupongsanugool, S. Teekachunhatean, N. Rojanasthien, S. Pongsatha, and C. Sangdee, "Pharmacokinetics of isoflavones, daidzein and genistein, after ingestion of soy beverage compared with soy extract capsules in postmenopausal Thai women," *BMC Clinical Pharmacology*, vol. 5, article 2, 2005.

[25] S. Teekachunhatean, S. Techatoei, N. Rojanasthein, M. Manorot, and C. Sangdee, "Influence of fructooligosaccharide on pharmacokinetics of isoflavones in postmenopausal women," *Evidence-Based Complementary and Alternative Medicine*, vol. 2012, Article ID 783802, 9 pages, 2012.

[26] P. Timan, N. Rojanasthien, M. Manorot, C. Sangdee, and S. Teekachunhatean, "Effect of synbiotic fermented milk on oral bioavailability of isoflavones in postmenopausal women," *International Journal of Food Sciences and Nutrition*, vol. 65, no. 6, pp. 761–767, 2014.

[27] S. Teekachunhatean, P. Pongnad, N. Rojanasthein, M. Manorot, and C. Sangdee, "Effects of vitamin D plus calcium supplements on pharmacokinetics of isoflavones in thai postmenopausal women," *Evidence-Based Complementary and Alternative Medicine*, vol. 2011, Article ID 895471, 7 pages, 2011.

[28] C.-C. Wang, J. K. Prasain, and S. Barnes, "Review of the methods used in the determination of phytoestrogens," *Journal of Chromatography B*, vol. 777, no. 1-2, pp. 3–28, 2002.

[29] L. Coward, N. C. Barnes, K. D. R. Setchell, and S. Barnes, "Genistein, daidzein, and their β-glycoside conjugates: antitumor isoflavones in soybean foods from American and Asian diets," *Journal of Agricultural and Food Chemistry*, vol. 41, no. 11, pp. 1961–1967, 1993.

[30] T. H. Kao and B. H. Chen, "An improved method for determination of isoflavones in soybean powder by liquid chromatography," *Chromatographia*, vol. 56, no. 7-8, pp. 423–430, 2002.

[31] U.S. Department of Health and Human Services, Food and Drug Administration, Center for Drug Evaluation and Research (CDER), Center for Veterinary Medicine (CVM), "Guidance for Industry, Bioanalytical Method Validation," May 2018, https://www.fda.gov/downloads/Drugs/Guidances/ucm070107.pdf.

[32] A. A. Franke, L. J. Custer, and S. A. Hundahl, "Determinants for urinary and plasma isoflavones in humans after soy intake," *Nutrition and Cancer*, vol. 50, no. 2, pp. 141–154, 2004.

[33] A. Scalbert and G. Williamson, "Dietary intake and bioavailability of polyphenols," *Journal of Nutrition*, vol. 130, no. 8S, pp. 2073S–2085S, 2000.

[34] A. J. Day, F. J. Cañada, J. C. Díaz et al., "Dietary flavonoid and isoflavone glycosides are hydrolysed by the lactase site of lactase phlorizin hydrolase," *FEBS Letters*, vol. 468, no. 2-3, pp. 166–170, 2000.

[35] A. J. Day, M. S. Dupont, S. Ridley et al., "Deglycosylation of flavonoid and isoflavonoid glycosides by human small intestine and liver β-glucosidase activity," *FEBS Letters*, vol. 436, no. 1, pp. 71–75, 1998.

[36] M. D'Archivio, C. Filesi, R. Varì, B. Scazzocchio, and R. Masella, "Bioavailability of the polyphenols: Status and controversies," *International Journal of Molecular Sciences*, vol. 11, no. 4, pp. 1321–1342, 2010.

[37] I. Rowland, M. Faughnan, L. Hoey, K. Wähälä, G. Williamson, and A. Cassidy, "Bioavailability of phyto-oestrogens," *British Journal of Nutrition*, vol. 89, Suppl. 1, pp. S45–S58, 2003.

[38] P. W. Parodi, "The role of intestinal bacteria in the causation and prevention of cancer: Modulation by diet and probiotics," *Australian Journal of Dairy Technology*, vol. 54, no. 2, pp. 103–121, 1999.

[39] K. Murota and J. Terao, "Antioxidative flavonoid quercetin: implication of its intestinal absorption and metabolism," *Archives of Biochemistry and Biophysics*, vol. 417, no. 1, pp. 12–17, 2003.

[40] N. J. Turner, B. M. Thomson, and I. C. Shaw, "Bioactive isoflavones in functional foods: The importance of gut microflora on bioavailability," *Nutrition Reviews*, vol. 61, no. 6, pp. 204–213, 2003.

[41] J. Wiström, L. O. Gentry, A.-C. Palmgren et al., "Ecological effects of short-term ciprofloxacin treatment of travellers' diarrhoea," *Journal of Antimicrobial Chemotherapy*, vol. 30, no. 5, pp. 693–706, 1992.

[42] T. Bergan, C. Delin, S. Johansen, I. M. Kolstad, C. E. Nord, and S. B. Thorsteinsson, "Pharmacokinetics of ciprofloxacin and effect of repeated dosage on salivary and fecal microflora," *Antimicrobial Agents and Chemotherapy*, vol. 29, no. 2, pp. 298–302, 1986.

[43] E. Borghi, F. Borgo, M. Severgnini, M. N. Savini, M. C. Casiraghi, and A. Vignoli, "Rett syndrome: a focus on gut microbiota," *International Journal of Molecular Sciences*, vol. 18, no. 2, 2017.

[44] T. Yatsunenko, F. E. Rey, M. J. Manary et al., "Human gut microbiome viewed across age and geography," *Nature*, vol. 486, no. 7402, pp. 222–227, 2012.

[45] S. Ruengsomwong, O. La-Ongkham, J. Jiang, B. Wannissorn, J. Nakayama, and S. Nitisinprasert, "Microbial community of healthy thai vegetarians and non-vegetarians, their core gut microbiota, and pathogen risk," *Journal of Microbiology and Biotechnology*, vol. 26, no. 10, pp. 1723–1735, 2016.

[46] S. Nishijima, W. Suda, K. Oshima et al., "The gut microbiome of healthy Japanese and its microbial and functional uniqueness," *DNA Research*, vol. 23, no. 2, pp. 125–133, 2016.

Hindawi
Evidence-Based Complementary and Alternative Medicine
Volume 2019, Article ID 2673769, 10 pages
https://doi.org/10.1155/2019/2673769

Research Article

Inhibition of Cytochrome P450 Activities by *Sophora flavescens* Extract and Its Prenylated Flavonoids in Human Liver Microsomes

Daeun Yim, Min Jung Kim, Yumi Shin, Su-Jun Lee, Jae Gook Shin, and Dong Hyun Kim

Department of Pharmacology and Pharmacogenomics Research Center, Inje University College of Medicine, Busan 614-735, Republic of Korea

Correspondence should be addressed to Dong Hyun Kim; dhkim5055@gmail.com

Received 15 November 2018; Revised 19 February 2019; Accepted 4 March 2019; Published 13 March 2019

Guest Editor: Jiang Ma

Sophora flavescens possesses several pharmacological properties and has been widely used for the treatment of diarrhea, inflammation, abscess, dysentery, and fever in East Asian countries. *S. flavescens* is a major source of prenylated flavonoids, such as sophoraflavone and kushenol. In this study, we examined the effects of *S. flavescens* extract and its prenylated flavonoids on cytochrome P450 (CYP) isoform activity in human liver microsomes. The extract inhibited CYP2C8, CYP2C9, CYP2C19, and CYP3A activities, with IC_{50} values of 1.42, 13.6, 19.1, and 50 μg/mL, respectively. CYP2B6 was only inhibited in human liver microsomes preincubated with the extract. CYP3A4 was more strongly inhibited by the extract in the presence of NADPH, suggesting that the extract may inhibit CYP2B6 and CYP3A4 via mechanism-based inactivation. Prenylated flavonoids also inhibited CYP isoforms with different selectivity and modes of action. Kushenol I, leachianone A, and sophoraflavone G inhibited CYP2B6, whereas kushenol C, kushenol I, kushenol M, leachianone A, and sophoraflavone G inhibited CYP3A4 via mechanism-based inhibition. Our results suggest that *S. flavescens* may contribute to herb–drug interactions when coadministered with drugs metabolized by CYP2B6, CYP2C8, CYP2C9, and CYP3A4.

1. Introduction

The dried roots of *Sophora flavescens*, a traditional Chinese medicine, have been widely used in Korea, Japan, and China for the treatment of solid tumors and inflammatory disease [1]. Moreover, *S. flavescens* exerts diverse pharmacological properties including antianaphylaxis, antimicrobial, immunoregulatory, and cardioprotective activities [2]. These therapeutic effects of *S. flavescens* may be derived from complex interactions among its various constituents. Phytochemical analysis revealed the presence of quinolizidine alkaloids and prenylated flavonoids in *S. flavescens* [3, 4]. These two chemicals have been shown to exert a wide spectrum of pharmacological effects, such as anti-inflammatory, antitumor, antimalarial, and antiviral effects [2, 5–8].

Recently, herb–drug interactions have drawn considerable attention, as they can lead to serious adverse effects or diminished drug efficacy. Herb–drug interactions may occur via modulation of hepatic and intestinal cytochrome P450 (CYP) drug-metabolizing enzymes and drug transporters [9, 10]. CYPs play a central role in the metabolism and elimination of xenobiotics including drugs, environmental pollutants, and food ingredients. Previous studies have reported potential herb–drug interactions for St. John's wort [11], gingko biloba [12], goldenseal [13], and ginseng [14] via induction and/or inhibition of CYPs. Furthermore, several *in vitro* and *in vivo* studies have shown that *S. flavescens* extract modulates CYP activities, both induction and inhibition depending on the experimental design. In rat models, oral administration of *S. flavescens* extract resulted in induction of CYP2D and inhibition of CYP1A2 and CYP2C [15]. Sophocarpine from *S. flavescens* was reported to inhibit CYP3A4 and CYP2C9 in human liver microsomes [16]. Induction of CYP1A, CYP2B1/2, CYP2C11, and CYP3A following treatment with *S. flavescens* was observed in rats and mice, and the alkaloids matrine and oxymatrine contributed to induction of CYP isoforms [17–19]. In rats, treatment with *S. flavescens* extract significantly reduced the exposure of indinavir, a

Table 1: . CYP isoform-selective substrates, concentrations, and corresponding metabolites.

CYP isoform	Substrate	Concentration used (μM)	Metabolites
1A2	Phenacetin	50	Acetaminophen
2A6	Coumarin	5	7-Hydroxycoumarin
2B6	Bupropion	50	6-Hydroxybupropion
2C8	Rosiglitazone	5	Hydroxyrosiglitazone
2C9	Diclofenac	10	Hydroxydiclofenac
2C19	*S*-Mephenytoin	80	4-Hydroxymephenytoin
2D6	Dextromethorphan	5	Dextrorphan
3A4	Midazolam	2	1-Hydroxymidazolam
			-

substrate of CYP3A and P-glycoprotein [20]. Nevertheless, studies evaluating the *in vitro* effects of *S. flavescens* extract and/or its flavonoids on human CYP isoform activity are limited.

The aim of the present study was to evaluate the effects of *S. flavescens* extract and its prenylated flavonoids on the activity of eight CYP isoforms in human liver microsomes, to further our understanding of the potential effects of *S. flavescens* on drugs metabolized primarily by CYP enzymes. We demonstrated that *S. flavescens* extract reversibly inhibited the activities of CYP2C8, CYP2C9, and CYP2C19 whereas it inhibited CYP2B6 and CYP3A4 in a mechanism-based inactivation manner.

2. Materials and Methods

2.1. Materials. *S. flavescens* root extract was purchased from the Korea Plant Extract Bank (Chungbuk, Korea). The extract was prepared by extraction with a 70% ethanol solution. Glucose 6-phosphate, β-NADP+, glucose-6-phosphate dehydrogenase, phenacetin, coumarin, bupropion, diclofenac, *S*-mephenytoin, dextromethorphan, and chlorpropamide were purchased from Sigma Aldrich (St. Louis, MO, USA); rosiglitazone and midazolam from Toronto Research Chemicals (Toronto, ON, Canada); and kushenols A, C, I, and M, leachianone A, and sophoraflavone G from Core Sciences (Seoul, Korea). Pooled human liver microsomes, and baculovirus-insect cell expressed 2B6 and 3A4 were purchased from BD Gentest (Woburn, MA, USA). All other reagents were of the highest grade commercially available.

2.2. CYP Inhibition Assay. The incubation mixture consisted of 0.5 mg/mL human liver microsomes or 20 pmol/mL recombinant CYPs, *S. flavescens* extract (0.1–100 μg/mL), and/or prenylated flavonoids (1–100 μM), probe substrates for each CYP isoform, and an NADPH-generating system (3.3 mM glucose-6-phosphate, 1.3 mM β-$NADP^+$, 3.3 mM $MgCl_2$, and 1.0 U/mL glucose-6-phosphate dehydrogenase) in a total volume of 200 μL potassium phosphate buffer (0.1 M, pH 7.4). As shown in Table 1, the probe substrates used in this experiment were 50 μM phenacetin for CYP1A2, 5 μM coumarin for CYP2A6, 50 μM bupropion for CYP2B6, 10 μM paclitaxel for CYP2C8, 100 μM tolbutamide for CYP2C9, 10 μM *S*-mephenytoin for CYP2C18, 5 μM dextromethorphan for CYP2D6, 50 μM chlorzoxazone for CYP2E1, and 5 μM midazolam for CYP3A4 as described previously [21]. The reaction was initiated by the addition of an NADPH-generating system, followed by incubation in a water bath at 37°C for 20 minutes. The reaction was stopped by the addition of 200 μL acetonitrile and 100 μM chlorpropamide. The samples were then centrifuged at 13,000 *g* for 5 minutes. The supernatants from each reaction were analyzed by LC-MS/MS. To determine if the extract or prenylated flavonoids were irreversible inhibitors of the various CYP isoforms, human liver microsomes were preincubated with the extract or prenylated flavonoids in the presence of an NADPH-generating system at 37°C for 30 minutes. The reaction was initiated by the addition of a CYP probe substrate, followed by a 20-minute incubation; the reaction was stopped by the addition of a 200 μL internal standard solution (100 μM chlorpropamide in acetonitrile). The samples were then centrifuged at 13,000 *g* for 5 minutes. The supernatants from each reaction were analyzed by LC-MS/MS.

2.3. Inactivation Assay. To characterize the time- and concentration-dependent inhibition of CYP3A4 by *S. flavescens* extract and kushenol I, an inactivation study was performed using human liver microsomes and recombinant CYP3A4. Human liver microsomes (1 mg/mL) or recombinant CYP3A4 (100 pmol/mL) was incubated with various concentrations of *S. flavescens* extract and kushenol I. The reaction mixture was incubated at 37°C for 5 minutes prior to initiation of the reaction by addition of an NADPH-generating system. Following 0, 5, 10, 20, or 30 minutes of incubation, a 10 μL aliquot from each reaction mixture was added to a second reaction containing 10 μM midazolam, an NADPH-generating system, and 0.2 M potassium phosphate buffer (pH 7.4), at a total reaction volume of 100 μL. After 20 minutes, the 1-hydroxymidazolam formed in the reaction was analyzed by LC-MS/MS.

2.4. HPLC-MS/MS Analysis. Chromatography was performed using the Agilent 1100 Series LC system (Agilent, Santa Clara, CA, USA), which consisted of an autosampler, binary pump, and column oven. The HPLC system was coupled to the 4000 QTRAP triple-quadrupole mass spectrometer (AB Sciex, Foster City, CA, USA) equipped with an electrospray ionization source. The turbo ion-spray interface was operated

in positive-ion mode using nitrogen as the nebulizing agent, turbo spray, and curtain gas, which were set to optimum values of 40, 50, and 20 psi, respectively. The turbo gas temperature was set to 600°C, and the electrospray ionization needle voltage was programmed to 5,500 V. Quadrupoles Q1 and Q3 were set to unit resolution.

For the quantitation of prenylated flavonoids, each flavonoid was dissolved in methanol to prepare the standard stock solution (1 mg/mL). Calibration and quality control samples were prepared by serial dilution of stock solutions to known concentration. *S. flavescens* extract was also dissolved in methanol. An aliquot of the sample (100 μL) was then spiked with 5 μL of a digoxin solution (internal standard, 100 μg/mL) and filtered through a 0.22 μm membrane filter. A 5 μL aliquot of each sample was injected into the LC-MS/MS. Separation was done using the Luna C18 column (100 × 2.0 mm, 3.0 μm, Phenomenex, Torrance, CA, USA). The mobile phase consisted of (A) 0.1% formic acid and (B) 100% acetonitrile containing 0.1% formic acid. Stepwise liner gradient elution was performed as follows: 30% B at 0 minutes, 60% B at 10 minutes, 80% B at 15 minutes, maintenance for 5 minutes, and return to 30% B at 21 minutes. The flow rate was 0.2 mL/min. Detection of the ions was performed by monitoring the transition of m/z 409.2 ⟶ 164.9 for kushenol A, 439.2 ⟶ 365.0 for kushenol C, 455.2 ⟶ 178.9 for kushenol I, 509.2 ⟶ 301.0 for kushenol M, 439.2 ⟶ 164.9 for leachianone A, 425.2 ⟶ 165.0 for sophoraflavone G, and 798 ⟶ 97 for digoxin. Calibration curves were linear ($r^2 > 0.997$) over the concentration range between 10 and 500 ng/mL. The lower limit of quantitation was set to 10 ng/mL for all prenylated flavonoids. The relative standard deviations for intra- and interday precision over the concentration range for the flavonoids were lower than 12.0% with accuracies between 86.0 and 108.6%.

The analysis of the primary metabolites produced by the CYP isoforms from selective substrates was done by the validated method described elsewhere [22] with minor modification. Separation was performed using a Luna C18 column (30 × 2.0 mm, 3 μm, Phenomenex). The mobile phase consisted of (A) 0.1% formic acid and (B) 100% acetonitrile containing 0.1% formic acid. A liner gradient elution from a 15% to 80% solvent (B) was performed for 2.6 minutes following reequilibration for 5 minutes at a flow rate of 0.2 mL/min. Analytes were quantified by multiple-reaction monitoring with specific precursor/product ion transitions. Detection of ion values was performed by monitoring the transitions of m/z 152 ⟶ 110 for acetaminophen, 163 ⟶ 107 for 7-OH-coumarin, 256 ⟶ 238 for 6-OH-bupropion, 374 ⟶ 151 for OH-rosiglitazone, 312 ⟶ 230 for 4-OH-mephenytoin, 258 ⟶ 157 for dextrorphan, 342 ⟶ 175 for 1-OH-midazolam, and 277 ⟶ 175 for chlorpropamide. Chlorpropamide was used as an internal standard. Data acquisition and processing were performed using the Analyst software (ver. 1.4.1; Applied Biosystems, Foster City, CA, USA).

2.5. Data Analysis. CYP isoform activity in the presence of *S. flavescens* extract and prenylated flavonoids was expressed as a percentage of the corresponding value in the control. The IC_{50} values were calculated by nonlinear least square regression analysis using WinNonlin, ver. 2.1 (Pharsight, Mountain View, CA, USA). The K_i and k_{inact} values were calculated using a secondary double reciprocal plot. The natural logarithm of remaining enzyme activity is plotted against the preincubation time (Figure 5). The observed inactivation rate constants (k_{obs}) were obtained by the slopes of the initial log-linear phases. K_i and k_{inact} were calculated using the following equation: $1/k_{obs} = 1/k_{inact} + K_i/k_{inact} \cdot 1/[I]$, where [I] denotes concentration of inhibitor.

3. Results

3.1. Relative Levels of Six Prenylated Flavonoids in S. flavescens Extract. Various flavonoids have been detected in *S. flavescens* [2]. Because prenylated flavonoids act as inhibitors of CYP isoforms [23], the CYP inhibitory potential of six prenylated flavonoids (kushenol A, kushenol C, kushenol I, kushenol M, leachianone A, and sophoraflavone G) from *S. flavescens* was evaluated in human liver microsomes (Figure 1). The relative levels of flavonoids in *S. flavescens* extract were determined using LC-MS/MS. A reconstituted MRM chromatogram obtained from the *S. flavescens* extract is presented in Figure 2. All six prenylated flavonoids were detected in the extract. The relative levels of kushenol A, kushenol C, kushenol M, kushenol I, leachianone A, and sophoraflavone G were 0.08%, 0.02%, 0.10%, 1.17%, 0.51%, and 1.07%, respectively. Kushenol I and sophoraflavone G were the most abundant prenylated flavonoids detected in the extract.

3.2. Inhibition of CYP Isoforms by S. flavescens Extract and Its Prenylated Flavonoids. The inhibitory effects of the *S. flavescens* extract and individual prenylated flavonoids on eight CYP isoforms were determined by measuring the IC_{50} values. CYP isoform-selective substrates were used for this experiment as described previously [21]. Inhibition of CYP activity was determined by evaluating the net signal change between naïve CYP reactions and test reactions. *S. flavescens* extract displayed strong inhibition of CYP2C8, moderate inhibition of CYP2C9 and CYP2C19, and weak inhibition of CYP2B6, CYP3A4, and CYP2C8 (Table 2 and Figure 3). CYP2C8 was most strongly inhibited by the extract with IC_{50} of 1.42 μg/mL. In human liver microsomes preincubated with the extract in the presence of an NADPH-generating system for 30 minutes, the inhibition of CYP2B6 and CYP3A4 was increased 10- to 50-fold, with IC_{50} values of 0.7 μg/mL and 6.2 μg/mL, respectively. These findings suggest that some active component within the extract inhibits CYP2B6 and CYP3A4 via mechanism-based inactivation. The IC_{50} values of the extract and prenylated flavonoids kushenol A, kushenol C, kushenol I, kushenol M, leachianone A, and sophoraflavone G are listed in Table 2. CYP3A4 was not inhibited by the prenylated flavonoids, even at 50 μM, when microsomes were not preincubated with the flavonoids. However, CYP3A4 was strongly inhibited by kushenol C, kushenol I, kushenol M, leachianone A, and sophoraflavone G in microsomes preincubated with the flavonoids, with IC_{50} values < 5 μM. CYP2B6 activity was more strongly inhibited by kushenol

Table 2: IC_{50} values of the standardized hop extract and individual prenylated flavonoids for inhibition of specific CYP isoforms in human liver microsomes.

CYP isoform	Preincubation	IC_{50} value						
		S. flavescens extract (μg/mL)	Kushenol A (μM)	Kushenol C (μM)	Kushenol I (μM)	Kushenol M (μM)	Leachianone A (μM)	Sophoraflavone G (μM)
1A2	-	>100	>50	5.00	>50	>50	>50	2.26
	+	54.6	>50	4.86	>50	>50	>50	0.17
2A6	-	>100	>50	>50	>50	>50	>50	>50
	+	>100	>50	>50	>50	>50	>50	>50
2B6	-	66.5	>50	>50	>50	>50	5.74	2.42
	+	0.7	>50	>50	0.12	>50	0.28	0.07
2C8	-	1.42	>50	>50	0.67	>50	0.75	0.32
	+	0.49	0.11	7.07	0.14	0.28	0.33	0.09
2C9	-	13.6	>50	9.3	7.35	>50	>50	1.25
	+	12.3	2.5	6.9	5.03	>50	2.05	0.42
2C19	-	19.1	>50	>50	>50	>50	>50	N.D
	+	18.7	>50	6.6	>50	>50	3.13	N.D
2D6	-	>100	>50	>50	>50	>50	>50	>50
	+	73.4	>50	>50	>50	>50	>50	>50
3A4	-	51.0	>50	>50	>50	>50	>50	>50
	+	6.2	>50	3.95	0.57	1.29	0.69	0.78

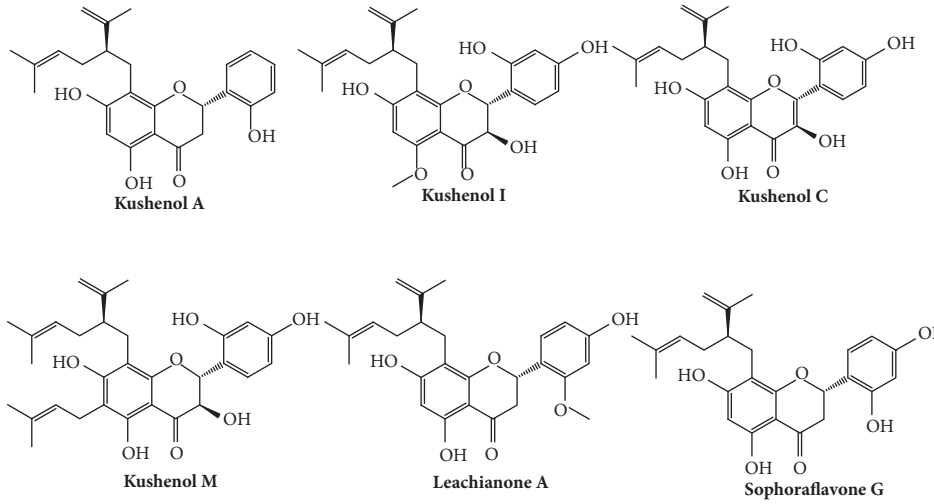

Figure 1: Structure of prenylated flavonoids in *S. flavescens* extract.

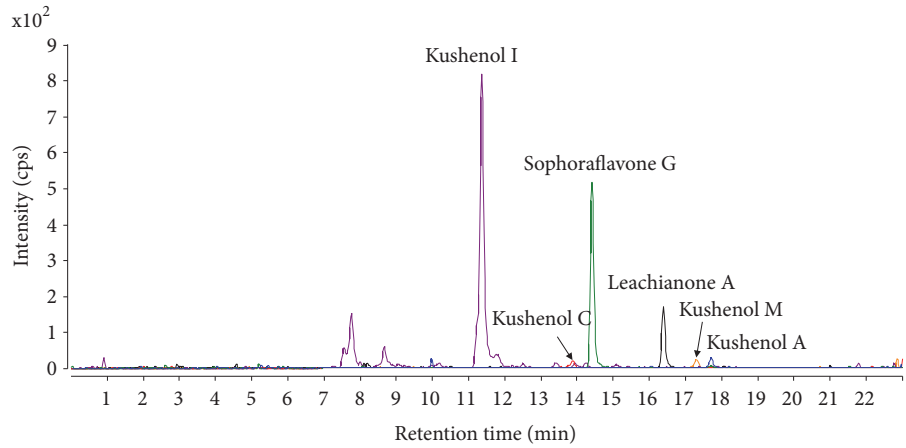

Figure 2: LC-MS/MS selected ion chromatogram of prenylated flavonoids in *S. flavescens* extract.

I, leachianone A, and sophoraflavone G after preincubation with the flavonoids, displaying IC_{50} values < 0.5 μM. CYP2A6 and CYP2D6 were not inhibited by the flavonoids regardless of preincubation. CYP2C8 was inhibited by all test flavonoids after preincubation, although kushenol I, leachianone A, and sophoraflavone G showed similar inhibitory effects without preincubation. Kushenol I and sophoraflavone G also inhibited CYP2C9 regardless of preincubation, and kushenol A and leachianone A inactivated CYP2C9. Similar to the inhibition profiles of CYP2B6 and CYP3A4 in microsomes, kushenol I also more strongly inhibited bupropion 6-hydroxylation and midazolam 1'-hydroxylation activities in recombinant CYP2B6 and CYP3A4, respectively, when CYPs were preincubated with kushenol I in the presence of the NADPH-generating system (Figure 4).

3.3. Inactivation of CYP3A4 by S. flavescens Extract and Kushenol I. The effects of the concentration and incubation time of *S. flavescens* extract and kushenol I on CYP3A4 inhibition were assessed. We chose kushenol I for these experiments as it was the most abundant prenylated flavonoid in the extract. Both *S. flavescens* extract and kushenol I demonstrated time- and concentration-dependent inhibition of CYP3A4 in human liver microsomes (Figures 5(a) and 5(b)). Preincubation of the test materials in the absence of NADPH abolished the time-dependent inhibitory effect, suggesting mechanism-based inactivation. The K_i and k_{inact} values of *S. flavescens* extract were 6.96 μM and 0.034/min for CYP3A4, respectively, and 0.24 μM and 0.022/min for CYP3A4, respectively. The efficiency of CYP3A4 inactivation was assessed by the ratio of k_{inact} to K_i, which was 0.0049 for *S. flavescens* extract and 0.092 for kushenol I. These findings suggest that kushenol I inhibits CYP3A4 more efficiently than does the extract. Kushenol I also showed time- and concentration-dependent inhibition of recombinant CYP3A4 with the K_i and k_{inact} values of 0.88 μM and 0.045/min, respectively (Figure 5(c)).

4. Discussion

We evaluated the effects of *S. flavescens* extract and its prenylated flavonoids (kushenol A, kushenol C, kushenol

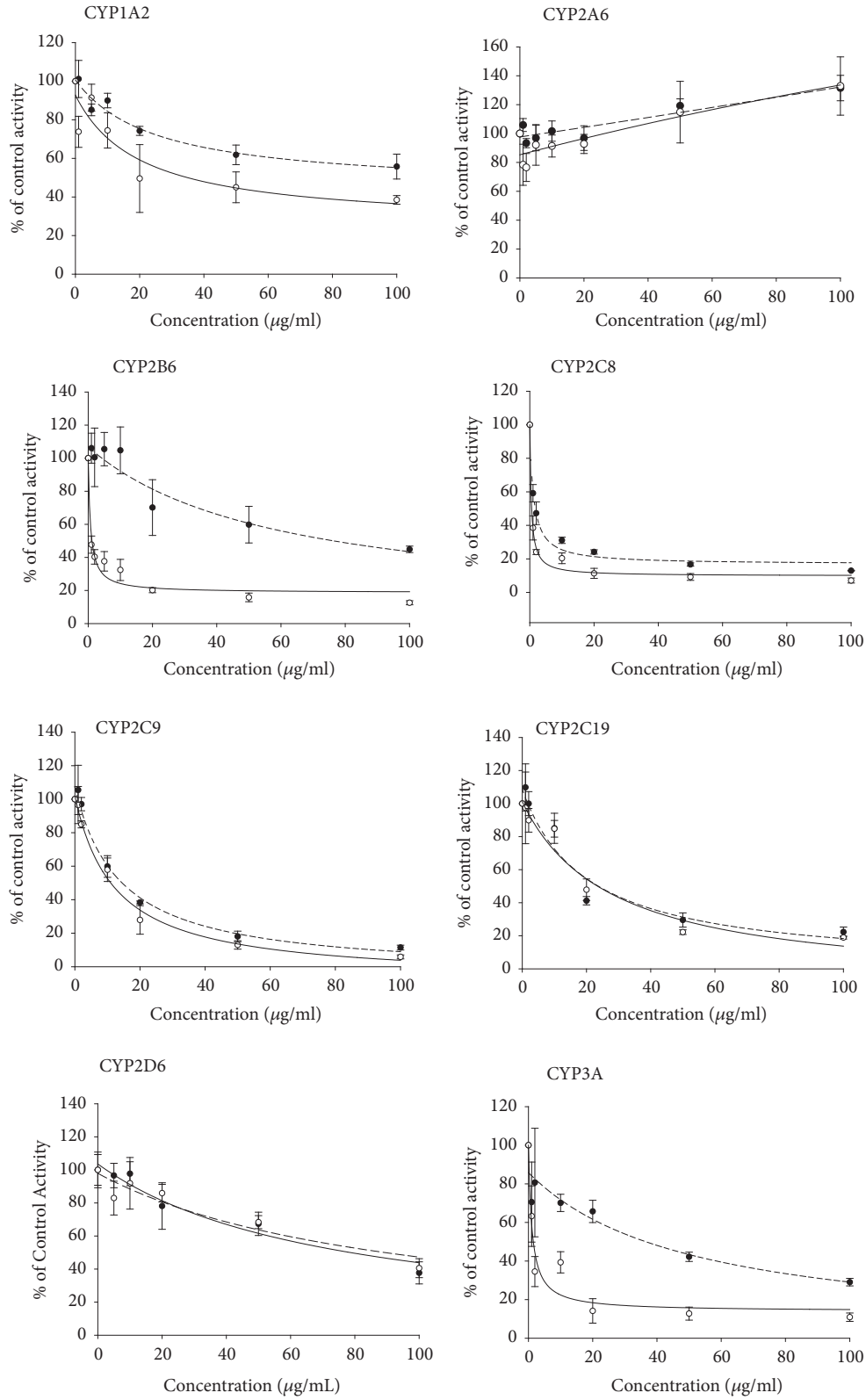

Figure 3: Concentration-dependent inhibition of CYP isoforms by *S. flavescens* extract and its prenylated flavonoids in human liver microsomes with (○) or without (●) preincubation in the presence of an NADPH-generating system. CYP activities are expressed as the relative percentage of the activity in the control. Each data point represents the mean of triplicate experiments.

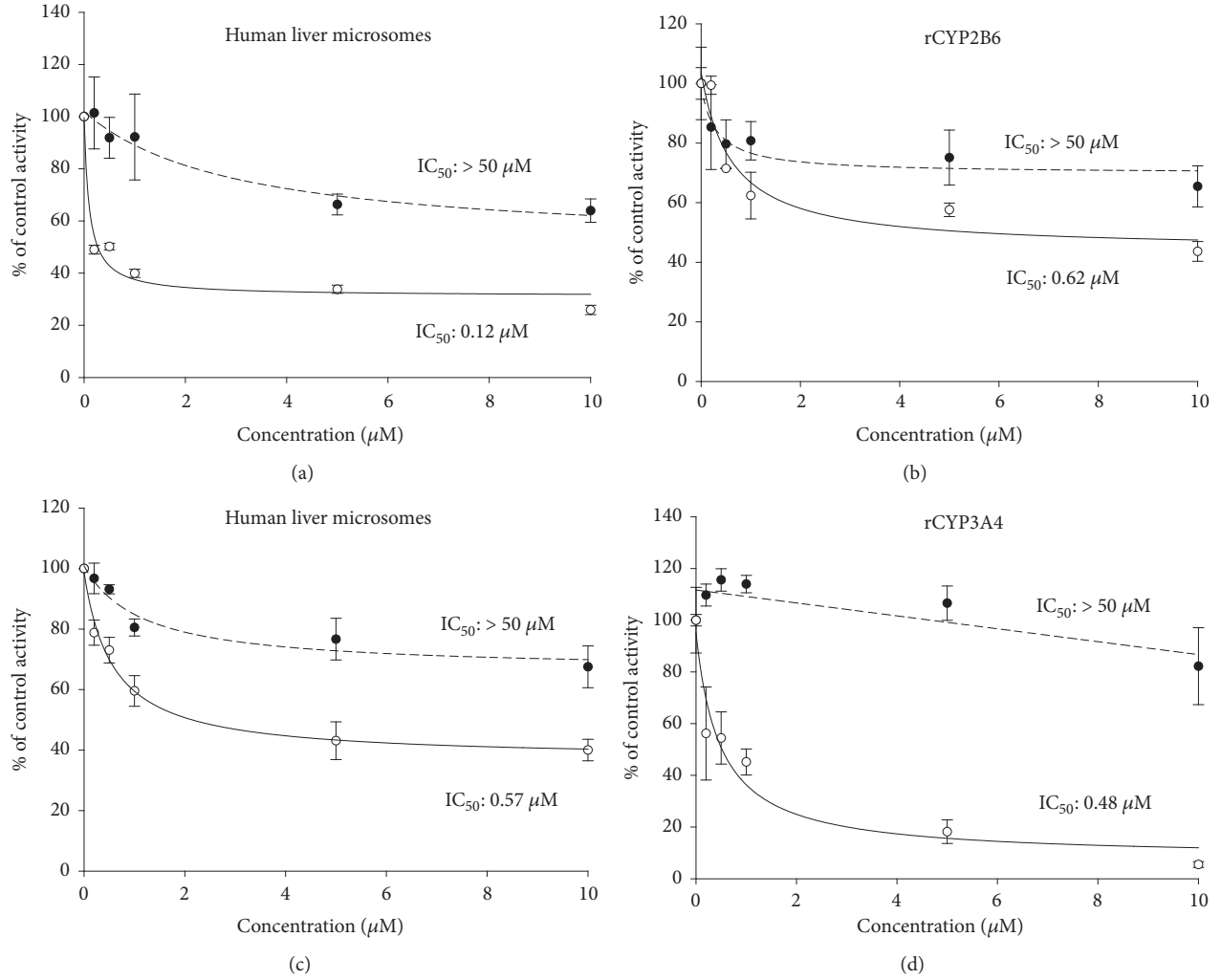

Figure 4: Concentration-dependent inhibition of bupropion 6-hydroxylation and midazolam 1'-hydroxylation by kushenol I with (○) or without (●) preincubation in the presence of an NADPH-generating system; microsomal- (a) and recombinant CYP2B6- (b) mediated bupropion 6-hydroxylation and microsomal- (c) and recombinant CYP3A4- (d) mediated midazolam 1'-hydroxylation. CYP activities are expressed as the relative percentage of the activity in the control. Each data point represents the mean of triplicate experiments.

I, kushenol M, leachianone A, and sophoraflavone G) on the activities of different CYP isoforms in human liver microsomes using CYP isoform-selective substrates. Considering the central role of CYP enzymes in drug metabolism and clearance, knowledge of the effects of herbal extracts and their active ingredients on CYP enzymes is critical to understanding herb–drug interactions in a clinical setting. *S. flavescens* was traditionally used as a decoction or powder, obtained from its dried roots (Kushen). More than 200 compounds have been identified in *S. flavescens*, with alkaloids and flavonoids exerting the observed pharmacological effects of this medicine [2, 24]. Among the flavonoids, prenylated flavonoids such as kushenols, leachianones, and sophoraflavones were found to exert several pharmacological properties [2, 5, 7]. All of the prenylated flavonoids evaluated in this study were identified in *S. flavescens* extract, although flavonoids may be preferentially extracted by 70% ethanol compared with alkaloids.

Our results indicated that the ethanolic extract of *S. flavescens* inhibited CYP2C8 most strongly, followed by CYP2C9, CYP2C19, CYP3A4, and CYP2B6, but did not inhibit CYP1A2, CYP2A6, or CYP2D6, in human liver microsomes. However, the IC_{50} values of the extract for inhibition of CYP2B6 and CYP3A4 were significantly decreased 10- to 50-fold in microsomes preincubated with the extract in the presence of NADPH, suggesting that the extracts inhibited CYP2B6 and CYP3A4 via mechanism-based inactivation (Table 2, Figure 4). Mechanism-based inactivation of CYP3A4 was further confirmed by kinetic analysis, which revealed K_i and k_{inact} values of 6.96 μg/mL and 0.034/min, respectively. The prenylated flavonoids evaluated in this study exhibited different inhibitory potential toward different CYP isoforms. Kushenol I, which was the most abundant of the prenylated flavonoids in the extract, inhibited CYP2C8 and CYP2C9 reversibly but inhibited CYP2B6 and CYP3A by mechanism-based inactivation.

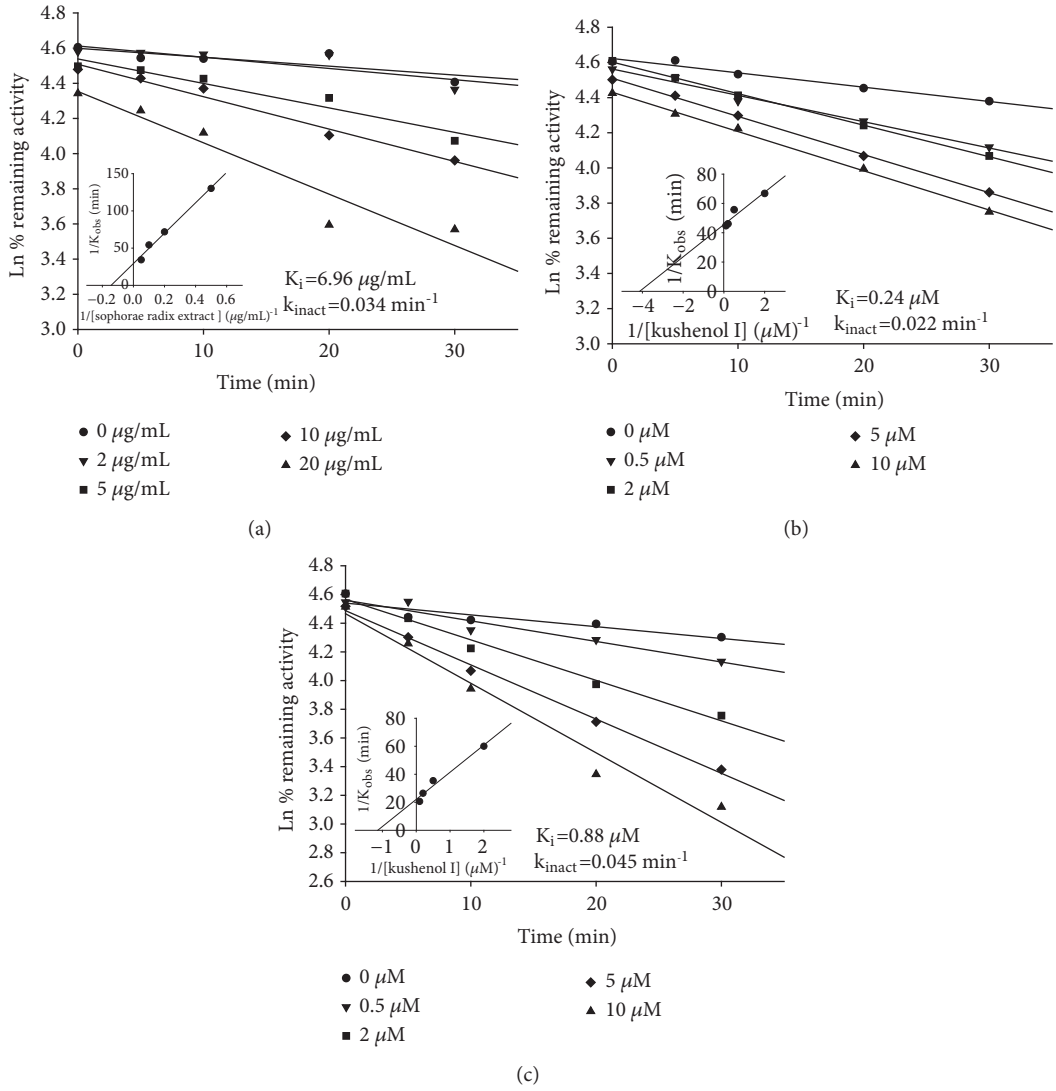

Figure 5: Concentration- and time-dependent inactivation of human liver microsomal CYP3A4 by *S. flavescens* extract (a) and kushenol I (b) and recombinant CYP3A4 by kushenol I (c) in the presence of an NADPH-generating system. The logarithm of the percentage of remaining activity (related to time 0 in the presence of solvent alone) was plotted as a function of time; the corresponding double reciprocal plots for the inactivation rate and the concentration of *S. flavescens* extract or kushenol I are shown. The K_i and k_{inact} values were obtained from the reciprocals of the x- and y-intercepts, respectively. Each data point represents the mean of duplicate experiments.

On the other hand, sophoraflavone G reversibly inhibited CYP1A2, CYP2B6, CYP2C8, and CYP2C9, whereas only CYP3A4 was irreversibly inhibited by this flavonoid. Inactivation of CYP3A by kushenol I was also observed, with K_i and k_{inact} values of 0.242 μM and 0.022/min, respectively. Iwata et al. [25] reported that the methanolic fraction of *Sophora* radix does not inhibit CYP2D6 or CYP3A4 in human liver microsomes. These results are consistent with our findings of limited CYP2D6 and CYP3A4 inhibition in microsomes without preincubation with the extract. Previous research showed that sophocarpine from *S. flavescens* inhibited CYP3A4 in a time-dependent manner and competitively inhibited CYP2C9 [16]. Prenylated flavonoids from *Humulus lupulus* almost completely inhibited CYP1A1 and CYP1B1 activities at a concentration of 10 μM [26]. The prenylated flavone isoxanthohumol also showed time-dependent inactivation of CYP1A2 [17]. Yilmazer and his colleagues [26] demonstrated that xanthohumol is transformed to a diol metabolite, presumably via an epoxide intermediate. The epoxide intermediate generated during the enzymatic reaction may be responsible for inactivation of the CYP enzymes.

The different effects of the active components in *S. flavescens* on CYP isoforms may complicate findings in experimental rats. Oral administration of *S. tonkinensis* extract to rats for 14 days resulted in increased plasma levels of bupropion and omeprazole, which were metabolized mainly by CYP2B and CYP2C, whereas the extract did not significantly modulate CYP1A or CYP3A activity [27]. In addition, administration of *S. flavescens* extract to rats for 7

days increased the plasma levels of phenacetin, omeprazole, and tolbutamide, suggesting inhibition of CYP1A and CYP2C activities [15]. Contrarily, concomitant oral administration of *S. flavescens* extract to rats for 7 days significantly decreased the concentration of plasma indinavir, which is primarily metabolized by CYP3A, whereas the ethyl acetate fraction of *S. flavescens* had no effect [20]. Dose-dependent increases in CYP1A2, CYP2B, and CYP3A activities were reported in rats treated with *S. flavescens* extract, as demonstrated by CYP isoform-selective activity and western blot analysis [18]. CYP3A4 mRNA expression was induced by *S. flavescens* aqueous extract in HepaRG and DPX2 cells via activation of the pregnane X receptor and the compounds N-methylcytisine partially contributed to CYP3A4 induction [28]. Yuan and his colleagues reported that matrine and oxymatrine induce CYP2B, but not CYP3A in experimental rats [17]. Because CYP inhibitors and inducers exist in *S. flavescens*, modulation of CYP isoforms by *S. flavescens* extract may be dependent on the preparation methods of the extract as well as experimental design.

Although the *S. flavescens* extract used in this experiment was prepared with 70% ethanol, and flavonoids may be preferentially extracted compared with alkaloids, the extract inhibited CYP2B6, CYP2C8, CYP2C9, CYP2C19, and CYP3A4 in human liver microsomes. In particular, CYP2B6 and CYP3A4 were inhibited by a mechanism-based mode of inhibition, suggesting that these CYPs may be significantly inhibited by administration of the extract to humans. The mechanism-based inactivation of CYP3A4 was confirmed using the prenylated flavonoid kushenol I. Given the inhibitory effects of prenylated flavonoids along with inductive effects of alkaloids, the overall modulation of CYP activity by *S. flavescens* extract in humans may be complex and dependent on treatment formulation and duration. To the best of our knowledge, no clinical trials have been conducted to evaluate the possible interactions between *S. flavescens* extract and concomitantly administered drugs. Therefore, clinical trials to investigate these herb–drug interactions are required to better predict the effects of *S. flavescens* extract on concomitantly administered drugs in humans.

5. Conclusion

In summary, *S. flavescens* extract strongly and reversibly inhibited CYP2C8, CYP2C9, and CYP2C19. CYP2B6 and CYP3A4 were inhibited by the extract via mechanism-based inactivation. The constituents kushenol A, kushenol C, kushenol M, kushenol I, leachianone A, and sophoraflavone G also displayed CYP inhibition, which was dependent on the selectivity of these compounds for the CYP isoforms and on the mode of inhibition. Considering the inhibitory effects of *S. flavescens* extract and its prenylated flavonoids on CYP enzymes, clinical interaction with coadministered drugs that are metabolized by CYP enzymes, especially CYP2B6 and CYP3A4, cannot be excluded. The potential interactions between *S. flavescens* extract and common drugs need further evaluation in human clinical trials.

Data Availability

The data used to support the findings of this study are available from the corresponding author upon request.

Conflicts of Interest

The authors declare no financial conflicts of interest that could inappropriately influence the outcome of this study.

Acknowledgments

This research was supported by the National Research Foundation of Korea (NRF), funded by the Ministry of Science, ICT & Future Planning (grant No. 2017R1A2N3008475 and grant No. 2018R1A5A2021242).

References

[1] Chinese Pharmacopoeia Commission, *The Pharmacopoeia of the People's Republic of China*, China Medical Science Press, Beijing, China, 2010.

[2] X. He, J. Fang, L. Huang, J. Wang, and X. Huang, "Sophora flavescens ait.: traditional usage, phytochemistry and pharmacology of an important traditional chinese medicine," *Journal of Ethnopharmacology*, vol. 172, pp. 10–29, 2015.

[3] L. Zhang, L. Xu, S.-S. Xiao et al., "Characterization of flavonoids in the extract of Sophora flavescens Ait. by high-performance liquid chromatography coupled with diode-array detector and electrospray ionization mass spectrometry," *Journal of Pharmaceutical and Biomedical Analysis*, vol. 44, no. 5, pp. 1019–1028, 2007.

[4] X. Chen, C. Yi, X. Yang, and X. Wang, "Liquid chromatography of active principles in Sophora flavescens root," *Journal of Chromatography B*, vol. 812, pp. 149–163, 2004.

[5] M. Sun, J. Han, J. Duan et al., "Novel antitumor activities of Kushen flavonoids in vitro and in vivo," *Phytotherapy Research*, vol. 21, no. 3, pp. 269–277, 2007.

[6] X. Y. Huang and C. X. Chen, "Effect of oxymatrine, the active component from Radix Sophorae flavescentis (Kushen), on ventricular remodeling in spontaneously hypertensive rats," *Phytomedicine*, vol. 20, no. 3-4, pp. 202–212, 2013.

[7] Y. C. Kim, H.-S. Kim, Y. Wataya et al., "Antimalarial Activity of Lavandulyl Flavanones Isolated from the Roots of Sophora Flavescens," *Biological & Pharmaceutical Bulletin*, vol. 27, no. 5, pp. 748–750, 2004.

[8] M. Kuroyanagi, T. Arakawa, Y. Hirayama, and T. Hayashi, "Antibacterial and antiandrogen flavonoids from Sophora flavescens," *Journal of Natural Products*, vol. 62, no. 12, pp. 1595–1599, 1999.

[9] H. J. Cho and I. S. Yoon, "Pharmacokinetic interactions of herbs with Cytochrome p450 and P-Glycoprotein," *Evid Based Complement Alternat Med*, vol. 2015, Article ID 736431, 10 pages, 2015.

[10] S. Zhou, Y. Gao, W. Jiang, M. Huang, A. Xu, and J. W. Paxton, "Interactions of herbs with cytochrome P450," *Drug Metabolism Reviews*, vol. 35, no. 1, pp. 35–98, 2003.

[11] F. Borrelli and A. A. Izzo, "Herb-drug interactions with St John's Wort (hypericum perforatum): an update on clinical observations," *The AAPS Journal*, vol. 11, no. 4, pp. 710–727, 2009.

[12] S. M. Robertson, R. T. Davey, J. Voell, E. Formentini, R. M. Alfaro, and S. R. Penzak, "Effect of *Ginkgo biloba* extract on lopinavir, midazolam and fexofenadine pharmacokinetics in healthy subjects," *Current Medical Research and Opinion*, vol. 24, no. 2, pp. 591–599, 2008.

[13] B. J. Gurley, S. F. Gardner, M. A. Hubbard et al., "*In vivo* effects of goldenseal, kava kava, black cohosh, and valerian on human cytochrome P450 1A2, 2D6, 2E1, and 3A4/5 phenotypes," *Clinical Pharmacology & Therapeutics*, vol. 77, no. 5, pp. 415–426, 2005.

[14] C.-S. Yuan, G. Wei, L. Dey et al., "Brief communication: American ginseng reduces warfarin's effect in healthy patients. A randomized, controlled trial," *Annals of Internal Medicine*, vol. 141, no. 1, pp. 23–27, 2004.

[15] L. Chen, J. Cai, S. Wang, L. Hu, and X. Yang, "Effect of radix sophorae flavescentis on activity of CYP450 isoforms in rats," *International Journal of Clinical and Experimental Medicine*, vol. 8, pp. 21365–21371, 2015.

[16] J. Zhang, C. Li, J. Zhang, and F. Zhang, "In vitro inhibitory effects of sophocarpine on human liver cytochrome P450 enzymes," *Xenobiotica*, pp. 1–14, 2018 (Basque).

[17] F. Yuan, J. Chen, W.-J. Wu et al., "Effects of matrine and oxymatrine on catalytic activity of cytochrome P450s in rats," *Basic & Clinical Pharmacology & Toxicology*, vol. 107, no. 5, pp. 906–913, 2010.

[18] Y. F. Ueng, C. C. Tsai, W. S. Lo, and C. H. Yun, "Induction of hepatic cytochrome p450s by the herbal medicine sophora flavescens extract in rats: impact on the elimination of theophylline," *Drug Metabolism and Pharmacokinetics*, vol. 25, no. 6, pp. 560–567, 2010.

[19] Y.-F. Ueng, C.-C. Chen, C.-C. Tsai, and P. Souček, "Differential inductive profiles of hepatic cytochrome P450s by the extracts of Sophora flavescens in male and female C57BL/6JNarl mice," *Journal of Ethnopharmacology*, vol. 126, no. 3, pp. 437–446, 2009.

[20] J.-M. Yang, S.-P. Ip, Y. Xian et al., "Impact of the Herbal Medicine Sophora Flavescens on the Oral Pharmacokinetics of Indinavir in Rats: The Involvement of CYP3A and P-Glycoprotein," *PLoS ONE*, vol. 7, no. 2, Article ID e31312, 2012.

[21] K.-A. Seo, S.-J. Lee, K.-B. Kim et al., "Ilaprazole, a new proton pump inhibitor, is primarily metabolized to ilaprazole sulfone by CYP3A4 and 3A5," *Xenobiotica*, vol. 42, no. 3, pp. 278–284, 2012.

[22] M.-J. Kim, H. Kim, I.-J. Cha et al., "High-throughput screening of inhibitory potential of nine cytochrome P450 enzymes in vitro using liquid chromatography/tandem mass spectrometry," *Rapid Communications in Mass Spectrometry*, vol. 19, no. 18, pp. 2651–2658, 2005.

[23] Y. Yuan, X. Qiu, D. Nikolić et al., "Inhibition of human cytochrome P450 enzymes by hops (Humulus lupulus) and hop prenylphenols," *European Journal of Pharmaceutical Sciences*, vol. 53, no. 1, pp. 55–61, 2014.

[24] M. Sun, H. Cao, L. Sun, S. Dong, Y. Bian, J. Han et al., "Antitumor activities of kushen: literature review," *Evidence-Based Complementary and Alternative Medicine*, vol. 2012, Article ID 373219, 11 pages, 2012.

[25] H. Iwata, Y. Tezuka, T. Usia, S. Kadota, A. Hiratsuka, and T. Watabe, "Inhibition of human liver microsomal CYP3A4 and CYP2D6 by extracts from 78 herbal medicines," *Journal of Traditional Medicines*, vol. 21, no. 1, pp. 42–50, 2004.

[26] M. C. Henderson, C. L. Miranda, J. F. Stevens, M. L. Deinzer, and D. R. Buhler, "In vitro inhibition of human P450 enzymes by prenylated flavonoids from hops, Humulus lupulus," *Xenobiotica*, vol. 30, no. 3, pp. 235–251, 2000.

[27] J. Cai, J. Ma, K. Xu, G. Gao, Y. Xiang, and C. Lin, "Effect of radix sophorae tonkinensis on the activity of cytochrome P450 Isoforms in Rats," *International Journal of Clinical and Experimental Medicine*, vol. 8, pp. 9737–9743, 2015.

[28] L. Wang, F. Li, J. Lu et al., "The Chinese herbal medicine Sophora flavescens activates pregnane X receptor," *Drug Metabolism and Disposition*, vol. 38, no. 12, pp. 2226–2231, 2010.

Hindawi
Evidence-Based Complementary and Alternative Medicine
Volume 2019, Article ID 1983780, 16 pages
https://doi.org/10.1155/2019/1983780

Review Article

Influence Factors of the Pharmacokinetics of Herbal Resourced Compounds in Clinical Practice

Shi Sun,[1] Yifang Wang,[1] Ailing Wu,[1] Zhen Ding,[1] and Xinguang Liu [2]

[1] *Department of Pharmacy, Luoyang Orthopedic Hospital of Henan Province, Orthopedic Hospital of Henan Province, Luoyang, China*
[2] *Institute of Integrative Medicine, Dalian Medical University, Dalian, China*

Correspondence should be addressed to Xinguang Liu; lxg1987519@163.com

Received 14 November 2018; Accepted 15 January 2019; Published 5 March 2019

Academic Editor: Giuseppe Caminiti

Herbal medicines have been used to prevent and cure diseases in eastern countries for thousands of years. In recent decades, these phytotherapies are becoming more and more popular in the West. As being nature-derived is the essential attribute of herbal medicines, people believe that taking them for diseases treatment is safe enough and has no side-effects. However, the efficacy of herbal resourced compounds (HRC) depends on the multiple constituents absorbed in the body and their pharmacokinetics. Thus, many factors will influence the clinical practice of HRC, i.e., their absorption, distribution, metabolism, and excretion (ADME). Among these factors, herb-drug interaction has been widely discussed, as these compounds may share the same drug-metabolizing enzymes and drug transporters. Meanwhile there are many other potential factors that can also change the ADME of HRC, including herb pretreatment, herb-herb interactions, pathological status, gender, age of patient, and chemical and physical modification of certain ingredients. With the aim of ensuring the efficacy of HRC and minimizing their clinical risks, this review provides and discusses the influence factors and artificial improvement of the pharmacokinetics of HRC.

1. Introduction

The history of people employing herbal medicines can be dated back as early as 2100 B.C. in ancient Asian countries [1]. Nowadays, approximately 25% of common medications contain herbs, and this proportion has been elevated to 30% and to 50% in China, especially [2]. Not only in the East, herbal medicines have contributed the largest proportion to complementary and alternative medicine consumption in the United States and about 20% of people have taken some herbal supplementation [2, 3].

With the increasing knowledge of diseases treatment, people found that pharmacokinetics of HRC and their tissue distribution behaviors are crucial to their pharmacological efficacy [4]. For instance, differences in physiological status of body such as gender, age, diseases, and external stimulus may influence the oral bioavailability, tissue distribution, half-time ($t_{1/2}$), maximum plasma concentration (C_{max}), and time to reach C_{max} (T_{max}), etc. of drugs or herbal medicines, and these changes in intrinsic pharmacokinetic parameters will cause variations in their therapeutic effects [4–8].

Meanwhile, unlike the widely employed chemical drugs, herbal medicines containing thousands of constituents are regarded as performing holistic effects through interactions among multiple active components and multiple targets [9]. Meanwhile, the internal metabolism processes of herbal medicines are complex due to these interactions, which may influence metabolism-related biological active substances, such as cytochrome P450 enzyme (CYP450) and P-glycoprotein (P-gp) [10]. Certainly, if herbal medicines were applied in combination with conventional drugs, the risk of possible interactions between constituents is increased. In addition, not all herb-drug or herb-herb interactions are harmful. Under some circumstances, these interactions can improve the bioavailability of target compounds and minimize side-effects of toxic ingredients [11, 12].

The pharmacokinetic changes of HRC are closely related to its pharmacodynamics, and the factors affecting the process *in vivo* are very complex and easy to be ignored. Thus, the aim of this review is to describe the common factors that influence the pharmacokinetics of HRC, thereby giving

some references to ensure the safety and efficacy of these medications.

2. The Influence of Processing on the HRC Pharmacokinetics

The processing of traditional Chinese medicines (TCM) is a routine procedure and is usually performed on raw herbs before clinical use. Various traditional methods have been applied to herbs processing, such as sautéing with Chinese rice wine or brine solution, stir-heating, frying with sand, salt, honey or bile, steaming with water, ginger juice or vinegar, and sulfur fumigation [13–19]. The purpose of herb processing is modifying the nature of crude herbal materials, which results in enhancing their therapeutic effects, as well as reducing their toxicity. The content of some ingredients in herbs may increase, and others may decrease or even disappear after processing. Changing the chemical profile usually influences the pharmacokinetics of HRC.

Wine is one of the most popular processing adjuvants. Tao et al. [20] compared the pharmacokinetic differences between crude and wine-processed *Dipsacus asper* (DA) in rats. After being processed, the contents of phenolic acids of DA were decreased more than those of the crude herb, while the contents of saponins and iridoids were increased significantly. Compared to rats in the group of crude herb administration, area under the plasma concentration-time from zero to the last quantifiable time-point ($AUC_{0\text{-}t}$) values along with C_{max} values of most compounds increased remarkably after wine-processed DA aqueous extracts administration. These differences might be attributed to the facilitating effect of wine that made ingredients absorb into the circulation more easily. Wine-processed herb exhibited more loose tissues, more small pores, larger total surface area, and smaller fractal dimension than those of crude herb, which allows the solvent to penetrate the loose tissue and to change internal structure, then increasing dissolution of herb containing components [21], and this might be another reason to explain this phenomenon. Similar results were observed in wine-processed *Rhizoma Coptidis* and *Schisandra Chinensis fructus* [22, 23].

The same adjuvant used in herbal materials processing can have different effects on pharmacokinetics of herbs. Vinegar-baked is another routine technology for herb preparation. On the one hand, during the procedure of vinegar processing, the hydrolyzation of saponins, flavonoids, and polysaccharides occurs, and the content of these components may be changed, because the main component of vinegar is acetic acid; this will result in deglycosylation of natural products with glycoside structure. The reaction makes the pharmacokinetic parameters of compounds significantly different between crude and vinegar-processed herbs and strengthens the effect of processed herbs [24]. On the other hand, some vinegar-processed herbs show less toxicity than crude herbs. This may be caused by the destruction of prototypes of some ingredients possessing the most toxicity and decreasing the bioavailability of toxic components after processing [14].

Animal-derived materials, such as pig's bile and mutton-fat, are a class of distinctive adjuvants in herb processing. There are researchers believing that bitter bile could increase the Cold nature of herbs and influence the energy metabolism of experimental animals [25]. Furthermore, a comparative pharmacokinetic study revealed that bile-processed *Rhizoma Coptidis* could increase the absorption rate of main active alkaloids into the plasma of heat syndrome rats more than raw herb [19]. These results are probably because alkaloids in *Rhizoma Coptidis* are hydrophobic, but when they meet the bile acids in processing adjuvant pig's bile, soluble salts are formed and then facilitate the water dissolving of these alkaloids, which finally leads to the absorption rate improvement of alkaloids by rats and strengthens their specific therapeutic effects.

In recent decades, a controversial processing technology named sulfur fumigation has taken the place of natural drying of postharvest medicinal herbs under sun or in the shade [26]. For one thing, this operation can make herbs look whiter and prettier and prevent them from insects and mildew with shortened drying time. For another, this processing procedure can cause chemical alteration of the herbs' origin ingredients, generate sulfonated derivatives, and then influence the pharmacokinetics of certain components [26–28]. *Radix Paeoniae Alba* (the root of *Paeonia lactiflora* Pall., PA) is the most representative medicinal herb that is always processed by sulfur fumigation. Some researchers suggested that sulfur fumigation could increase the absorption time and improve the bioavailability of the active components of PA [29], whereas another study showed that the safety and efficacy of PA were reduced after this processing procedure [28]. In consideration of the debatable safety of sulfur-fumigated medicinal materials, most herbs are forbidden to be processed by sulfur fumigation in China now. Meanwhile, the permitted herbs should have sulfur dioxide residual amount less than 400 mg/kg, but this residue limitation lacks scientific evidence [26]. Overall, in order to standardize the practice of sulfur fumigation and ensure the safety and efficacy of sulfur-fumigated herbs, further studies are needed.

Different from traditional processing, new methods like ultrafine powders of Chinese herbs (D 90 < 45 μm) have made great progress in clinical use for their convenience for carrying and oral administration [30]. As the pulverized herbal medicine owns a relatively larger surface area than traditional applied forms, bioavailability of many constituents *in vivo* increased [30, 31]. Consequently, this feature will help patients in taking lower dosage of herbal medicine in prescriptions and saving cost, which may improve medication compliance to ensure therapeutic effects

3. The Influence of Coadministration with Herbal Medicines or Drugs

In general, many people believe that herbal remedies present moderate and harmless effects to patients. Admittedly, the use of herbal medicines alone may not be dangerous, but they ignore the fact that herbal medicines contain various constituents with multiple pharmacological actions on the body. If conventional drugs are taken in combination,

probable interactions of pharmacokinetics and/or pharmacodynamics may occur between them. A report reveals that nearly 80% of the world's population take herbs as their primary medications. In particular, older people tend to become the largest consuming groups of herbal prescriptions due to their commonly multiple health problems, such as chronic diseases [32]. They often take herbal medicines coupled with conventional medications, which is raising the potential for herb-drug interactions. Therefore, the risk of possible interactions between drug and co- or preadministration herbal medicine, single substance, and other components in traditional herbal compound prescriptions, even occurring in the multiconstituent herb itself, should not be disregarded. Several reviews have discussed the issue of herb-drug interactions [3, 10, 32–35]. In these reviews, they mainly focus on the effects of natural products on the pharmacokinetics or pharmacodynamics of drugs. However, on the one hand, the coadministration of chemical drug may also influence the pharmacokinetics of HRC; on the other hand, the interactions between HRC are also little discussed. Hence, we will place especial emphasis on herb-herb interactions and multicomponent interaction in an herb in this section.

3.1. Herb-Drug Interaction. The metabolism of HRC *in vivo* mostly depends on common drug-metabolizing enzymes and transporters, such as CYP450 or P-gp. Many papers reported that the coadministration of herbal medicines interferes in the pharmacokinetics of chemical drugs because of their sharing the same metabolizing enzymes and transporters, while the chemical drugs would also affect the pharmacokinetics of HRC by the same mechanism. Therefore, intensive studies are needed to ensure the safety and effectiveness of drugs when they coadministrated with herbal medicines.

CYP450 is a group of oxygenases, which plays a key role in the metabolism of endogenous substances and exogenous xenobiotics. Meanwhile, approximately 90% of current drugs are metabolized by CYP450 subtypes [10]. If the chemical drugs inducted or inhibited specific CYP450 isoforms, the metabolism of coadministration HRC would be influenced. Yin and Cheng et al. [36] used CYP450 probe drugs as a tool to investigate the effects of notoginsenoside R1 on the activities of several CYP450 isoforms *in vivo*. The results exhibited that compared with the pharmacokinetic parameters of the control group, the C_{max} and area under the plasma concentration-time from zero to infinity ($AUC_{0-\infty}$) of caffeine, which is mainly metabolized by CYP1A2, were increased, while the total plasma clearance (CL) was decreased in the notoginsenoside R1 treated group. However, other probe drugs corresponding to CYP2C11, CYP2D1, and CYP3A1/2 like tolbutamide, metoprolol, and dapsone were not affected by notoginsenoside R1 administration. These consequences indicated that patients who took drugs metabolized by CYP1A2 together with notoginsenoside R1 should evaluate the potential herb-drug interactions and be paid more attention.

Drug transporters are another important group that affects the metabolism of drugs. Until now, a lot of transporters have been characterized in humans, while P-gp is the most extensively studied one and affects the bioavailability of many oral medications [33]. *Schisandra chinensis* is a commonly used herb and its extract was reported to regulate P-gp along with other transporters such as multidrug resistance-associated proteins and organic anion transporting polypeptides, as well as some drug-metabolizing enzymes. Therefore, coadministration of *Schisandra chinensis* and other drugs which are substrates of the reported transporters and enzymes may cause unfavorable herb-drug interactions [37].

Although many studies indicate that herbal medicines could alter the pharmacokinetics of coadministration drugs [38, 39], there are still some reports suggesting that no significant influence is observed in combination use of herbs with drugs [40, 41].

3.2. Herb-Herb Interaction. According to many fork medicine theories, the most dominant clinical application form of herbal medicines is "formula", which is prescribed in combination of two or more herbs. Compatibility of multiple herbs is a key characteristic of formula and has exhibited its enormous influence in long-term clinical practices. It depends on both the clinical efficacy and the properties of each herb and possesses intention to obtain synergistic therapeutic effects and minimize or diminish the possible side-effects [42–44]. The chemical material basis of compatibility may be due to their interactions between the multiple constituents in the compound prescription, sequentially influencing the ADME of individual active ingredients. Hence, it is meaningful to reveal the complex mechanism of formula compatibility. Some common herb-herb interactions are summarized in Table 1.

Many works have been demonstrated to study the regularity of recipe composition. Da Chuanxiong decoction consists of *Gastrodia elata* Bl. (GE) and *Ligusticum chuanxiong* Hort. (LC), and Hu et al. compared the pharmacokinetics of gastrodin after orally administrating GE extract alone and in combination with different components of LC in rats [54]. They found that total phenolic acids and alkaloids but not tetramethylpyrazine of LC significantly affected the pharmacokinetic parameters of gastrodin. Another case investigated the pharmacokinetic compatibility of several ingredients in Sheng Mai San, a compound prescription consisting of *Panax ginseng*, *Ophiopogon japonicus*, and *Schisandra chinensis* and exhibiting curative effects on cardiovascular diseases [44]. Experiment results showed that *Schisandra* lignans extract could significantly enhance the exposure of several ginsenosides both *in vitro* and *in vivo*. Recently, a comparative pharmacokinetic study in rats was carried out to evaluate the herb-herb interactions in Guanxin Shutong Capsule (GSC) following oral administration of single herb extract and different herb extract combinations [45]. With the composing of *Choerospondias axillaris*, *Salvia miltiorrhiza Bunge*, *Syzigium aromaticum* (SA), *Borneolum syntheticum* (BS), and *Tabaschir*, GSC has been used for treating cardiovascular-related disease in clinical practice. As a result, GSC treated group showed significant promotion of the bioavailability of eugenol and reduction of the rate of its elimination processes, and the AUC_{0-t}, $AUC_{0-\infty}$, and C_{max} of bicyclic monoterpenes (isoborneol, borneol, and camphor) were more prominently

Table 1: Possible herb-herb interactions.

Herb1	Herb2	Monitoring indexes	Pharmacokinetic parameters of indexes comparing to administration herb1 alone										Ref.
			$AUC_{0\text{-}t}$	$AUC_{0\text{-}\infty}$	$t_{1/2}$	T_{max}	C_{max}	$MRT_{0\text{-}\infty}$	$MRT_{0\text{-}t}$	K	V_d	CL	
Borneolum	GuanxinShutong Capsule	Camphor	↓		↓		↓						[45]
		Isoborneol	↓	↓	↑		↓						
		Borneol	↓	↓			↓						
		Eugenol	↑	↑	↑	↑	↓						
	Syzigiumaromaticum	Camphor			↓		↓						
		Isoborneol					↓						
		Borneol			↓								
		Eugenol				↑	↓						
Salviaemiltiorrhi-zae	Borneol	Rosmarinicacid		↑			↑	↑					[46]
		Salvianolic acid A		↑			↑						
		Salvianolic acid B		↑	↑			↑					
Radix et Rhizoma Rhei	Dahuang-Fuzi Decoction	Chrysophanol	↓	↓	↑	↑	↓						[43]
		Physcion	↓	↓		↑	↓						
Paeonia lactiflora	ZengmianYiliu Formula	Albiflorin	↓	↓			↓			↓[a]	↑	↑	[47]
		Paeoniflorin			-[c]					↓[b]			
Raidx Kansui and *Radix et Rhizoma Glycyrrhizae*	Gansui-Banxia Decoction	Liquiritigenin	↑	↑	↑	↓	↑						[48]
		Isoliquiritigenin	↑	↑	↑	↑	↑						
		Liquiritin	↓	↓	↑	↓	↑						
		Glycyrrhetinic acid	↑	↑		↓	↑						
		Glycyrrhizic acid	↑	↑	↑								
Radix Paeoniae	*Radix et Rhizoma Glycyrrhizae*	Liquiritigenin	↑	↑			↑						[48]
		Isoliquiritingenin	↑	↑			↑						
		Liquiritin	↑	↑	↑	↑	↑						
		Glycyrrhetinic acid	↑	↑	↑		↑						
		Glycyrrhizic acid		↑	↑	↑	↑						
Cortex Mori	*Radix Pueraria* Flavonoids	1-deoxynojirimycin				↑	↑	↑					[49]

Table 1: Continued.

Herb1	Herb2	Monitoring indexes	Pharmacokinetic parameters of indexes comparing to administration herb1 alone										Ref.
			$AUC_{0\text{-}t}$	$AUC_{0\text{-}\infty}$	$t_{1/2}$	T_{max}	C_{max}	$MRT_{0\text{-}\infty}$	$MRT_{0\text{-}t}$	K	V_d	CL	
Ramulus Cinnamomi	*Ephedrae Herba*	Coumarin	↑	↑	↑			↑	↑				[50]
		Cinnamic alcohol	↑	↑					↑				
		Cinnamic acid	↑	↑	↓			↑	↑				
HuoluoXiaoling Dan	*Radix Paeoniae Rubra*	Paeoniflorin	↓	↓		↓						↑	[51]
		Albiflorin	↓	↓		↓						↑	
		Oxypaeoniflorin	↓	↓		↓						↑	
	Corydalis yanhusuo	Tetrahydropalmatine	↑	↑	↓	↓	↑					↓	
		Corydaline	↑	↑		↓	↑						
		Dehydrocorydaline	↑	↑		↓	↑					↓	
		Berberine	↑	↑		↓	↑						
HuoluoXiaoling Dan	*Radix Angelica sinensis* and *Rhizome Ligusticum chuanxiong*	Senkyunolide A	↑				↑						[42]
		Ligustilide	↑	↑	↓		↑						
		Butylidenephthalide	↑	↑	↓	↓	↑						
		3-butyl-phthalide	↑	↑			↑						
		Levistilide A	↑	↑	↓	↓	↑						
Panax Ginseng glycosides	*Schisandra lignans*	Ginsenoside Rb2[d]	↑	↑									[44]
		Ginsenoside Rc[d]	↑	↑									
		Ginsenoside Rd[d]	↑	↑									
		Ginsenoside Rb1[e]	↑	↑									
		Ginsenoside Rb2[e]	↑	↑									
		Ginsenoside Rd[e]		↑									
Quercetin and Rutin	Leaves of *Bacopa onnieri*, Fruits of *Hipphophae rhamnoides* and Bulbs of *Dioscoreabulbifera*	Quercetin	↓				↓						[52]
		Rutin	↑	↑			↑	↑					
Radix Paeoniae Alba and *Radix et Rhizoma Glycyrr-hizae* (1:1)	*Radix Paeoniae Alba* and *Radix et Rhizoma Glycyrr-hizae* (4:1)	Albiflorin	↑				↑					↓	[53]
		Oxypaeoniflorin	↑				↑					↓	
		Paeoniflorin	↑				↑					↓	
		Isoliquiritin	↑										
		Liquiritigenin	↑									↓	
		Isoliquiritingenin	↓				↓					↑	
		Ononin	↑									↓	
		Glycyrrhizin	↑				↑					↓	
		Glycyrrhetinic acid	↓				↓						
Rhizoma Tianma	Ferulic acid	Gastrodin		↑	↑			↓					[54]
	Total phenolic acid of *Rhizoma Chuanxiong*	Gastrodin		↑			↑						
Rhizoma Tianma	Total alkaloids of *Rhizoma Chuanxiong*	Gastrodin		↑									[54]
	Rhizoma Chuanxiong	Gastrodin		↑	↑		↓	↑				↓	

Blanks are no mention or no significant changes
a. decreased in elimination rate constant
b. decreased in distribution/absorption rate constant
c: decreased in elimination half-life and increased in distribution half-life
d: single dose
e: multiple dose

decreased than in SA-BS coextract treated group. As the accumulation of bicyclic monoterpenes proved to be toxic in long-term administration, the reduced absorption of these compounds owing to the herb-herb interactions in GSC could alleviate the toxicity of bicyclic monoterpenes to some extent. From the cases discussed above, we can speculate that improving the exposure of some bioactive components and reducing toxic ingredients absorption may be possible explanations to elucidate the mechanism of formula compatibility.

Although many researchers suggested that interactions between herbs in compound prescriptions are of common occurrence [44–47, 50–54], herbs demonstrate almost no interference with each other in some cases. Li et al. [61] reported that Honghua constituents demonstrated nearly no influences on the metabolism of Danshen polyphenols from Danhong injection via monitoring the plasma concentrations of eight Danshen polyphenols and comparing their pharmacokinetic parameters between Danshen injection and Danhong injection treated rats. Therefore, the interaction among herbs cannot be generalized, and specific discussion is required.

Nowadays, the safety of herbal medicines has been attracted more and more attention, and confirming the compatibility of herbs is a key point to ensure the safety of clinical usage of herbal remedies. "Eighteen Incompatible Medicaments" is the typical representative of TCM incompatibility. The theory proposes that specific agents in the eighteen-herb list can produce toxicity if they were used in combination. Gansui-Gancao is an incompatible herb pair recorded in "Eighteen Incompatible Medicaments". Gansui is the root of *Euphorbia kansui* T.N. Liou ex T.P. Wang (GS) and exhibited a notable efficacy in treating malignant pleural effusion, but its efficacy could be weakened and even caused serious toxicity when used in combination with gancao, the root of *Glycyrrhiza uralensis* Fisch. or *Glycyrrhiza glabra* L (GC) [62, 63]. In general, these two herbs will not appear in one TCM formulae. Interestingly, a compound prescription called Gansuibanxia decoction (GSD) is composed of the tuber of *Pinellia ternata* (Thunb.) Breit. (BX) and the root of *Paeonia lactiflora* Pall. (SY), along with the incompatible herb pair of GS and GC, and the decoction exhibits great curative effect on phlegm retention syndrome. This is a surprising example, and it seems to violate the principles of formulating prescription. Cui et al. [48] elucidated the reasonability of this application of GSD from the pharmacokinetic prospective. They found that GS could inhibit the absorption of liquiritigenin, isoliquiritigenin, liquiritin, glycyrrhetinic acid, and glycyrrhizic acid of GC, which reduced the detoxification ability of GC and increased the toxicity of GS immediately. Nevertheless, SY demonstrated the opposite effects on the bioavailability of the main bioactive components of GC and alleviated the absorption inhibition of GS on GC in GSD. These results provided a possible explanation of this application of the incompatible herb pair.

Synergistic effect is another pivotal characteristic of TCM and demonstrates enhancement of their therapeutic effects; for example, Danshen-Sanqi (the root and rhizome of *Salvia miltiorrhiza* Bge. and the root and rhizome of *Panax notoginseng* (Burk.) F. H. Chen) and Zhishi-Baizhu (the immature fruit of *Citrus aurantium* L. or *Citrus sinensis* Osbeck and the root of *Atractylodes macrocephala* Koidz) exert synergistic actions to treat coronary heart disease and functional dyspepsia, respectively [64, 65]. *Cortex Mori* (CM), the root bark of *Morus alba* L, exhibits α-glycosidase inhibition effect and plays an important role in regulating the postprandial blood glucose level. As the main biological active constituent of CM, 1-Deoxynojirimycin (DXM) is considered as a potent α-glycosidase inhibitor. Coadministration of *Radix Pueraria* (the root of *Pueraria lobata* (Wild) Ohwi, RP) flavonoids with CM extract could reduce the absorption rate of DXM significantly and thus elevate the relative concentration and duration of DMX in small intestine, which demonstrated a stronger hypoglycemic effect of CM extract compared with the herb administration alone [49]. These results agree with the principle of composition of TCM, referring to enhancing the efficacy and reducing the toxic side-effects.

3.3. Multicomponent Interaction in an Herb. Since multiple components constitute the connotation of herbal medicines, possible interactions between complex ingredients in a single herb may occur. Ma et al. [12] reported that interaction between stilbene glucoside and emodin, two major constituents of *Radix Polygoni Multiflori* (the root of *Polygonum multiflorum* Thunb.), was observed. This interaction subsequently elevated the degree of absorption of emodin into rat plasma and prolonged its duration time *in vivo* after the stilbene glucoside treatment. The mechanism might involve inhibition of UDP-glucuronosyl-transferases 1A8 and thus prohibit the glucuronidation of emodin. Sinomenine is the prime alkaloid of *Sinomenium acutum*, Rehder & E.H. Wilson (SA). Co-dosing sinomenine with SA extract reduced the C_{max} and $AUC_{0\text{-}t}$ in rat plasma by comparison with pure sinomenine treated group, especially at the higher dosage of 60 mg/kg. These results suggested that the SA extract was able to decrease the bioavailability of its main constituent [60]. Similar results were observed in coadministration of pure osthole and *Libanotis buchtormensis* supercritical extract [55]. Of course, there are studies suggesting that interactions between components can also increase the absorption and improve the bioavailability of other components [11, 56, 57]. In addition, some reports indicate that the pharmacokinetic parameters of a class of compounds having similar characteristics, like flavonoids, tend to be affected together by coexisting compounds in rats [58, 59]. These results may be attributed to the competition or inhibition of the same transporters between those certain group compounds and other complex ingredients in one herb. The function and direction of interaction are uncertain, further studies should be carried out monitoring the clinical use of herbal medicines to ensure their safety and efficacy. Table 2 represents possible interactions among multiple components in single herb.

4. The Influence of Pathological Status

Pharmacokinetics of certain compounds may be influenced by the pathological status of host [5, 66]. For the past few years, many researches have focused on this issue. They found that pathological factors such as liver injury, diabetes, stroke,

Table 2: Possible multi-components interaction in an herb.

HRC1	HRC2/Herb	Monitoring indexes	Pharmacokinetic parameters of indexes comparing to administration HRC1 alone									Ref.
			$AUC_{0\text{-}t}$	$AUC_{0\text{-}\infty}$	$t_{1/2}$	T_{max}	C_{max}	$MRT_{0\text{-}\infty}$	$MRT_{0\text{-}t}$	V_d	CL	
Osthole	*Libanotis buchtormensis*	Osthole	↓		↑	↓	↓				↑	[55]
Epimedin C	*Herba Epimedii*	Epimedin C	↓			↓	↓			↑	↑	[56]
Tectoridin	*Iris tectorum*	Tectoridin	↑	↑	↑		↑				↑	[57]
Emodin	Stilbene glucoside of *Radix Polygoni Multiflori*	Emodin	↑	↑	↑		↑		↑	↑	↓	[12]
		Emodin glucuronide	↓	↓	↑		↓		↑	↑		
Magnoflorine	*Cortex Phellodendri*	Magnoflorine	↑	↑	↑	↑		↑	↑		↓	[11]
	Berberine	Magnoflorine	↑	↑			↑				↓	
Favonoid fraction of *Abelmoschus manihot*	Macromolecular fraction of *Abelmoschus manihot*	Rutin				↑						[58]
		Isoquercitrin			↓	↑	↑					
		Hibifolin				↑						
		Quercetin-3'-O-glucose				↑						
		Quercetin			↓	↑						
	Small molecule fraction of *Abelmoschus manihot*	Rutin	↑		↑		↑					
		Hyperiode	↑									
		Isoquercitrin	↑									
		Hibifolin	↑			↑						
		Myricetin	↑			↑	↑					
		Quercetin-3'-O-glucose	↑				↑					
		Quercetin			↓							
	Macromolecular and Small molecule fraction of *Abelmoschus manihot*	Rutin	↑									
		Hyperiode	↑		↑	↑						
		Isoquercitrin	↑			↑						
		Hibifolin				↑						
		Myricetin				↑						
		Quercetin-3'-O-glucose	↑			↑						
		Quercetin	↑		↓							
Ginkgo flavonoids	*Ginkgo biloba*	Apigenin	↑			↓	↑		↓	↓	↓	[59]
		Leteolin	↑			↑	↑		↑	↓	↓	
		Naringenin	↑			↑			↓		↓	
		Quercetin			↑	↑	↑		↑	↑	↓	
		Diosmetin	↑			↑	↑			↓	↓	
		Kaempferol	↑				↑		↑		↓	
		Isohamnetin	↑				↑			↓	↓	
Sinomenine	*Sinomeniumacutum*	Sinomenine	↓	↓			↓			↑	↑	[60]

fever, rheumatoid arthritis, migraine, coronary atherosclerotic heart disease, cancer, and neurodegenerative diseases demonstrate deep impact on metabolism of HRC [8, 67–75]. Hepatocytes are the parenchymal cells of liver which can improve the excretion of xenobiotics through urine or feces by modifying their structure, including phase I xenobiotic metabolism like oxidation or hydrolysis, followed by phase II metabolism like glucuronidation, sulfation, acetylation, or glutathione conjugation. Meanwhile, cytochrome P450 enzymes are mainly located in the pericentral area of the liver lobule, and glutathione peroxidase shows a higher expression in periportal zone [76]. So drugs are primarily metabolized in liver as this important organ generates the highest drug-metabolizing activity. Therefore, liver lesions will result in changing the pharmacokinetics of drugs [8, 77]. For instance, *dl*-Praeruptorin A (PA) is the prime active ingredient of *Peucedanum praeruptorum* Dunn and the substance of CYP 450 isozymes 3A1 and 3A2 in rats. A comparative pharmacokinetic experiment was conducted in liver cirrhosis and normal rats with single-dose intravenous administration to evaluate the pharmacokinetic variability of PA under hepatic damage condition. Compared to the control group, PA exhibited significant higher $AUC_{0\text{-}\infty}$ and slower hepatic elimination rate in model group. Those results might be partly caused by the lower hepatic blood flow rate and levels of CYP450 isoforms in liver cirrhosis rats [78].

Diabetes mellitus has become one of the most widespread metabolic diseases in the world, and patients suffering from type 2 diabetes mellitus (T2DM) approximately account for 90% of the diabetic totality [79]. In terms of metabolism, T2DM can induce gastrointestinal impairments, resulting in changes of the gut microbiome and slowing gastric emptying. Meanwhile, nephropathy and liver disease can be also observed in T2DM patients [80–82]. These physiological changes will affect the ADME of HRC. Wei et al. [80] invested the pharmacokinetic alteration of Sanhuang Xiexin decoction (SXD) extracts between T2DM and normal rats. They found that, compared to the control group, the AUC, C_{max}, $t_{1/2}$, and T_{max} of the six main components of SXD, namely, rhein, baicalin, wogonoside, berberine, palmatine, and coptisine, were remarkably enhanced in T2DM rats after oral administration of SXD. These results indicated that the bioavailability of the target compounds was improved and the elimination was slower in T2DM rats. Similar metabolism process *in vivo* was observed in cyanidin-3-O-glucoside and *Maydis stigma* extract treated T2DM rats [82, 83].

Stroke is one of the most serious causes of death in China and the United States [84]. Moreover, this malignant disease can cause hepatic dysfunction, affecting the secretion of glucocorticoid and gastric mucus, suppressing the gastric mucus bicarbonate barrier function and the peristalsis of stomach and small intestine. These alterations may increase bioavailability of HRC and prolong their retention time in the body [70, 85]. Meanwhile, stroke can activate a sequence of cascade reactions and damage the blood brain barrier (BBB). This makes it easier for HRC to cross BBB, thus changing the distribution of HRC [84].

It is worth noting that some model-inducement agents, such as streptozotocin and nitroglycerin, can elicit liver and kidney damage and increase microvascular permeability [80, 86]. Streptozotocin induces insulin deficiency due to its selective pancreatic β-cell cytotoxicity caused by DNA alkylation and nitric oxide generation. And diabetes causes structural and functional abnormalities in the liver by affecting glycogen and lipid metabolism. Nitroglycerine will induce vasodilation due to the vascular dilatory response of the brachial artery. These compounds also affect the metabolism of HRC. The metabolic changes caused by model-inducement agents do not agree with normal pathological process; perhaps some of the metabolism changes are not caused by the diseases themselves, so the results in these studies inducing models with nonself substances should be confirmed and evaluated.

5. The Influence of Physical and Chemical Modifications of Natural Product

Although many herbal medicines demonstrate good biological activities in tests *in vitro*, the *in vivo* assays do not exhibit reproducible results [87]. This may be attributed to the diversity of various constituents of herbal remedies, which affect the bioavailability, the internal duration, and the amount reaching the target tissue of the curative compounds. Many efforts have been made trying to solve the mentioned problems above, concerning physical and chemical modifications of active candidates derived from herbal medicines, to develop various drug delivery systems, (DDS) and change their properties and behaviors *in vivo*.

5.1. Promoting Bioavailability and Internal Duration of Natural Products. Most HRCs, such as flavonoids, tannins, and terpenoids, possess high water solubility or high molecular size; thus it is difficult for them to cross cell lipid membranes, leading to decreased bioavailability and efficacy [87]. Nevertheless, ingredients with hydrophobic property, like β-elemene, also affect their oral absorption due to the poor water solubility [88]. Low bioavailability seems to become the biggest obstacle of herbal medicines application in treating disease and brought about many problems in clinical trials [89]. Meanwhile, fast systemic clearance of HRCs also limits their therapeutic usage [90].

Poly lactic-co-glycolic acid (PLGA) is a widely used class of polymers and has been approved by US Food and Administration and European Medicine Agency for developing therapeutic nanoparticle DDS for their good biocompatible and biodegradable properties. The biodegradation process of PLGA occurs by hydrolysis and generates lactic acid and glycolic acid, which finally enter the tricarboxylic acid cycle being metabolized into carbon dioxide and water [91–93]. So, the polymers are safe enough and usually used to improve bioavailability and solubility of certain drugs [94]. Solvent evaporation, nanoprecipitation, and emulsification-diffusion technologies are commonly employed methods of PLGA nanoparticles synthesis [91]. Curcumin is a widely concerning polyphenol, which is derived from the herbal spice *Curcuma longa* L., and exhibits many physiological activities such as antioxidant, anti-inflammation, and antitumor. However, this promising bioactive compound exhibits

low bioavailability and a short half-life [92]. To overcome the shortages of curcumin and improve its therapeutic effect, Tsai et al. [92] designed curcumin-loaded PLGA nanoparticles (C-NPs). The *in vivo* test results showed that the curcumin exposure (AUC/dose) dramatically increased, 55% and 21-fold, after intravenous and oral administration of C-NPs more than conventional curcumin in rats, respectively. Meanwhile, C-NPs treated rats demonstrated 22-fold relative higher oral bioavailability, extended retention time, and decreased excretion of curcumin than those of rats in the control group. All the results above revealed that C-NPs could prolong internal retention time and elevate bioavailability of curcumin. Another attempt aiming to improve the oral bioavailability of resveratrol, a poorly water-soluble anti-inflammatory and antioxidant compound, was performed via formation of resveratrol-loaded galactosylated PLGA nanoparticles (RGP-NPs) [95]. These newly synthesized RGP-NPs exhibited more than 3 times higher oral bioavailability of resveratrol than those of rats dosing resveratrol suspensions alone, as well as exhibiting increased anti-inflammatory efficacy. From these examples, we can see clearly that PLGA-conjugates significantly affect the metabolism of modified HRC.

Emulsions are a class of mixtures consisting of two immiscible liquids and stabilizing with surfactants or emulsifiers. These DDS can be divided into two types, oil-in-water (O/W) and water-in-oil (W/O), and O/W type holds dominant position in parenteral or oral administration [91, 96]. Due to the hydrophilic property and smaller particle size, emulsions can be used to deliver many hydrophobic HRCs and enhance their bioavailability and *in vivo* duration time by turning them into dissolved forms, increasing their intestinal epithelial permeability, and decreasing their hepatic uptake [97–100]. The common methods to prepare emulsions in laboratory are sonication and homogenization, with high-pressure homogenization and microfluidization on a large scale [91]. Ligustrazine is an active alkaloid derived from *Ligusticum wallichii* Franchat and has various biological effects on cardiovascular and neurovascular disorders. However, like curcumin, the low oral bioavailability and short *in vivo* half-life of ligustrazine require multiple doses to obtain optimum clinical efficacy, but this application also ascends the its toxic risk to patients [100]. Wei et al. developed a ligustrazine-loaded lipid emulsion (LLE) and invested the influence of pharmacokinetics and tissue distribution of this application form on ligustrazine. Compared with routine ligustrazine injection, the optimized LLE demonstrated a sustained release profile *in vitro*, as well as an enhanced bioavailability and improved distribution pattern in all rat tissues *in vivo*. These results made lipid emulsion a potential delivery system of ligustrazine for its clinical use [100]. Moreover, Ke et al. [99] designed a cyclovirobuxine D-loaded self-nanoemulsifying DDS and significantly enhanced the relative bioavailability of the loaded drug to 200.22% in comparison with the commercial dosage form in rabbits. Besides carrying monomers, emulsion DDS can be also loaded with multiple phytochemicals like the total flavones of *Hippophae rhamnoides* L and *Corydalis decumbens* (Thunb.) Pers. extracts, improving the relative bioavailability of those hydrophobic ingredients [98, 101]. These results show the great potential of emulsion in developing DDS for poorly water-soluble HRC.

PEGylation technique, which refers to covalent attachment of polyethylene glycol (PEG) chains to target compound with ester bonds, is a widely used chemical functionalization method of biomolecules to improve their stability, water solubility, and pharmacokinetic properties such as $t_{1/2}$ and CL [102, 103]. Moreover, PEGylation molecules often demonstrated advantages in being protected against enzymatic degradation, as well as reducing immunogenicity and toxicity compared to their parent compounds [103, 104]. So many distinguishing properties make PEGylation technology very suitable to be applied to HRC modification. Lu et al. [102] synthesized PEGylated triacontanol (PEG-TA) as prodrug of triacontanol (TA), which exhibited antibacterial, antioxidant, antisenescence, etc. activities with low water solubility, established a gas chromatography tandem mass spectrometric method, and finally applied it to the pharmacokinetic study of PEG-TA and its metabolite TA in rats. Comparing the pharmacokinetic parameters, involving C_{max}, T_{max}, AUC, and mean residence time (MRT), between PEG-TA and TA treated rats via oral dosing and intravenous injection, they found that administration of PEG-TA in both ways conspicuously enhanced exposure levels and prolonged plasma half-life of TA. Namely, these results indicated that PEGylation might be a potential way to improve the pharmacodynamic properties of TA and promote its application. *Radix Ophiopogonis* polysaccharide (ROP) is a natural fraction possessing great therapeutic efficacy on myocardial ischemia. However, the poor oral bioavailability and short half-life limit its clinical application. In consideration of overcoming aforementioned shortages of ROP, Lin et al. synthesized two forms of PEGylated ROP. Finally, they found that these two newly synthesized conjugates exhibited approximate 11-13 times longer $t_{1/2}$ *in vivo* than ROP alone, showing good absorption following subcutaneous administration [105]. In addition, other technologies like micronization, salt formation, and hydroxypropyl-β-cyclodextrin inclusion were reported to enhance oral bioavailability of target compounds [106].

5.2. Target Delivering of HRC. The poor concentration of drug in target tissue prevents many drugs from exerting their therapeutic effects [107]. Hence, researchers took more and more attempts to apply plenty of methods to solve this problem. Among them, drug-targeting, including passive targeting and active targeting, is a promising technology that improves the bioavailability of HRC in desired loci *in vivo*, as well as reducing toxicity due to the localized area release of certain constituents of herbal medicines [89].

Since tissue lesions are direct manifestations of many diseases, tissue-targeting is the most important strategy in targeting DDS design. Meanwhile, the changes of tissue distribution of loaded HRC are obvious. For instance, Huang et al. [108] developed a bone-targeting liposome loaded with icaritin, an osteogenic flavonoid isolated from *Herba Epimedii*. They found that the developed targeting DDS could increase distribution of icaritin to the bone and enhance bone

formation in ovariectomized mice compared to the control group. In addition, other cases also indicated tissue-targeting DDS can enhance the therapeutic effects of loaded HRC on certain disease and, of course, proved changes of their tissue distribution indirectly [109–111].

Cells are the basic structures and functional units of organisms. Interfering with the physiological activities of pathological cells has become one of the means to treat diseases, especially in cancer therapy. Therefore, many cell-targeting DDS are developed to improve the bioactive HRC uptake into concerning cells. These attempts will change the distribution of loaded components between normal and diseased cells. Recognized as an anti-inflammation and anti-cancer agent, celastrol, an active constituent of *Tripterygium wilfordii* Hook. F., possesses the property of poor water solubility and target selectivity [112]. To surmount these challenges, Niemelä et al. designed sugar-decorated mesoporous silica nanoparticles (SDMSN) as vectors of celastrol and investigated the target-specific efficacy on induction of apoptosis of cancer cells. Consequently, the uptake of SDMSN in HeLa and A549 cancer cells was four and five times higher than mouse embryonic fibroblasts and shows no toxicity to normal cells [112]. As tumor cells extensively produce acidic metabolites and export acid to the extracellular space, these characteristics result in a peripheral acidic microenvironment around tumor cells [113]. Based on this feature of tumor cells, researchers have developed pH-sensitive DDS, and the loaded HRC release is facilitated in the acidic microenvironment of tumor, rather than normal cells, thereby changing the distribution of curative compounds and enhancing their target-specificity [114].

Organelles are fundamental structures of cells and keep cells working normally. Among them, mitochondria are very important organelles and their dysfunctions are linked with cancer, diabetes, and other diseases [115]. More and more attention has been attracted by mitochondria-mediated apoptosis of tumor cells, and researchers believe that this may be a promising approach in cancer therapy. Therefore, mitochondria-targeting DDS emerge at the right moment. Recently, glycyrrhetinic acid [116] and hypericin [117] functionalized graphene oxide carriers were reported to exhibit mitochondria-targeting property, improve mitochondrial permeability, and enhance the uptake of loaded drug into mitochondria.

6. Influence of Other Factors

Gender is a very important influence factor in drug metabolism, especially for women. The inter-gender pharmacokinetic alterations are mainly attributed to the differences of sex hormones secretion, the variety of intestinal and hepatic CYPs and transporters, the body fat percentage and the average body weight, plasma volume, and organ blood flow between male and female [118, 119]. These discrepancies have overall effects on drug ADME. Some reports indicate that women suffered high risk of adverse drug reaction in certain circumstances than men [118, 120]. Therefore, it is particularly important to study the sex-based impact on drug metabolism. Yang et al. [6] performed a study to investigate the gender-related differences of pharmacokinetics of diosbulbin B (DB) in rats. As a result, the female rats exhibited approximately 7 times higher oral absolute bioavailability of DB than male rats. Moreover, a bigger apparent volume of distribution (Vd), longer internal retention, and faster clearance were observed in female group after intravenous administration of DB. Xu et al. [9] explored the sex-related pharmacokinetic differences of *Schisandra* lignans after oral-dose of *Schisandra chinensis* extract in rats and found that female rats demonstrated a higher internal amount and slower elimination rate of focused compounds than male group. In detail, the $t_{1/2}$ of all the five marker ingredients, namely, schisandrin, schisandrol B, deoxyschisandrin, γ-schisandrin, and schisantherin A, was 2-9 times longer, along with 5-50 times higher C_{max} and $AUC_{0\text{-}t}$ of the tested compounds except schisantherin A, compared to those achieved in male rats. Nevertheless, it has been pointed out that gender difference did not significantly influence the pharmacokinetic parameters of paeoniflorin [121]. As the results showed above, the gender-related changes of pharmacokinetics seem to be unpredictable, so more attention is needed to explore the differences of herbal medicine applications between genders.

Age appears to be another influence factor of pharmacokinetics, for the age-related differences in gastric emptying rate, the concentration of serum proteins, and the activity levels of drug-metabolizing enzymes, as well as the function of liver and kidney [122, 123]. Specifically, children exhibit increased CL of certain drugs, while elders show the opposite trend. Meanwhile, elder people show decreased absorption rate and increased unbound drug concentration in plasma due to the slower gastric emptying and lower concentration of serum proteins than adults [122]. A population pharmacokinetic study suggested that the population estimate of the Vd of artesunate and dihydroartemisinin, two derivatives of artemisinin treating severe malaria, was higher in adults than children, but CL was not significantly changed [124]. Another population pharmacokinetic study concerning daikenchuto, a traditional Kampo used in Japan to treat various gastrointestinal complications, also revealed that age is an important index in drug metabolism [125]. In summary, dosage adjusting to different age is a vital issue during the drug treatment, and age-related pharmacokinetic changes should be taken into account.

Acupuncture is a traditional therapy and has been used in China for thousands of years. It is always applied by inserting thin needles into specific points, which is called “acupoints”, of the body of people being treated and then rolling the needles manually or simulating by electricity [126, 127]. Due to the oddity of its theory and operation method, it was considered to be a Chinese equivalent of voodoo decades ago [128]. Nevertheless, acupuncture is becoming a distinguished alternative therapy and being adopted in countries worldwide to treat chronic pain, osteoarthritis, asthma, rhinitis, heroin addiction, rheumatoid arthritis, etc. [127–129]. Moreover, acupuncture is the most popular alternative treatment in US fertility clinics for couples desiring fertility care [130]. Additionally, evidence shows that acupuncture can promote the release of several neuropeptides in the central nervous system

and demonstrate meaningful physiological effects [131]. In a word, acupuncture shows great potential therapeutic effect on certain body disorders. As acupuncture is an external stimulus, it can disturb the internal balance of the body and affect the metabolism of herbal medicines. Zhou et al. [132] reported that acupuncture could improve the absorption and reduce the elimination of baicalin in normal rats, and they found that stimulating specific acupoints, such as Jizhong (Du6), Dazhui (Du14), and Zhongwan (Ren12), was able to cause a bimodal phenomenon of the concentration-time course of baicalin. The synergistic effect on pharmacokinetics was also observed in combination with acupuncture at Zusanli (ST36) and oral administration of *Schisandra chinensis* in rats, as well as improving the target tissue distribution of three main lignans of *Schisandra chinensis*, namely, schisandrin, deoxyschisandrin, and schisandrin B, in comparison with the herb-alone treated group [4, 127]. All the published data above suggests that acupuncture seems to be able to decrease the required dosage of herbal medicines, thus economizing the total amount of herb consumption and reducing the possibility of adverse drug reactions.

7. Conclusion

According to evidence presented in this review, numerous factors like preliminary treatment, combination with drugs or herbs, pathological status, chemical or physical modifications, age, gender, and acupuncture will influence the pharmacokinetics of herbal medicines. In particular, as aging society is coming, the population of elder people with multiple health disorders and taking multiple medications is growing larger and larger. The occurrence of interactions between herbal medicines and drugs or internal body environment should be paid more attention particularly. Knowledge of factors affecting the pharmacokinetics of herbal medicines can lead to better guidance of their rational administration, whereas studies of these factors are mainly limited to animals at present and clinical research is lacking. Therefore, clinical research is required to focus in the future on elucidating and verifying the mechanism of the interactions between the influence factors and herbal medicines. The better knowledge of factors affecting the pharmacokinetics of herbal medicines we gain, the better guidance of their rational administration we can apply.

Conflicts of Interest

The authors declare that they have no conflicts of interest.

Acknowledgments

The authors sincerely appreciate the financial support from the National Natural Science Foundation of China (No: 81703678), Basic Scientific Research Projects of Colleges and Universities (LQ2017041), and the Scientific Research Project for Traditional Chinese Medicine of Henan Province (No: 2017ZY1001).

References

[1] D. Schuppan, J. I.-D. Jia, B. Brinkhaus, and E. G. Hahn, "Herbal products for liver diseases: a therapeutic challenge for the new millennium," *Hepatology*, vol. 30, no. 4, pp. 1099–1104, 1999.

[2] R. Liperoti, D. L. Vetrano, R. Bernabei, and G. Onder, "Herbal medications in cardiovascular medicine," *Journal of the American College of Cardiology*, vol. 69, no. 9, pp. 1188–1199, 2017.

[3] A. Tachjian, V. Maria, and A. Jahangir, "Use of herbal products and potential interactions in patients with cardiovascular diseases," *Journal of the American College of Cardiology*, vol. 55, no. 6, pp. 515–525, 2010.

[4] X. Wu, Y. Zhou, F. Yin et al., "Comparative pharmacokinetics and tissue distribution of schisandrin, deoxyschisandrin and schisandrin B in rats after combining acupuncture and herb medicine (schisandra chinensis)," *Biomedical Chromatography*, vol. 28, no. 8, pp. 1075–1083, 2014.

[5] M. D'Archivio, C. Filesi, R. Varì, B. Scazzocchio, and R. Masella, "Bioavailability of the polyphenols: Status and controversies," *International Journal of Molecular Sciences*, vol. 11, no. 4, pp. 1321–1342, 2010.

[6] B. Yang, X. Wang, W. Liu et al., "Gender-related pharmacokinetics and absolute bioavailability of diosbulbin B in rats determined by ultra-performance liquid chromatography-tandem mass spectrometry," *Journal of Ethnopharmacology*, vol. 149, no. 3, pp. 810–815, 2013.

[7] L. Zhou, J. Li, and C. Yan, "Simultaneous determination of three flavonoids and one coumarin by LC–MS/MS: Application to a comparative pharmacokinetic study in normal and arthritic rats after oral administration of Daphne genkwa extract," *Biomedical Chromatography*, vol. 32, no. 7, Article ID e4233, 2018.

[8] T. Yang, S. Liu, C.-H. Wang, Y.-Y. Tao, H. Zhou, and C.-H. Liu, "Comparative pharmacokinetic and tissue distribution profiles of four major bioactive components in normal and hepatic fibrosis rats after oral administration of Fuzheng Huayu recipe," *Journal of Pharmaceutical and Biomedical Analysis*, vol. 114, pp. 152–158, 2015.

[9] H. Xu, J. Gan, X. Liu et al., "Gender-dependent pharmacokinetics of lignans in rats after single and multiple oral administration of Schisandra chinensis extract," *Journal of Ethnopharmacology*, vol. 147, no. 1, pp. 224–231, 2013.

[10] S. Soleymani, R. Bahramsoltani, R. Rahimi, and M. Abdollahi, "Clinical risks of St John's Wort (Hypericum perforatum) co-administration," *Expert Opinion on Drug Metabolism & Toxicology*, vol. 13, no. 10, pp. 1047–1062, 2017.

[11] X. Tian, Z. Li, Y. Lin, M. Chen, G. Pan, and C. Huang, "Study on the PK profiles of magnoflorine and its potential interaction in Cortex phellodendri decoction by LC-MS/MS," *Analytical and Bioanalytical Chemistry*, vol. 406, no. 3, pp. 841–849, 2014.

[12] J. Ma, L. Zheng, T. Deng et al., "Stilbene glucoside inhibits the glucuronidation of emodin in rats through the down-regulation of UDP-glucuronosyltransferases 1A8: application to a drug–drug interaction study in Radix Polygoni Multiflori," *Journal of Ethnopharmacology*, vol. 147, no. 2, pp. 335–340, 2013.

[13] X.-B. Cui, X.-C. Qian, P. Huang et al., "Simultaneous determination of ten flavonoids of crude and wine-processed Radix Scutellariae aqueous extracts in rat plasma by UPLC-ESI-MS/MS and its application to a comparative pharmacokinetic study," *Biomedical Chromatography*, vol. 29, no. 7, pp. 1112–1123, 2015.

[14] Y. Tao, D. Su, W. Li, and B. Cai, "Pharmacokinetic comparisons of six components from raw and vinegar-processed Daphne

genkwa aqueous extracts following oral administration in rats by employing UHPLC–MS/MS approaches," *Journal of Chromatography B*, vol. 1079, pp. 34–40, 2018.

[15] Y. Cheng, Y. Zhang, H. Xing, K. Qian, L. Zhao, and X. Chen, "Comparative pharmacokinetics and bioavailability of three ephedrines in rat after oral administration of unprocessed and honey-fried ephedra extract by response surface experimental design," *Evidence-Based Complementary and Alternative Medicine*, vol. 2017, Article ID 2802193, 12 pages, 2017.

[16] Y. Tao, Y. Du, W. Li, and B. Cai, "Development and validation of an UHPLC–MS/MS approach for simultaneous quantification of five bioactive saponins in rat plasma: Application to a comparative pharmacokinetic study of aqueous extracts of raw and salt-processed Achyranthes bidentata," *Journal of Pharmaceutical and Biomedical Analysis*, vol. 151, pp. 164–169, 2018.

[17] W. Gu, J. C. Li, D. Ji et al., "Pharmacokinetic comparisons of typical constituents in curcumae rhizoma and vinegar-processed curcumae rhizoma after oral administration to rats," *Evidence-Based Complementary and Alternative Medicine*, vol. 2018, Article ID 6809497, 11 pages, 2018.

[18] R. Guo, H. Wu, X. Yu et al., "Simultaneous determination of seven anthraquinone aglycones of crude and processed semen cassiae extracts in rat plasma by UPLC-MS/MS and its application to a comparative pharmacokinetic study," *Molecules*, vol. 22, no. 11, Article ID 1803, 2017.

[19] Y. Zi-Min, C. Yue, G. Hui, L. Jia, C. Gui-Rong, and J. Wang, "Comparative pharmacokinetic profiles of three protoberberine-type alkaloids from raw and bile-processed Rhizoma coptidis in heat syndrome rats," *Pharmacognosy Magazine*, vol. 13, no. 49, pp. 51–57, 2017.

[20] Y. Tao, Y. Ren, W. Li et al., "Comparative pharmacokinetic analysis of extracts of crude and wine-processed Dipsacus asper in rats by a sensitive ultra performance liquid chromatography–tandem mass spectrometry approach," *Journal of Chromatography B*, vol. 1036-1037, pp. 33–41, 2016.

[21] C. L. Cui, X. He, C. L. Dong et al., "The enhancement mechanism of wine-processed Radix Scutellaria on NTG-induced migraine rats," *Biomedicine and Pharmacotherapy*, vol. 91, pp. 138–146, 2017.

[22] X.-C. Qian, L. Zhang, Y. Tao et al., "Simultaneous determination of ten alkaloids of crude and wine-processed Rhizoma Coptidis aqueous extracts in rat plasma by UHPLC-ESI-MS/MS and its application to a comparative pharmacokinetic study," *Journal of Pharmaceutical and Biomedical Analysis*, vol. 105, pp. 64–73, 2015.

[23] K. Liu, Y. Song, Y. Liu et al., "An integrated strategy using UPLC–QTOF-MSE and UPLC–QTOF-MRM (enhanced target) for pharmacokinetics study of wine processed Schisandra Chinensis fructus in rats," *Journal of Pharmaceutical and Biomedical Analysis*, vol. 139, pp. 165–178, 2017.

[24] T. Lei, D. Zhang, K. Guo et al., "Validated UPLC-MS/MS method for simultaneous quantification of eight saikosaponins in rat plasma: Application to a comparative pharmacokinetic study in depression rats after oral administration of extracts of raw and vinegar-baked Bupleuri Radix," *Journal of Chromatography B*, vol. 1060, pp. 231–239, 2017.

[25] C. Zhou, J. Wang, X. Zhang et al., "Investigation of the differences between the "Cold" and "Hot" nature of Coptis chinensis Franch and its processed materials based on animal's temperature tropism," *Science in China Series C: Life Sciences*, vol. 52, no. 11, pp. 1073–1080, 2009.

[26] W. L. T. Kan, B. Ma, and G. Lin, "Sulfur fumigation processing of traditional Chinese medicinal herbs: beneficial or detrimental?" *Frontiers in Pharmacology*, vol. 2, article 84, 2011.

[27] K. Cheng, H. Cai, X. Liu et al., "Evaluation of the influence of sulfur fumigation on the pharmacokinetics of four active ingredients in Si Wu Tang," *Journal of Separation Science*, vol. 38, no. 1, pp. 25–33, 2015.

[28] M. Kong, H. H. Liu, and J. Wu, "Effects of sulfur-fumigation on the pharmacokinetics, metabolites and analgesic activity of Radix Paeoniae Alba," *Journal of Ethnopharmacology*, vol. 212, pp. 95–105, 2018.

[29] Y. S. Cheng, C. Peng, F. Y. Wen, and H. Zhang, "Pharmacokinetic comparisons of typical constituents in white peony root and sulfur fumigated white peony root after oral administration to mice," *Journal of Ethnopharmacology*, vol. 129, no. 2, pp. 167–173, 2010.

[30] H. Zhi, Z. Li, Y. Deng et al., "Comparative in vivo constituents and pharmacokinetic study in rats after oral administration of ultrafine granular powder and traditional decoction slices of Chinese Salvia," *Biomedical Chromatography*, Article ID e4385, 2018.

[31] Y. Tao, S. Huang, G. Yang, W. Li, and B. Cai, "A simple and sensitive LC-MS/MS approach for simultaneous quantification of six bioactive compounds in rats following oral administration of aqueous extract and ultrafine powder of Astragalus propinquus: application to a comparative pharmacokinetic study," *Journal of Chromatography B*, vol. 1096, pp. 31–38, 2018.

[32] E. M. Alissa, "Medicinal herbs and therapeutic drugs interactions," *Therapeutic Drug Monitoring*, vol. 36, no. 4, pp. 413–422, 2014.

[33] S. Shi and U. Klotz, "Drug interactions with herbal medicines," *Clinical Pharmacokinetics*, vol. 51, no. 2, pp. 77–104, 2012.

[34] D. Singh, R. Gupta, and S. A. Saraf, "Herbs-are they safe enough? An overview," *Critical Reviews in Food Science and Nutrition*, vol. 52, no. 10, pp. 876–898, 2012.

[35] A. Di Minno, B. Frigerio, G. Spadarella et al., "Old and new oral anticoagulants: food, herbal medicines and drug interactions," *Blood Reviews*, vol. 31, no. 4, pp. 193–203, 2017.

[36] S. Yin, Y. Cheng, T. Li, M. Dong, H. Zhao, and G. Liu, "Effects of notoginsenoside R1 on CYP1A2, CYP2C11, CYP2D1, and CYP3A1/2 activities in rats by cocktail probe drugs," *Pharmaceutical Biology*, vol. 54, no. 2, pp. 231–236, 2016.

[37] J.-L. He, Z. W. Zhou, J.-J. Yin et al., "Schisandra chinensis regulates drug metabolizing enzymes and drug transporters via activation of Nrf2-mediated signaling pathway," *Drug Design, Development and Therapy*, vol. 9, pp. 127–146, 2015.

[38] Y. Liu, S. Liu, Y. Shi, M. Qin, Z. Sun, and G. Liu, "Effects of safflower injection on the pharmacodynamics and pharmacokinetics of warfarin in rats," *Xenobiotica*, vol. 48, no. 8, pp. 818–823, 2018.

[39] T. H. Kim, S. Shin, J. C. Shin et al., "Effect of sipjeondaebotang on the pharmacokinetics of S-1, an anticancer agent, in rats evaluated by population pharmacokinetic modeling," *Molecules*, vol. 22, no. 9, Article ID 1488, 2017.

[40] C.-M. Lu, M.-L. Hou, L.-C. Lin, and T.-H. Tsai, "Development of a microdialysis system to monitor lamivudine in blood and liver for the pharmacokinetic application in herbal drug interaction and the gene expression in rats," *Journal of Pharmaceutical and Biomedical Analysis*, vol. 96, pp. 231–240, 2014.

[41] C. T. Ting, Y.-Y. Cheng, and T. H. Tsai, "Herb-drug interaction between the traditional hepatoprotective formulation and

sorafenib on hepatotoxicity, histopathology and pharmacokinetics in rats," *Molecules*, vol. 22, no. 7, Article ID 1034, 2017.

[42] W. Ma, W. Wang, Y. Peng et al., "Ultra-high performance liquid chromatography with tandem mass spectrometry method for the simultaneous quantitation of five phthalides in rat plasma: application to a comparative pharmacokinetic study of Huo Luo Xiao Ling Dan and herb-pair extract," *Journal of Separation Science*, vol. 39, no. 11, pp. 2057–2067, 2016.

[43] X. Liu, H. Li, L. Wu et al., "Simultaneous quantification of chrysophanol and physcion in rat plasma by ultra fast liquid chromatography-tandem mass spectrometry and application of the technique to comparative pharmacokinetic studies of *Radix et Rhei Rhizoma* extract alone and Dahuang Fuzi Decoction," *Journal of Chromatography B*, vol. 980, pp. 88–93, 2015.

[44] Y. Liang, Y. Zhou, J. Zhang et al., "Pharmacokinetic compatibility of ginsenosides and Schisandra Lignans in Shengmai-san: from the perspective of p-glycoprotein," *PLoS ONE*, vol. 9, no. 6, Article ID e98797, 2014.

[45] J. Mu, X. Gao, Q. Li et al., "Vortex-ultrasound-assisted dispersive liquid–liquid microextraction coupled with gas chromatography–mass spectrometry for the analysis of volatile bioactive components and comparative pharmacokinetic study of the herb–herb interactions in Guanxin Shutong Capsule," *Journal of Separation Science*, vol. 40, no. 16, pp. 3267–3278, 2017.

[46] X.-J. Lai, L. Z. Zhang, J.-S. Li et al., "Comparative pharmacokinetic and bioavailability studies of three salvianolic acids after the administration of Salviae miltiorrhizae alone or with synthetical borneol in rats," *Fitoterapia*, vol. 82, no. 6, pp. 883–888, 2011.

[47] C. Gong, H. Yang, H. Wei, C. Qi, and C.-H. Wang, "Pharmacokinetic comparisons by UPLC-MS/MS of isomer paeoniflorin and albiflorin after oral administration decoctions of single-herb Radix Paeoniae Alba and Zengmian Yiliu prescription to rats," *Biomedical Chromatography*, vol. 29, no. 3, pp. 416–424, 2015.

[48] Y. Cui, T. Liu, Y. Zhang et al., "Simultaneous determination of five bioactive components of Gancao in rat plasma by UHPLC-MS/MS and its application to comparative pharmacokinetic study of incompatible herb pair Gansui-Gancao and Gansuibanxia Decoction," *Journal of Pharmaceutical and Biomedical Analysis*, vol. 159, pp. 318–325, 2018.

[49] B.-X. Xiao, Q. Wang, L.-Q. Fan, L.-T. Kong, S.-R. Guo, and Q. Chang, "Pharmacokinetic mechanism of enhancement by Radix Pueraria flavonoids on the hyperglycemic effects of Cortex Mori extract in rats," *Journal of Ethnopharmacology*, vol. 151, no. 2, pp. 846–851, 2014.

[50] P. Wei, Q.-F. Tang, H.-L. Huo et al., "Comparative pharmacokinetics of three phenylpropanoids in rat plasma after oral administration of Ramulus Cinnamomi and Ramulus Cinnamomi-Ephedrae Herba herb-couple extract," *Chinese Journal of Integrative Medicine*, pp. 1–7, 2017.

[51] Y. Ai, Y. Wu, F. Wang et al., "A UPLC-MS/MS method for simultaneous quantitation of three monoterpene glycosides and four alkaloids in rat plasma: Application to a comparative pharmacokinetic study of Huo Luo Xiao Ling Dan and single herb extract," *Journal of Mass Spectrometry*, vol. 50, no. 3, pp. 567–577, 2015.

[52] A. K. Kammalla, M. K. Ramasamy, J. Chintala, G. P. Dubey, A. Agrawal, and I. Kaliappan, "Comparative pharmacokinetic interactions of Quercetin and Rutin in rats after oral administration of European patented formulation containing Hippophae rhamnoides and Co-administration of Quercetin and Rutin," *European Journal of Drug Metabolism and Pharmacokinetics*, vol. 40, no. 3, pp. 277–284, 2015.

[53] C.-H. Xu, P. Wang, Y. Wang et al., "Pharmacokinetic comparisons of two different combinations of Shaoyao-Gancao Decoction in rats: competing mechanisms between paeoniflorin and glycyrrhetinic acid," *Journal of Ethnopharmacology*, vol. 149, no. 2, pp. 443–452, 2013.

[54] P.-Y. Hu, P.-F. Yue, Q. Zheng et al., "Pharmacokinetic comparative study of gastrodin after oral administration of Gastrodia elata Bl. extract and its compatibility with the different indigents of Ligusticum chuanxiong Hort. to rats," *Journal of Ethnopharmacology*, vol. 191, pp. 82–86, 2016.

[55] J. Shi, Q. Fu, W. Chen et al., "Comparative study of pharmacokinetics and tissue distribution of osthole in rats after oral administration of pure osthole and Libanotis buchtormensis supercritical extract," *Journal of Ethnopharmacology*, vol. 145, no. 1, pp. 25–31, 2013.

[56] C.-J. Lee, Y.-T. Wu, T. Y. Hsueh, L.-C. Lin, and T.-H. Tsai, "Pharmacokinetics and oral bioavailability of epimedin C after oral administration of epimedin C and Herba Epimedii extract in rats," *Biomedical Chromatography*, vol. 28, no. 5, pp. 630–636, 2014.

[57] M. Yang, X. Yang, J. An et al., "Comparative pharmacokinetic profiles of tectorigenin in rat plasma by UPLC-MS/MS after oral administration of Iris tectorum maxim extract and pure tectoridin," *Journal of Pharmaceutical and Biomedical Analysis*, vol. 114, pp. 34–41, 2015.

[58] L. Lu, D. Qian, J. Guo et al., "Abelmoschi Corolla non-flavonoid components altered the pharmacokinetic profile of its flavonoids in rat," *Journal of Ethnopharmacology*, vol. 148, no. 3, pp. 804–811, 2013.

[59] T. Wang, J. Xiao, H. Hou et al., "Development of an ultra-fast liquid chromatography–tandem mass spectrometry method for simultaneous determination of seven flavonoids in rat plasma: application to a comparative pharmacokinetic investigation of Ginkgo biloba extract and single pure ginkgo flavonoids after oral administration," *Journal of Chromatography B*, vol. 1060, pp. 173–181, 2017.

[60] M.-F. Zhang, Y. Zhao, K.-Y. Jiang et al., "Comparative pharmacokinetics study of sinomenine in rats after oral administration of sinomenine monomer and sinomenium acutum extract," *Molecules*, vol. 19, no. 8, pp. 12065–12077, 2014.

[61] X. Li, F. Du, W. Jia et al., "Simultaneous determination of eight Danshen polyphenols in rat plasma and its application to a comparative pharmacokinetic study of DanHong injection and Danshen injection," *Journal of Separation Science*, vol. 40, no. 7, pp. 1470–1481, 2017.

[62] J. Shen, J. Wang, E.-X. Shang et al., "The dosage-toxicity-efficacy relationship of kansui and licorice in malignant pleural effusion rats based on factor analysis," *Journal of Ethnopharmacology*, vol. 186, pp. 251–256, 2016.

[63] X. Zhang, Y. Wang, Q. Liang et al., "The correlation between chemical composition, as determined by UPLC-TOF-MS, and acute toxicity of Veratrum nigrum L. and Radix paeoniae alba," *Evidence-Based Complementary and Alternative Medicine*, vol. 2014, Article ID 892797, 13 pages, 2014.

[64] X. Zhou, V. Razmovski-Naumovski, D. Chang et al., "Synergistic effects of danshen (salvia miltiorrhiza radix et rhizoma) and sanqi (notoginseng radix et rhizoma) combination in inhibiting inflammation mediators in RAW264.7 cells," *BioMed Research International*, vol. 2016, Article ID 5758195, 12 pages, 2016.

[65] C. Wang, Q. Ren, X. T. Chen et al., "System pharmacology-based strategy to decode the synergistic mechanism of Zhi-zhu Wan for functional dyspepsia," *Frontiers in Pharmacology*, vol. 9, Article ID 841, 2018.

[66] Y. Wang, M. Zhao, H. Ye et al., "Comparative pharmacokinetic study of the main components of cortex fraxini after oral administration in normal and hyperuricemic rats," *Biomedical Chromatography*, vol. 31, no. 8, Article ID e3934, 2017.

[67] X.-K. Huo, B. Wang, L. Zheng et al., "Comparative pharmacokinetic study of baicalin and its metabolites after oral administration of baicalin and Chaiqin Qingning capsule in normal and febrile rats," *Journal of Chromatography B*, vol. 1059, pp. 14–20, 2017.

[68] Y. Wu, Y. Ai, F. Wang et al., "Simultaneous determination of four secoiridoid and iridoid glycosides in rat plasma by ultra performance liquid chromatography-tandem mass spectrometry and its application to a comparative pharmacokinetic study," *Biomedical Chromatography*, vol. 30, no. 2, pp. 97–104, 2016.

[69] B. Kamble, A. Gupta, I. Moothedath et al., "Effects of Gymnema sylvestre extract on the pharmacokinetics and pharmacodynamics of glimepiride in streptozotocin induced diabetic rats," *Chemico-Biological Interactions*, vol. 245, pp. 30–38, 2016.

[70] Y. Li, Y. Lu, J. Hu et al., "Pharmacokinetic comparison of scutellarin and paeoniflorin in sham-operated and middle cerebral artery occlusion ischemia and reperfusion injury rats after intravenous administration of xin-shao formula," *Molecules*, vol. 21, no. 9, Article ID 1191, 2016.

[71] J. Guan, X. Zhang, B. Feng et al., "Simultaneous determination of ferulic acid and gastrodin of Tianshu Capsule in rat plasma by ultra-fast liquid chromatography with tandem mass spectrometry and its application to a comparative pharmacokinetic study in normal and migraine rats," *Journal of Separation Science*, vol. 40, no. 21, pp. 4120–4127, 2017.

[72] X. Gao, J. Mu, S. Guan et al., "Simultaneous determination of phenolic acids and diterpenoids and their comparative pharmacokinetic study in normal and acute blood stasis rats by UFLC–MS/MS after oral administration of Guan-Xin-Shu-Tong capsules," *Journal of Chromatography B*, vol. 1072, pp. 221–228, 2018.

[73] W. Chen, J. Li, Z. Sun et al., "Comparative pharmacokinetics of six coumarins in normal and breast cancer bone-metastatic mice after oral administration of Wenshen Zhuanggu Formula," *Journal of Ethnopharmacology*, vol. 224, pp. 36–44, 2018.

[74] Y. Shi, C. Cao, Y. Zhu et al., "Comparative pharmacokinetic study of the components of Jia-Wei-Kai-Xin-San in normal and vascular dementia rats by ultra-fast liquid chromatography coupled with tandem mass spectrometry," *Journal of Separation Science*, vol. 41, no. 12, pp. 2504–2516, 2018.

[75] X. Wang, Y. Zhang, H. Niu et al., "Ultra-fast liquid chromatography with tandem mass spectrometry determination of eight bioactive components of Kai-Xin-San in rat plasma and its application to a comparative pharmacokinetic study in normal and Alzheimer's disease rats," *Journal of Separation Science*, vol. 40, no. 10, pp. 2131–2140, 2017.

[76] A. Schenk, A. Ghallab, U. Hofmann et al., "Physiologically-based modelling in mice suggests an aggravated loss of clearance capacity after toxic liver damage," *Scientific Reports*, vol. 7, no. 1, Article ID 6224, 2017.

[77] K. Thelen and J. B. Dressman, "Cytochrome P450-mediated metabolism in the human gut wall," *Journal of Pharmacy and Pharmacology*, vol. 61, no. 5, pp. 541–558, 2009.

[78] Z. Zhang, X. Liang, M. Su et al., "Pharmacokinetics of dl-praeruptorin A after single-dose intravenous administration to rats with liver cirrhosis," *DARU Journal of Pharmaceutical Sciences*, vol. 19, no. 3, pp. 210–215, 2011.

[79] S. Sun, Z.-S. Xie, E.-H. Liu, Y.-T. Yan, X.-J. Xu, and P. Li, "Chemical profiling of Jinqi Jiangtang tablets by HPLC-ESI-Q-TOF/MS," *Chinese Journal of Natural Medicines*, vol. 12, no. 3, pp. 229–240, 2014.

[80] X.-Y. Wei, J.-H. Tao, X. Cui, S. Jiang, D.-W. Qian, and J.-A. Duan, "Comparative pharmacokinetics of six major bioactive components in normal and type 2 diabetic rats after oral administration of Sanhuang Xiexin Decoction extracts by UPLC-TQ MS/MS," *Journal of Chromatography B*, vol. 1061-1062, pp. 248–255, 2017.

[81] X. Zhang, L. Wang, Z. Zheng, Z. Pi, Z. Liu, and F. Song, "Online microdialysis-ultra performance liquid chromatography–mass spectrometry method for comparative pharmacokinetic investigation on iridoids from Gardenia jasminoides Ellis in rats with different progressions of type 2 diabetic complications," *Journal of Pharmaceutical and Biomedical Analysis*, vol. 140, pp. 146–154, 2017.

[82] B. B. Wei, Z. X. Chen, M. Y. Liu, and M. J. Wei, "Development of a UPLC-MS/MS method for simultaneous determination of six flavonoids in rat plasma after administration of maydis stigma extract and its application to a comparative pharmacokinetic study in normal and diabetic rats," *Molecules*, vol. 22, no. 8, Article ID 1267, 2017.

[83] C. Yang, Q. Wang, S. Yang, Q. Yang, and Y. Wei, "An LC–MS/MS method for quantitation of cyanidin-3-O-glucoside in rat plasma: Application to a comparative pharmacokinetic study in normal and streptozotocin-induced diabetic rats," *Biomedical Chromatography*, vol. 32, no. 2, Article ID e4042, 2018.

[84] L. Yu, H. F. Wan, C. Li et al., "Pharmacokinetics of active components from guhong injection in normal and pathological rat models of cerebral ischemia: a comparative study," *Frontiers in Pharmacology*, vol. 9, Article ID 493, 2018.

[85] S. Chen, M. Li, Y. Li et al., "A UPLC-ESI-MS/MS method for simultaneous quantitation of chlorogenic acid, scutellarin, and scutellarein in rat plasma: application to a comparative pharmacokinetic study in sham-operated and MCAO rats after oral administration of erigeron breviscapus extract," *Molecules*, vol. 23, no. 7, Article ID 1808, 2018.

[86] X. Zhao, T. Ma, C. Zhang et al., "Simultaneous determination of senkyunolide I and senkyunolide H in rat plasma by LC-MS: Application to a comparative pharmacokinetic study in normal and migrainous rats after oral administration of Chuanxiong Rhizoma extract," *Biomedical Chromatography*, vol. 29, no. 9, pp. 1297–1303, 2015.

[87] B. V. Bonifacio, P. B. Silva, M. A. Ramos et al., "Nanotechnology-based drug delivery systems and herbal medicines: a review," *International Journal of Nanomedicine*, vol. 9, pp. 1–15, 2014.

[88] M. Chen, S. Wang, M. Tan, and Y. Wang, "Applications of nanoparticles in herbal medicine: Zedoary turmeric oil and its active compound β-elemene," *American Journal of Chinese Medicine*, vol. 39, no. 6, pp. 1093–1102, 2011.

[89] R. Watkins, L. Wu, C. Zhang, R. M. Davis, and B. Xu, "Natural product-based nanomedicine: recent advances and issues," *International Journal of Nanomedicine*, vol. 10, pp. 6055–6074, 2015.

[90] M. Namdari, A. Eatemadi, M. Soleimaninejad, and A. T. Hammed, "A brief review on the application of nanoparticle

enclosed herbal medicine for the treatment of infective endocarditis," *Biomedicine & Pharmacotherapy*, vol. 87, pp. 321–331, 2017.

[91] S. Wang, R. Su, S. Nie et al., "Application of nanotechnology in improving bioavailability and bioactivity of diet-derived phytochemicals," *The Journal of Nutritional Biochemistry*, vol. 25, no. 4, pp. 363–376, 2014.

[92] Y. Tsai, W. Jan, C. Chien, W. Lee, L. Lin, and T. Tsai, "Optimised nano-formulation on the bioavailability of hydrophobic polyphenol, curcumin, in freely-moving rats," *Food Chemistry*, vol. 127, no. 3, pp. 918–925, 2011.

[93] L. Zou, F. Chen, J. Bao et al., "Preparation, characterization, and anticancer efficacy of evodiamine-loaded PLGA nanoparticles," *Drug Delivery*, vol. 23, no. 3, pp. 908–916, 2016.

[94] Y.-Y. Wu, J.-H. Zhang, J.-H. Gao, and Y.-S. Li, "Aloe-emodin (AE) nanoparticles suppresses proliferation and induces apoptosis in human lung squamous carcinoma via ROS generation in vitro and in vivo," *Biochemical and Biophysical Research Communications*, vol. 490, no. 3, pp. 601–607, 2017.

[95] F. Y. Siu, S. Ye, H. Lin, and S. Li, "Galactosylated PLGA nanoparticles for the oral delivery of resveratrol: enhanced bioavailability and in vitro anti-inflammatory activity," *International Journal of Nanomedicine*, vol. 13, pp. 4133–4144, 2018.

[96] Y. Cai, W. Zhang, Z. Chen, Z. Shi, C. He, and M. Chen, "Recent insights into the biological activities and drug delivery systems of tanshinones," *International Journal of Nanomedicine*, vol. 11, pp. 121–130, 2016.

[97] N. Chouhan, V. Mittal, D. Kaushik, A. Khatkar, and M. Raina, "Self emulsifying drug delivery system (SEDDS) for phytoconstituents: a review," *Current Drug Delivery*, vol. 12, no. 2, pp. 244–253, 2015.

[98] R. Guo, X. Guo, X. Hu et al., "Fabrication and optimization of self-microemulsions to improve the oral bioavailability of total flavones of Hippophaë rhamnoides L," *Journal of Food Science*, vol. 82, no. 12, pp. 2901–2909, 2017.

[99] Z. Ke, X. Hou, and X.-B. Jia, "Design and optimization of self-nanoemulsifying drug delivery systems for improved bioavailability of cyclovirobuxine D," *Drug Design, Development and Therapy*, vol. 10, pp. 2049–2060, 2016.

[100] L. J. Wei, N. Marasinib, G. Li et al., "Development of ligustrazine-loaded lipid emulsion: formulation optimization, characterization and biodistribution," *International Journal of Pharmaceutics*, vol. 437, no. 1-2, pp. 203–212, 2012.

[101] H. Ma, Q. Zhao, Y. Wang et al., "Design and evaluation of self-emulsifying drug delivery systems of Rhizoma corydalis decumbentis extracts," *Drug Development and Industrial Pharmacy*, vol. 38, no. 10, pp. 1200–1206, 2012.

[102] X. Lu, M. Fang, Y. Dai et al., "Quantification of triacontanol and its PEGylated prodrug in rat plasma by GC-MS/MS: application to a pre-clinical pharmacokinetic study," *Journal of Chromatography B*, vol. 1089, pp. 8–15, 2018.

[103] P. Esposito, L. Barbero, P. Caccia et al., "PEGylation of growth hormone-releasing hormone (GRF) analogues," *Advanced Drug Delivery Reviews*, vol. 55, no. 10, pp. 1279–1291, 2003.

[104] G. Pasut and F. M. Veronese, "State of the art in PEGylation: the great versatility achieved after forty years of research," *Journal of Controlled Release*, vol. 161, no. 2, pp. 461–472, 2012.

[105] X. Lin, Z.-J. Wang, F. Huang et al., "Long-circulating delivery of bioactive polysaccharide from radix ophiopogonis by PEGylation.," *International Journal of Nanomedicine*, vol. 6, pp. 2865–2872, 2011.

[106] J. Huang, Y. Liu, X. Li et al., "Comparative pharmacokinetic profiles of five poorly soluble pulchinenosides in different formulations from Pulsatilla chinensis saponins extracts for enhanced bioavailability," *Biomedical Chromatography*, vol. 29, no. 12, pp. 1885–1892, 2015.

[107] T. Chen, C. Li, Y. Li, X. Yi, S. M.-Y. Lee, and Y. Zheng, "Oral delivery of a nanocrystal formulation of schisantherin a with improved bioavailability and brain delivery for the treatment of Parkinson's disease," *Molecular Pharmaceutics*, vol. 13, no. 11, pp. 3864–3875, 2016.

[108] L. Huang, X. Wang, H. Cao et al., "A bone-targeting delivery system carrying osteogenic phytomolecule icaritin prevents osteoporosis in mice," *Biomaterials*, vol. 182, pp. 58–71, 2018.

[109] H. Wu, T. Yu, Y. Tian, Y. Wang, R. Zhao, and S. Mao, "Enhanced liver-targeting via coadministration of 10-Hydroxycamptothecin polymeric micelles with vinegar baked Radix Bupleuri," *Phytomedicine*, vol. 44, pp. 1–8, 2018.

[110] S. Yum, S. Jeong, S. Lee et al., "Colon-targeted delivery of piceatannol enhances anti-colitic effects of the natural product: Potential molecular mechanisms for therapeutic enhancement," *Drug Design, Development and Therapy*, vol. 9, pp. 4247–4258, 2015.

[111] J. H. Park, H. A. Kim, J. H. Park, and M. Lee, "Amphiphilic peptide carrier for the combined delivery of curcumin and plasmid DNA into the lungs," *Biomaterials*, vol. 33, no. 27, pp. 6542–6550, 2012.

[112] E. Niemelä, D. Desai, Y. Nkizinkiko, J. E. Eriksson, and J. M. Rosenholm, "Sugar-decorated mesoporous silica nanoparticles as delivery vehicles for the poorly soluble drug celastrol enables targeted induction of apoptosis in cancer cells," *European Journal of Pharmaceutics and Biopharmaceutics*, vol. 96, pp. 11–21, 2015.

[113] I. Böhme and A. K. Bosserhoff, "Acidic tumor microenvironment in human melanoma," *Pigment Cell & Melanoma Research*, vol. 29, no. 5, pp. 508–523, 2016.

[114] X. Wang, F. Wu, G. Li et al., "Lipid-modified cell-penetrating peptide-based self-assembly micelles for co-delivery of narciclasine and siULK1 in hepatocellular carcinoma therapy," *Acta Biomaterialia*, vol. 74, pp. 414–429, 2018.

[115] L. Saso and O. Firuzi, "Pharmacological applications of antioxidants: lights and shadows," *Current Drug Targets*, vol. 15, no. 13, pp. 1177–1199, 2014.

[116] C. Zhang, Z. Liu, Y. Zheng et al., "Glycyrrhetinic acid functionalized graphene oxide for mitochondria targeting and cancer treatment in vivo," *Small*, vol. 14, no. 4, Article ID 1703306, 2018.

[117] C. Han, C. Zhang, T. Ma et al., "Hypericin-functionalized graphene oxide for enhanced mitochondria-targeting and synergistic anticancer effect," *Acta Biomaterialia*, vol. 77, pp. 268–281, 2018.

[118] M. Gandhi, F. Aweeka, R. M. Greenblatt, and T. F. Blaschke, "Sex Differences in Pharmacokinetics and Pharmacodynamics," *Annual Review of Pharmacology and Toxicology*, vol. 44, pp. 499–523, 2004.

[119] F. Hu, J. An, W. Li et al., "UPLC-MS/MS determination and gender-related pharmacokinetic study of five active ingredients in rat plasma after oral administration of Eucommia cortex extract," *Journal of Ethnopharmacology*, vol. 169, pp. 145–155, 2015.

[120] R. G. Ulrich, "Idiosyncratic toxicity: a convergence of risk factors," *Annual Review of Medicine*, vol. 58, pp. 17–34, 2007.

[121] Y.-H. Hwang, T. Kim, W.-K. Cho, D. Jang, J.-H. Ha, and J. Y. Ma, "Food- and gender-dependent pharmacokinetics of

paeoniflorin after oral administration with Samul-tang in rats," *Journal of Ethnopharmacology*, vol. 142, no. 1, pp. 161–167, 2012.

[122] C. J. Landmark, S. I. Johannessen, and T. Tomson, "Host factors affecting antiepileptic drug delivery—pharmacokinetic variability," *Advanced Drug Delivery Reviews*, vol. 64, no. 10, pp. 896–910, 2012.

[123] H. Soraoka, K. Oniki, K. Matsuda et al., "The effect of Yokukansan, a traditional herbal preparation used for the behavioral and psychological symptoms of dementia, on the drug-metabolizing enzyme activities in healthy male volunteers," *Biological & Pharmaceutical Bulletin*, vol. 39, no. 9, pp. 1468–1474, 2016.

[124] J. A. Simpson, T. Agbenyega, K. I. Barnes et al., "Population pharmacokinetics of artesunate and dihydroartemisinin following intra-rectal dosing of artesunate in malaria patients," *PLoS Medicine*, vol. 11, no. 3, Article ID e444, 2006.

[125] M. Munekage, K. Ichikawa, H. Kitagawa et al., "Population pharmacokinetic analysis of daikenchuto, a traditional Japanese medicine (kampo) in Japanese and US health volunteers," *Drug Metabolism and Disposition*, vol. 41, no. 6, pp. 1256–1263, 2013.

[126] L. Cavalli, L. Briscese, T. Cavalli, P. Andre, and M. C. Carboncini, "Role of acupuncture in the management of severe acquired brain injuries (sABIs)," *Evidence-Based Complementary and Alternative Medicine*, vol. 2018, Article ID 8107508, 10 pages, 2018.

[127] D. Ji, Z. Ning, C. Mao et al., "Effects of acupuncture at ST36 on pharmacokinetics of Schisandra lignans in rats," *Acupuncture in Medicine*, vol. 33, no. 3, pp. 223–229, 2015.

[128] T. J. Kaptchuk, "Acupuncture: theory, efficacy, and practice," *Annals of Internal Medicine*, vol. 136, no. 5, pp. 374–383, 2002.

[129] F. Zhang, J. Ma, Y. Lu et al., "Acupuncture combined with curcumin attenuates carbon tetrachloride-induced hepatic fibrosis in rats," *Acupuncture in Medicine*, vol. 30, no. 2, pp. 132–138, 2012.

[130] E. Manheimer, D. van derWindt, K. Cheng et al., "The effects of acupuncture on rates of clinical pregnancy among women undergoing in vitro fertilization: a systematic review and meta-analysis," *Human Reproduction Update*, vol. 19, no. 6, pp. 696–713, 2013.

[131] J. S. Han, "Acupuncture: neuropeptide release produced by electrical stimulation of different frequencies," *Trends in Neurosciences*, vol. 26, no. 1, pp. 17–22, 2003.

[132] J. Zhou, F. Qu, E. Burrows, Y. Yu, and R. Nan, "Acupuncture can improve absorption of baicalin from extracts of Scutellaria baicalensis Georgi in rats," *Phytotherapy Research*, vol. 23, no. 10, pp. 1415–1420, 2009.

Hindawi
Evidence-Based Complementary and Alternative Medicine
Volume 2019, Article ID 4016323, 9 pages
https://doi.org/10.1155/2019/4016323

Research Article

Evidence on Integrating Pharmacokinetics to Find Truly Therapeutic Agent for Alzheimer's Disease: Comparative Pharmacokinetics and Disposition Kinetics Profiles of Stereoisomers Isorhynchophylline and Rhynchophylline in Rats

Chunyuan Zhang,[1] **Xu Wu**,[1,2] **Yanfang Xian**,[1] **Lin Zhu**,[3] **Ge Lin**,[3] **and Zhi-Xiu Lin**[1]

[1]*School of Chinese Medicine, Faculty of Medicine, The Chinese University of Hong Kong, Hong Kong SAR, Hong Kong*
[2]*Laboratory of Molecular Pharmacology, Department of Pharmacology, School of Pharmacy, Southwest Medical University, Luzhou 646000, Sichuan, China*
[3]*School of Biomedical Sciences, Faculty of Medicine, The Chinese University of Hong Kong, Hong Kong SAR, Hong Kong*

Correspondence should be addressed to Ge Lin; linge@cuhk.edu.hk and Zhi-Xiu Lin; linzx@cuhk.edu.hk

Chunyuan Zhang and Xu Wu contributed equally to this work.

Received 27 September 2018; Revised 4 December 2018; Accepted 9 January 2019; Published 3 February 2019

Guest Editor: Yong Ai

Isorhynchophylline (IRN) and rhynchophylline (RN), a pair of stereoisomers, are tetracyclic oxindole alkaloids isolated from *Uncaria rhynchophylla*, a commonly used Chinese medicinal herb. These two compounds have drawn extensive attention due to their potent neuroprotective effects with promising therapeutic potential for the treatment of Alzheimer's disease (AD). However, IRN and RN can interconvert into each other *in vivo* after oral administration. The present study aimed to elucidate the pharmacokinetic profiles and disposition kinetics of the administered and generated stereoisomers in the brain and cerebrospinal fluid (CSF) after oral administration of equal dose of IRN or RN to rats. Our study demonstrated that after oral administration, RN showed significantly higher systemic exposure (6.5 folds of IRN, $p < 0.001$) and disposition in the brain (2.5 folds of IRN, $p < 0.01$) and CSF (3 folds of IRN, $p < 0.001$) than IRN. The results indicated that interconversion between IRN and RN occurred. Notably, regardless of the orally administered IRN or RN, RN would always be one of the major or predominant forms present in the body. Our results provided sound evidence supporting further development of RN as a potential therapeutic agent for the treatment of AD. Moreover, the present study sets a solid example that integrating pharmacokinetics is crucial to identify the truly therapeutic agent.

1. Introduction

Alzheimer's disease (AD) is the most common form of neurodegenerative disease in the elderly population [1, 2]. Alkaloids-containing herbal extracts have been widely used as therapeutic agents in traditional medicine for thousands of years [3]. The use of naturally occurring alkaloids as therapeutic agents for AD treatment has drawn extensive attention, and the U.S. Food and Drug Administration has recently approved two alkaloids, i.e., galantamine and rivastigmine, which act as cholinesterase inhibitors, for the treatment of AD [4, 5].

Uncaria rhynchophylla (Gou-Teng in Chinese) has been demonstrated as a promising herbal medicine for the treatment of AD. The extract of *U. rhynchophylla* has been reported to have potent antiaggregation effects on amyloid-β proteins [6] and was demonstrated to improve cognitive deficits induced by D-galactose in mice [7]. The major active components in *U. rhynchophylla* have been revealed to be oxindole alkaloids. Isorhynchophylline (IRN) and rhynchophylline (RN) (Figure 1) are tetracyclic oxindole alkaloids accounting for more than 43% of the total alkaloid content in *U. rhynchophylla* [8] and have been regarded as the major pharmacologically active components in the

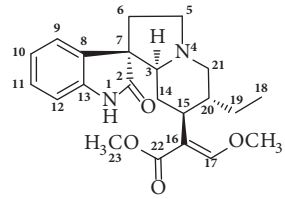

IRN

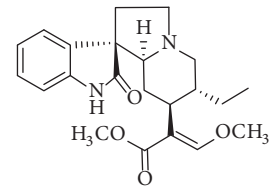

RN

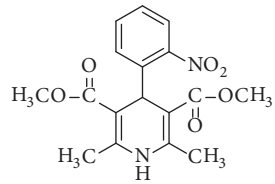

Nifedipine

Figure 1: Chemical structures of isorhynchophylline (IRN), rhynchophylline (RN) and nifedipine (internal standard, IS).

herb [9–11]. Investigations of the pharmacological effects of IRN and RN have revealed that they could exert beneficial effects on AD. Recent studies conducted by our group have indicated that IRN could rescue PC12 cells from amyloid-β-induced apoptosis [12] and also exhibited neuroprotective effect in amyloid-β-treated PC12 cells [13]. Both IRN and RN were able to exert neuroprotective effect by protecting amyloid-β-treated PC12 cells from cell death [14]. Furthermore, IRN could ameliorate cognitive deficits, enhance the antioxidative status, and reduce inflammation via inhibition of the NF-κB signaling pathway in the brain tissues of the D-galactose-induced mice [15]. IRN was also able to improve cognitive deficits via the inhibition of neuronal apoptosis and tau protein hyperphosphorylation in the hippocampus of the amyloid-β-treated rats [16]. More recently, other research groups identified RN as an inhibitor of tyrosine kinase EphA4 receptor and demonstrated that RN could restore the synaptic impairment in the transgenic mouse models of AD [17] and could ameliorate amyloid-β-induced perturbation of hippocampal CA1 neuronal activity [18].

Because both IRN and RN are promising candidates for further development into therapeutic agents for AD, understanding their disposition kinetics in the brain and cerebrospinal fluid (CSF) and plasma levels of IRN and RN is important. In addition, IRN and RN are a pair of stereoisomers at C7 chiral position. Interconversion between IRN and RN was firstly discovered by Wenkert et al. in 1959 [19], and this phenomenon has been observed both *in vitro* and *in vivo* [20–29]. It is worth noting that stereoconfiguration at C7 position of IRN and RN may lead to differences in their pharmacokinetics. Therefore, knowledge of the difference in pharmacokinetic profiles and disposition kinetics of IRN and RN and the epimerization between them is critical for further development of their therapeutic usage. However, previous pharmacokinetic studies on IRN and RN were only conducted separately [20–22]. The most recent stereoselective pharmacokinetic study on IRN and RN failed to reveal the disposition kinetics in the brain and the pharmacokinetic profiles of generated stereoisomers [27, 29]. In the present study, we aimed to elucidate the kinetic profiles of the orally administered and metabolically generated stereoisomers in the brain, CSF, and plasma of rats via studying in parallel both IRN and RN.

2. Materials and Methods

2.1. Chemicals and Reagents. IRN (purity ≥ 98%) and RN (purity ≥ 98%) were purchased from Chengdu Mansite Pharmaceutical Co. Ltd. (Chengdu, Sichuan, China). Nifedipine (purity ≥ 98%), used as internal standard (IS, Figure 1), was purchased from Sigma-Aldrich Chemical Co. (St. Louis, MO, US). Heparin and Tween 80 were purchased from Sigma-Aldrich Chemical Co. (St. Louis, MO, US). Acetonitrile of HPLC grade was obtained from Duksan Pure Chemicals (South Korea). All other compounds and reagents not listed were of analytical grade.

2.2. Investigation of the Kinetic Profiles of Administered and Generated Stereoisomers in the Brain, CSF, and Plasma of the Rats. Male Sprague-Dawley (SD) rats were provided by the Laboratory Animal Service Center of The Chinese University of Hong Kong, Hong Kong, China. Animals were housed in cages during the study period under standard conditions of temperature, humidity, and light. All animal experiments were approved by the Animal Ethics Committee of The Chinese University of Hong Kong.

One day before the experiment, the male SD rats (160-200 g) were fasted overnight with free access to water. On the following day, the rats were randomly divided into two groups (n = 18 per group) for oral administration of either IRN or RN at a dosage of 20 mg/kg. The dosage was the same as used in the previous pharmacodynamics studies [15, 16]. The suspension solutions of IRN and RN were prepared in 5% Tween 80, respectively. The SD rats in the two groups

were orally administered at a dose of 20 mg/kg IRN or RN and sacrificed at 15, 30, 60, 90, 120, and 180 min postdosing (n = 3 per time interval). The rats were exsanguinated by cardiac puncture under anesthesia, followed by collecting their CSF (about 100 μL) through a single puncture in the cisterna magna. Plasma was obtained by centrifugation of blood at 6,000 × g for 8 min at 4°C. After blood collection, the animals were perfused transcardially with normal saline until total blood volume was removed. Then, the whole brain was promptly collected, and the surface water was blotted dry with Kimwipes (Kimberly-Clark™). Blood vessels and meninges were carefully removed with forceps and the brain was weighted. All samples were stored at −20°C until analysis.

2.3. Brain, CSF, and Plasma Sample Preparations. Brain homogenate was freshly prepared by homogenizing brain tissues in normal saline (1:2, w/v). Homogenization was conducted in an ice bath using the IKA T10 basic ULTRA-TURRAX Homogenizer for 20–30 s.

The biological samples including brain homogenate, CSF, and plasma (50 μL each) were deproteinized by adding 150 μL of acetonitrile (containing 20 ng/mL IS). After vortex mixing for 1 min, the mixture was centrifuged (20,000 × g) for 10 min at 4°C. After centrifugation, an aliquot (5 μL) of supernatant was subjected to the LC-MS/MS analysis.

2.4. Quantitation of IRN and RN in Various Biological Samples by LC-MS/MS. Quantitation of IRN and RN in biological samples was performed on an Agilent 1290 Infinity LC system coupled with an Agilent 6460 Triple Quad tandem mass spectrometry with an ESI interface system (Agilent Technologies Inc., US). The chromatographic separation was achieved on ZORBAX Eclipse Plus C18 column (2.1 × 100 mm, 1.8 μm, Agilent) maintained at 40°C temperature at a flow rate of 0.3 mL/min. A gradient mobile phase consisting of 0.1% formic acid in acetonitrile (A) and 0.1% formic acid in water (B) was eluted as follows: 0–1 min, A, 15–20%; 1–5 min, A, 20–25%; 5–7 min, A, 25–95%; 7–10 min, A held at 95% and returned to the initial condition (acetonitrile-water ratio 15 : 85) for a 3 min equilibration. The temperature of the autosampler was kept at 4°C.

The MS/MS system was operated in positive mode and multiple reaction monitoring (MRM) mode under the following operation parameters: gas temperature, 300°C; gas flow, 5 L/min; nebulizer gas, 45 psi; capillary voltage, 3500 V; Fragmentor, 150 V (for IRN and RN), 76 V (for IS); cell accelerator, 4 V; Dwell, 80 ms. IRN and RN were monitored at the *m/z* 385 ($[M+H]^+$) to *m/z* 160 ($[M+H-225]^+$) transition and the IS at the *m/z* 347 ($[M+H]^+$) to *m/z* 315 ($[M+H-32]^+$) transition. All the data were processed using Agilent MassHunter Workstation Software Quantitative Analysis Version B.07.00/Build 7.0.457.0 (Agilent).

2.5. Data Analysis. Kinetic parameters were calculated using the WinNonlin software (Version 4.0, Pharsight Corp, Mountain View, CA, US) employing a noncompartmental model approach. Epimerization ratio was calculated by $AUC_{(\text{generated stereoisomer})}/(AUC_{(\text{generated stereoisomer})} + AUC_{(\text{administered stereoisomer})}) \times 100\%$. The brain-to-plasma partition coefficient (K_p, Brain) was calculated by AUC_{Brain}/AUC_{Plasma}, and the CSF-to-plasma partition coefficient (K_p, CSF) was calculated by AUC_{CSF}/AUC_{Plasma}.

All the data in the study were expressed as mean ± SEM. Statistical analyses were performed using GraphPad Prism 6.0 (GraphPad Software Inc, San Diego, CA, US) using two tailed unpaired *t*-test for two groups comparison. Statistical significance was set at p value less than 0.05.

3. Results

3.1. Disposition Kinetics of Administered Stereoisomers in the Rat Brain, CSF, and Plasma. The developed LC-MS/MS method that could separate the stereoisomers IRN and RN was successfully applied for the quantitation of both stereoisomers in all collected biological specimens. The typical MRM chromatograms of the blank biological specimen, blank biological specimen spiked with both analytes and samples obtained after oral administration of IRN or RN were shown in the supplementary data. The MRM chromatograms of blank plasma, brain tissues, and CSF (Figure S1) did not show any interfering peaks or signal at the retention times of the target analytes IRN (4.59 min) and RN (5.44 min). The calibration curves were generated by plotting the peak area ratio of IRN or RN to IS against the concentration of IRN or RN. The regression equations, linearity ranges, and correlation coefficients for individual standard curves are summarized in Table 1. The mean concentration-time profiles of administered and generated stereoisomers in the rat plasma, brain, and CSF after oral administration of IRN or RN at 20 mg/kg were obtained (Figures 2 and 3), and kinetic parameters were determined (Table 2).

The results showed that, after oral administration of equal dosage of IRN or RN, both rapidly reached their peak concentration in plasma at 30 min (Figure 2(a)), while the absorption and systemic exposure of the administered RN (C_{max}: 190.87 ± 6.34 ng/mL; AUC_{Plasma}: 16382.06 ± 269.22 ng·min/mL) were significantly higher than those of the administered IRN (C_{max}: 31.29 ± 1.59 ng/mL; AUC_{Plasma}: 2483.43 ± 83.83 ng·min/mL). On the other hand, the elimination of IRN was significantly faster than that of RN ($t_{1/2}$: 64.31 ± 3.19 min *vs.* 129.53 ± 9.30, $p < 0.01$) (Figure 2(a) and Table 2). Similarly, the overall brain exposure of RN (AUC_{Brain}: 1587.03 ± 127.82 ng·min/g and C_{max}: 16.96 ± 1.92 ng/mL) was also significantly higher than IRN (AUC_{Brain}: 627.37 ± 43.31 ng·min/g and C_{max}: 7.35 ± 0.74 ng/mL) (Figure 2(b) and Table 2). Moreover, RN also had significantly greater exposure in CSF, with AUC_{CSF} and C_{max} being more than 3-fold of those of IRN ($p < 0.001$) (Figure 2(c) and Table 2).

All the findings revealed that after oral administration of IRN or RN at the same dose, the systemic exposure of RN was significantly higher (about 6.5-fold, $p < 0.001$) than that of IRN due to its significantly greater oral absorption and slower clearance. Consequently, the higher plasma concentrations of RN also resulted in significantly higher exposure in both brain and CSF when comparing with that of IRN ($p < 0.01$).

3.2. Epimerization and Disposition Kinetics of Generated Stereoisomers in the Rat Brain, CSF, and Plasma. After

Table 1: Regression equations, linearity ranges, and correlation coefficients of the calibration curves.

Analyte	Biological specimen	Regression equation	Linear ranges (ng/mL)	Correlation coefficient
IRN	Brain	$y = 0.2100x + 0.0016$	0.1–5.0	0.9996
	CSF	$y = 0.3187x + 0.0042$	0.1–5.0	0.9994
	Plasma	$y = 0.7395x - 0.0137$	1.0–50.0	0.9991
RN	Brain	$y = 1.5308x + 0.0081$	0.5–10.0	0.9992
		$y = 1.5308x + 0.0081$	0.1–5.0	0.9991
	CSF	$y = 1.3104x - 0.0124$	0.5–10.0	0.9994
		$y = 1.3029x - 0.0002$	0.1–5.0	0.9991
	Plasma	$y = 1.4469x - 0.2262$	25.0–500.0	0.9992
		$y = 0.6529x + 0.1385$	1.0–50.0	0.9996

oral administration of the same dose, at least 47% of the administered IRN were metabolically converted to RN and then distributed into plasma (47.54 ± 0.22%), brain (32.21 ± 1.22%), and CSF (43.09 ± 0.92%) (Figures 3(a), 3(b), and 3(c) and Table 2). The systemic exposure of the administered IRN and generated RN in plasma was similar (epimerization ratio: 47.54 ± 0.22%), while the exposure in the brain (AUC_{Brain}) and CSF (AUC_{CSF}) of the generated RN was about half of the administered IRN. Whereas, after oral administration of RN, significantly less conversion to IRN occurred and approximately 2.20%, 8.23%, and 16.91% of the generated IRN were found in the plasma, brain, and CSF, respectively (Figures 3(d), 3(e), and 3(f) and Table 2). The results demonstrated that after oral administration of the same dosage of IRN or RN, the plasma concentrations of RN were always higher, with its systemic exposure significantly higher than that of IRN after administration of RN.

Moreover, for both IRN and RN administration, the patterns of the mean concentration-time profiles in plasma, CSF, and brain of the administered and generated stereoisomers were all comparable (Figure 3). For instance, after oral administration of RN, similar T_{max} (30 min) and $t_{1/2}$ (129.53 ± 9.0 (RN) *vs.* 116.60 ± 13.58 min (IRN)) values were observed for the administered RN and the generated IRN. These results indicated that the concentrations of the generated stereoisomers altered along with the changes of the concentrations of the administered stereoisomers in the plasma followed by the brain.

On the other hand, it was noted that after oral administration of RN, the $K_{p,Brain}$ and $K_{p,CSF}$ values of the generated IRN were significantly higher than those of administered RN ($p < 0.001$), and the epimerization ratios of RN in the brain (8.23 ± 0.56%) and CSF (16.91 ± 0.51%) were significantly higher than that in the plasma (2.2 ± 0.04%), indicating that IRN had a better capability than RN to penetrate into the brain. In addition, for the oral administration of IRN, although similar systemic exposure of the administered IRN and the generated RN was determined, the exposures in the brain (AUC_{Brain}) and CSF (AUC_{CSF}) of the administered IRN were significantly higher than that of the generated RN. These data further confirmed the higher permeability of IRN than RN into the brain. These results further indicated that (1) after oral administration of equal dosage of IRN or RN, both were absorbed rapidly into the systemic circulation and subsequently reached the brain via penetration through the blood-brain barrier (BBB); (2) the systemic exposure of RN was always pronounced with either similar to (after IRN administration) or significantly higher than that of IRN (after RN administration) due to significantly more extensive conversion of IRN to RN than that of RN to IRN, and significantly greater oral absorption and slower clearance of RN; and (3) after IRN administration, the concentrations of IRN in brain were significantly higher than that of RN due to the significantly higher permeability of IRN into the brain.

4. Discussion

Although both IRN and RN exhibited potent neuroprotective effects with promising therapeutic potential for the treatment of AD, differences in their pharmacological action exist. RN but not IRN was identified as a potent inhibitor of EphA4 to restore the synaptic impairment in AD [17]. On the other hand, IRN showed significant neuroprotective activity against glutamate-induced HT22 cell injury, while RN only displayed weak effect [25]. Meanwhile, it should be noted that IRN and RN can be interconverted *in vivo*. This indicates that the stereoselective pharmacokinetic study of these stereoisomers is crucial for identifying truly therapeutic agent for AD. Therefore, in the present study, we for the first time simultaneously investigated the kinetic profiles of the administered and generated stereoisomers in the brain, CSF, and plasma of the rats after oral administration of equal dose of IRN or RN.

We firstly observed significant stereoselective pharmacokinetics and epimerization of IRN and RN in the rats. After oral administration, both IRN and RN absorbed rapidly and reached their peak concentration in the plasma within 30 min. However, the systemic exposure (AUC_{Plasma}) of IRN was 6.5-fold lower than that of RN. These results were in good agreement with the data reported previously for the intact IRN and RN orally administered [29], where it was found that the bioavailability of RN (25.9 ± 8.7%) was 7.8-fold higher than that of IRN (3.3 ± 0.8%). Recent studies showed that this was mainly attributable to the stereoselective metabolism in liver. IRN was much more favorable to be metabolized than RN in the rat liver microsomes, and this stereo selectivity in hepatic metabolism of two stereoisomers was mainly mediated by CYP3A4 [28]. Moreover, the favorable conversion

Table 2: Kinetic parameters of the administered and generated stereoisomers in the brain, CSF, and plasma (mean ± SEM, n = 3 per time interval).

Samples	Parameters	IRN (20 mg/kg, *p.o.*)		RN (20 mg/kg, *p.o.*)	
		IRN	Generated RN	RN	Generated IRN
Plasma	$AUC_{0\text{-}180\,min}$ (ng·min/mL)	2483.43 ± 83.83	2249.95 ± 63.83	16382.06 ± 269.22***	369.30 ± 7.65†††
	C_{max} (ng/mL)	31.29 ± 1.59	29.00 ± 1.44	190.87 ± 6.34***	3.35 ± 0.06†††
	T_{max} (min)	30.00	30.00	30.00	30.00
	$t_{1/2}$ (min)	64.31 ± 3.19	89.65 ± 14.09	129.53 ± 9.30**	116.60 ± 13.58
	Epimerization ratio (%)	—	47.54 ± 0.22	—	2.20 ± 0.04$^{\#\#\#}$
Brain	$AUC_{0\text{-}180\,min}$ (ng·min/g)	627.37 ± 43.31	296.63 ± 9.49**	1587.03 ± 127.82**	140.76 ± 1.50†††
	$K_{p,Brain}$[b]	0.2530 ± 0.0187	0.1322 ± 0.0068**	0.0967 ± 0.0063**	0.3814 ± 0.0065†††
	C_{max} (ng/g)	7.35 ± 0.74	6.53 ± 0.25	16.96 ± 1.92**	1.22 ± 0.01††
	Epimerization ratio (%)	—	32.21 ± 1.22	—	8.23 ± 0.56$^{\#\#\#}$
CSF	$AUC_{0\text{-}180\,min}$ (ng·min/mL)	204.25 ± 16.53	153.93 ± 7.87	742.69 ± 12.80***	151.15 ± 5.09†††
	$K_{p,CSF}$[c]	0.0821 ± 0.0050	0.0683 ± 0.0016	0.0453 ± 0.0002**	0.4092 ± 0.0098†††
	C_{max} (ng/mL)	2.14 ± 0.34	1.72 ± 0.06	7.39 ± 0.17***	1.71 ± 0.05†††
	Epimerization ratio (%)	—	43.09 ± 0.92	—	16.91 ± 0.51$^{\#\#\#}$

Epimerization ratio was calculated by $AUC_{(generated\ stereoisomer)}/(AUC_{(generated\ stereoisomer)} + AUC_{(administered\ stereoisomer)}) \times 100\%$. The brain-to-plasma partition coefficient ($K_{p,Brain}$) was calculated by AUC_{Brain}/AUC_{Plasma}, and the CSF-to-plasma partition coefficient ($K_{p,CSF}$) was calculated by AUC_{CSF}/AUC_{Plasma}.

$^{**}p < 0.01$, $^{***}p < 0.001$, compared with IRN group (administered with 20 mg/kg IRN).

$^{\dagger\dagger}p < 0.01$, $^{\dagger\dagger\dagger}p < 0.001$, compared with RN group (administered with 20 mg/kg RN).

$^{\#\#\#}p < 0.001$, compared with generated RN group (administered with 20 mg/kg IRN).

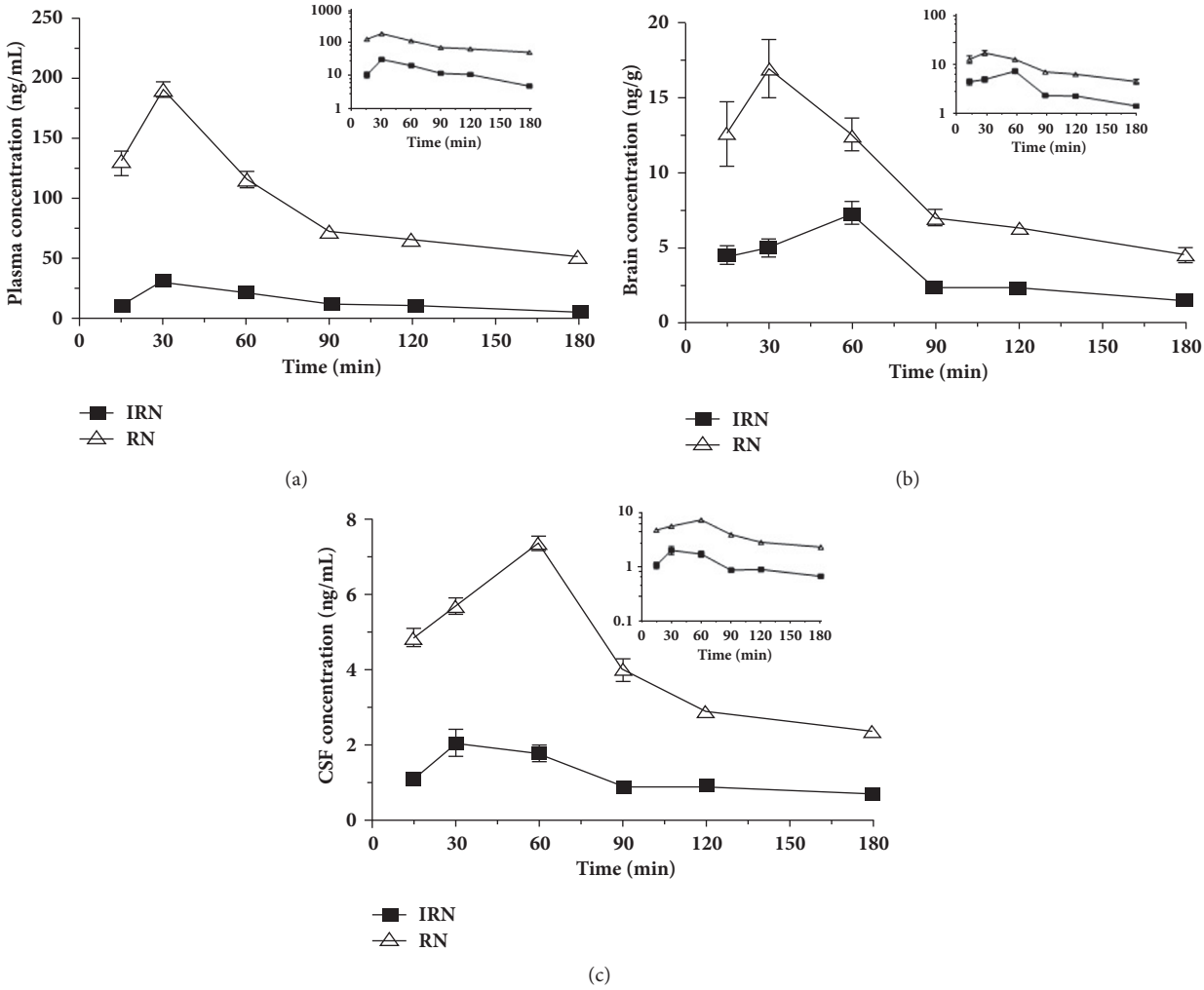

Figure 2: Mean concentration-time profiles of the administered IRN and RN in the rat plasma (a), brain (b) and CSF (c) after oral administration (The semi-logarithmic plots were inserted in the corresponding figures).

of IRN to RN also accounted for the low bioavailability of IRN [27]. The epimerization ratio of IRN to RN was 47.54 ± 0.22% in plasma while the epimerization ratio of RN to IRN is only 2.20 ± 0.04%. However, the AUC_{Plasma} of generated RN after IRN administration was much lower (2249.95 ± 63.83 *vs.* 16382.06 ± 269.22 ng·min/mL) than that of RN after RN administration, suggesting that the stereoselective interconversion made a smaller contribution to the difference in bioavailability of IRN and RN. Overall, RN might be a better choice for further development into an anti-AD agent due to its high bioavailability.

Importantly, in this study, the kinetic profiles of the metabolic converted stereoisomers (the generated RN from IRN and the generated IRN from RN) in the rat brain, CSF, and plasma were simultaneously elucidated after oral administration of IRN or RN. It is interesting to find that, regardless of the orally administered IRN or RN, RN was always one of the major or predominant forms present in the body. Our results showed that after administration of IRN, approximately half of IRN was metabolically converted to RN as identified in the plasma, brain, and CSF. On the other hand, after administration of RN, about 2.20%, 8.23%, and 16.91% of the generated IRN were found in the plasma, brain, and CSF, respectively; and both AUC_{Brain} and AUC_{CSF} of the generated IRN were significantly lower than those of RN. It has been reported that the interconversion between IRN and RN was partially based on their pK_a values. RN (pK_a 6.32) is a stronger base than IRN (pK_a 5.20) [30]. In the acidic condition, RN predominates because it could be stabilized by hydrogen bonding between the protonated nitrogen and oxindole carbonyl [30]. In addition, according to a previous report, after intravenous administration of equal dosage of IRN or RN, there was no significant difference between IRN and RN in the systemic exposure [29]. Therefore, the conversion between IRN and RN might take place in the GI tract, especially in the acidic compartment (pH 3.0-3.8) like stomach [31]. Moreover, epimerases, which are ubiquitous and catalyze versatile epimerization in all organisms [32], could also interconvert IRN into RN by catalyzing an epimerization on the C7 stereocenter. The significant difference in epimerization ratios between IRN and RN might also be due to the stereospecificity of epimerization.

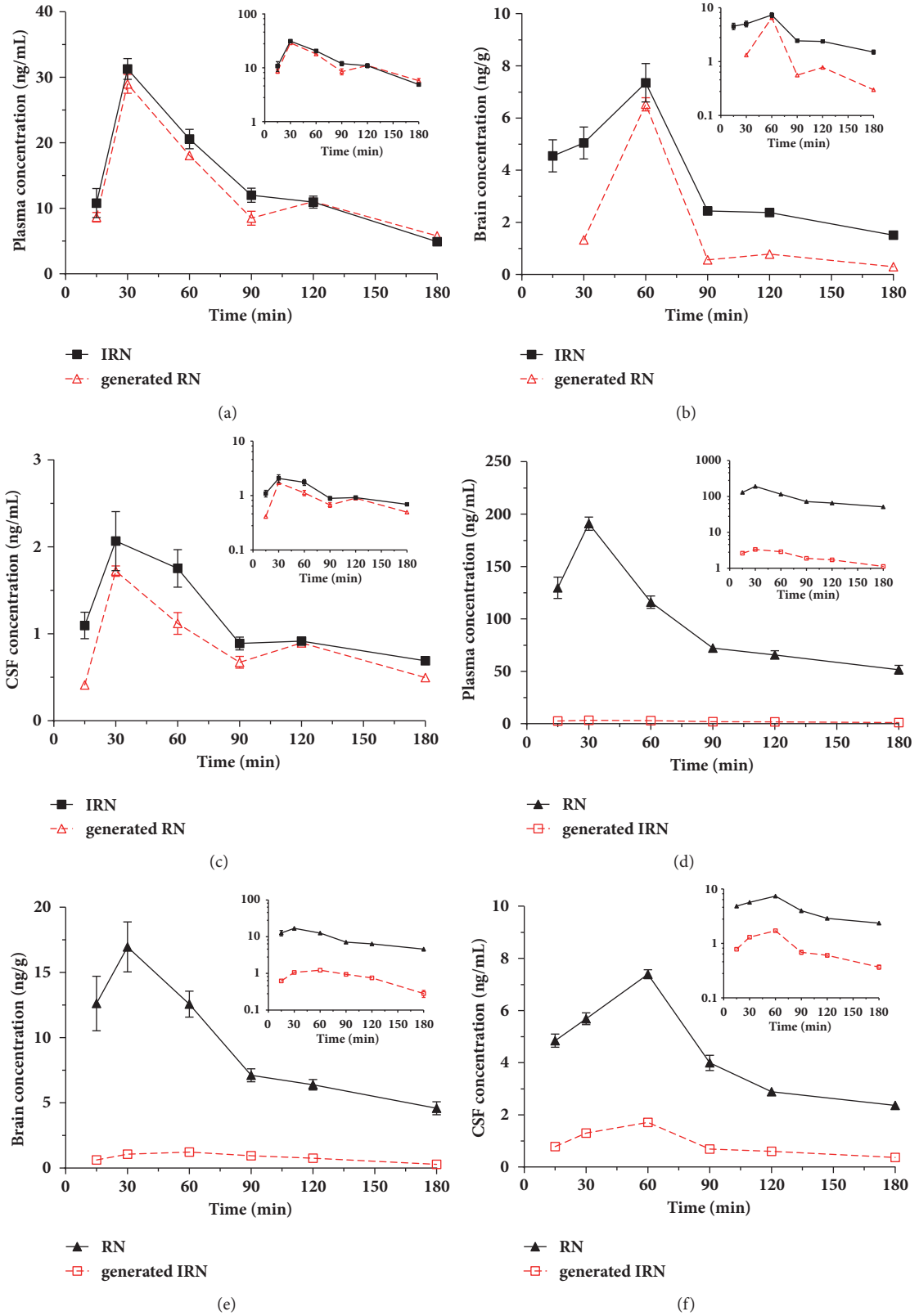

FIGURE 3: Mean concentration-time profiles of the administered IRN and generated RN in the rat plasma (a), brain (b) and CSF (c) after oral administration of IRN at 20 mg/kg. Concentration-time profiles of the administered RN and generated IRN in the rat plasma (d), brain (e) and CSF (f) after oral administration of RN at 20 mg/kg. (Semi-logarithmic plots were inserted in the corresponding figures).

Our results also revealed that IRN had significantly higher $K_{p,Brain}$ and $K_{p,CSF}$ than that of RN ($p < 0.01$), suggesting that IRN had better brain penetration capability. This was consistent with a previously reported study of *in vitro* BBB permeability, in which the BBB permeability of IRN and RN was measured using a coculture model composed of three types of cells, namely endothelial cells, pericytes, and astrocytes. Both IRN and RN could pass through brain endothelial cells, while IRN showed a 1-fold higher BBB permeability than RN [33]. Additionally, the membrane permeability of RN was affected by P-gp efflux transporter [27, 34]. Overall, our study for the first time confirmed the *in vivo* BBB permeability of IRN and RN, with IRN more permeable than RN. However, despite the higher BBB permeability of IRN, its BBB penetration was still lower than RN due to the poor bioavailability.

The therapeutic effects of both IRN and RN in AD have been recently investigated in different animal models [15, 17, 18]. Fu et al. found that oral administration of RN (50 mg/kg/day for 3-4 weeks) restored the impaired long-term potentiation in the hippocampus of APP/PS1 transgenic mice [17], while Xian et al. showed that oral administration of IRN (20 or 40 mg/kg for 3 weeks) ameliorated cognitive deficits induced by $A\beta_{25\text{-}35}$ in rats [15]. It should be noted that although both IRN and RN were capable of exerting anti-AD effect *in vivo*, the present kinetic study provided new evidence supporting that RN was more suitable than IRN for further development into an anti-AD agent, mainly due to the following: (1) low bioavailability of IRN; (2) high epimerization ratio of IRN; and (3) after oral administration of an equal dose of RN or IRN, the overall exposure of RN in the plasma, brain, and CSF was much higher than that of IRN.

5. Conclusion

The present study for the first time simultaneously probed the plasma pharmacokinetics and disposition kinetics of administered and generated stereoisomers in the brain and CSF after oral treatment of equal dose of IRN or RN in rats. Our findings unambiguously demonstrated that after oral administration, RN exhibited markedly higher systemic exposure and disposition in the brain and CSF than IRN. Moreover, with the same oral dose, regardless of the orally administration of IRN or RN, RN would always be one of the major or predominant forms present in the body. The results obtained from the present study provided sound experimental evidence to support further development of RN into a potential therapeutic agent for the treatment of AD. Our present study also set a good example on integrating pharmacokinetics for identifying the truly therapeutic agent.

Abbreviations

AD: Alzheimer's disease
BBB: Blood-brain barrier
CSF: Cerebrospinal fluid
IRN: Isorhynchophylline
IS: Internal standard
MRM: Multiple reaction monitoring
RN: Rhynchophylline
SD: Sprague-Dawley.

Data Availability

The current data used to support the findings of this study are included within the article.

Conflicts of Interest

The authors declare that they have no conflicts of interest.

Acknowledgments

This study was supported by a General Research Fund of the University Grants Council of Hong Kong SAR (Project no. 14110814).

Supplementary Materials

The typical MRM chromatograms of the blank biological specimen, blank biological specimen spiked with both analytes and samples obtained after oral administration of IRN or RN were shown in Figure S1. *(Supplementary Materials)*

References

[1] K. Blennow, M. J. de Leon, and H. Zetterberg, "Alzheimer's disease," *The Lancet*, vol. 368, no. 9533, pp. 387–403, 2006.

[2] A. Kumar, A. Singh, and A. Ekavali, "A review on Alzheimer's disease pathophysiology and its management: an update," *Pharmacological Reports*, vol. 67, no. 2, pp. 195–203, 2015.

[3] Y. P. Ng, T. C. Or, and N. Y. Ip, "Plant alkaloids as drug leads for Alzheimer's disease," *Neurochem Int*, vol. 89, pp. 260–270, 2015.

[4] E. L. Konrath, C. S. Passos, L. C. J. Klein-Júnior, and A. T. Henriques, "Alkaloids as a source of potential anticholinesterase inhibitors for the treatment of Alzheimer's disease," *Journal of Pharmacy and Pharmacology*, vol. 65, no. 12, pp. 1701–1725, 2013.

[5] K. Matsuzono, N. Hishikawa, Y. Ohta et al., "Combination Therapy of Cholinesterase Inhibitor (Donepezil or Galantamine) plus Memantine in the Okayama Memantine Study," *Journal of Alzheimer's Disease*, vol. 45, no. 3, pp. 771–780, 2015.

[6] Y.-F. Xian, Z.-X. Lin, M. Zhao, Q.-Q. Mao, S.-P. Ip, and C.-T. Che, "Uncaria rhynchophylla Ameliorates Cognitive Deficits Induced by D-galactose in Mice," *Planta Medica*, vol. 77, no. 18, pp. 1977–1983, 2011.

[7] H. Fujiwara, K. Iwasaki, K. Furukawa et al., "Uncaria rhynchophylla, a Chinese medicinal herb, has potent antiaggregation effects on Alzheimer's β-amyloid proteins," *Journal of Neuroscience Research*, vol. 84, no. 2, pp. 427–433, 2006.

[8] J. D. Phillipson and S. R. Hemingway, "Chromatographic and spectroscopic methods for the identification of alkaloids from herbarium samples of the genus uncaria," *Journal of Chromatography A*, vol. 105, no. 1, pp. 163–178, 1975.

[9] J. S. Shi, Y. U. JX, X. P. Chen, and R. X. Xu, "Pharmacological actions of Uncaria alkaloids, rhynchophylline and isorhynchophylline," *Acta Pharmacol Sin*, vol. 24, pp. 97–101, 2003.

[10] T.-H. Kang, Y. Murakami, H. Takayama et al., "Protective effect of rhynchophylline and isorhynchophylline on in vitro

ischemia-induced neuronal damage in the hippocampus: Putative neurotransmitter receptors involved in their action," *Life Sciences*, vol. 76, no. 3, pp. 331–343, 2004.

[11] D. Yuan, B. Ma, J.-Y. Yang et al., "Anti-inflammatory effects of rhynchophylline and isorhynchophylline in mouse N9 microglial cells and the molecular mechanism," *International Immunopharmacology*, vol. 9, no. 13-14, pp. 1549–1554, 2009.

[12] Y. F. Xian, Z. X. Lin, Q. Q. Mao, J. N. Chen, S. u. ZR, X. P. Lai et al., "Isorhynchophylline protects PC12 cells against beta-amyloid-induced apoptosis via PI3K/Akt signaling pathway," *Evidence-Based Complementary and Alternative Medicine*, vol. 2013, Article ID 163057, 2013.

[13] Y. F. Xian, Z. X. Lin, Q. Q. Mao et al., "Protective Effect of Isorhynchophylline Against β-Amyloid-Induced Neurotoxicity in PC12 Cells," *Cellular and Molecular Neurobiology*, vol. 32, no. 3, pp. 353–360, 2012.

[14] Y. F. Xian, Z. X. Lin, Q. Q. Mao et al., "Bioassay-guided isolation of neuroprotective compounds from uncaria rhynchophylla against beta-amyloid-induced neurotoxicity," *Evidence-Based Complementary and Alternative Medicine*, vol. 2012, Article ID 802625, 2012.

[15] Y.-F. Xian, Z.-R. Su, J.-N. Chen et al., "Isorhynchophylline improves learning and memory impairments induced by D-galactose in mice," *Neurochemistry International*, vol. 76, no. 10, pp. 42–49, 2014.

[16] Y. F. Xian, Q. Q. Mao, J. C. Wu et al., "Isorhynchophylline treatment improves the amyloid-β-induced cognitive impairment in rats via inhibition of neuronal apoptosis and tau protein hyperphosphorylation," *Journal of Alzheimer's Disease*, vol. 39, no. 2, pp. 331–346, 2014.

[17] A. K. Y. Fu, K.-W. Hung, H. Huang et al., "Blockade of EphA4 signaling ameliorates hippocampal synaptic dysfunctions in mouse models of Alzheimer's disease," *Proceedings of the National Acadamy of Sciences of the United States of America*, vol. 111, no. 27, pp. 9959–9964, 2014.

[18] H. Shao, Z. Mi, W. Ji et al., "Rhynchophylline Protects Against the Amyloid β-Induced Increase of Spontaneous Discharges in the Hippocampal CA1 Region of Rats," *Neurochemical Research*, vol. 40, no. 11, pp. 2365–2373, 2015.

[19] E. Wenkert, J. H. Udelhofen, and N. K. Bhattacharyya, "3-Hydroxymethyleneoxindole and its Derivatives," *Journal of the American Chemical Society*, vol. 81, no. 14, pp. 3763–3768, 1959.

[20] J. Cai, C. Lin, J. Ma, L. Hu, G. Lin, and X. Wang, "Determination of rhynchophylline in rat plasma by liquid chromatography mass spectrometry and its application," *Journal of Chromatographic Science*, vol. 52, pp. 661–665, 2014.

[21] W. Wang, C.-M. Ma, and M. Hattori, "Metabolism and pharmacokinetics of rhynchophylline in rats," *Biological & Pharmaceutical Bulletin*, vol. 33, no. 4, pp. 669–676, 2010.

[22] W. Wang, C. M. Ma, and M. Hattori, "Metabolism of isorhynchophylline in rats detected by LC-MS," *Journal of Pharmacy & Pharmaceutical Sciences*, vol. 13, no. 1, pp. 27–37, 2010.

[23] Z.-F. Wu, Y.-Q. Wang, N. Wan et al., "Structural stabilities and transformation mechanism of rhynchophylline and isorhynchophylline by ultra performance liquid chromatography/Time-of-flight mass spectrometry (UPLC/Q-TOF-MS)," *Molecules*, vol. 20, no. 8, pp. 14849–14859, 2015.

[24] J. Wang, P. Qi, J. Hou et al., "Profiling and identification of metabolites of isorhynchophylline in rats by ultra high performance liquid chromatography and linear ion trap Orbitrap mass spectrometry," *Journal of Chromatography B*, vol. 1033-1034, pp. 147–156, 2016.

[25] F. Chen, W. Qi, J. Sun, J. W. Simpkins, and D. Yuan, "Urinary metabolites of isorhynchophylline in rats and their neuroprotective activities in the HT22 cell assay," *Fitoterapia*, vol. 97, pp. 156–163, 2014.

[26] G. Laus, "Kinetics of isomerization of tetracyclic spiro oxindole alkaloids," *Journal of the Chemical Society, Perkin Transactions 2*, no. 2, pp. 315–317, 1998.

[27] X. Wang, M. Zheng, J. Liu et al., "Differences of first-pass effect in the liver and intestine contribute to the stereoselective pharmacokinetics of rhynchophylline and isorhynchophylline epimers in rats," *Journal of Ethnopharmacology*, vol. 209, pp. 175–183, 2017.

[28] X. Wang, Z. Qiao, J. Liu, M. Zheng, W. Liu, and C. Wu, "Stereoselective in vitro metabolism of rhynchophylline and isorhynchophylline epimers of Uncaria rhynchophylla in rat liver microsomes," *Xenobiotica*, vol. 10, pp. 1–9, 2017.

[29] X. Wang, M. Zheng, J. Liu, Z. Qiao, W. Liu, and F. Feng, "Stereoselective pharmacokinetic study of rhynchophylline and isorhynchophylline epimers in rat plasma by liquid chromatography–tandem mass spectrometry," *Xenobiotica*, vol. 47, no. 6, pp. 479–487, 2017.

[30] J. E. Saxton, *The Indoles: The Monoterpenoid Indole Alkaloids. The Chemistry of Heterocyclic Compounds*, Wiley, New York, NY, USA, 1983.

[31] Y. Kwon, *Handbook of Essential Pharmacokinetics, Pharmacodynamics and Drug Metabolism for Industrial Scientists*, Kluwer Academic/Plenum Publishers, New York, NY, USA, 2001.

[32] S. T. M. Allard, M.-F. Giraud, and J. H. Naismith, "Epimerases: Structure, function and mechanism," *Cellular and Molecular Life Sciences*, vol. 58, no. 11, pp. 1650–1665, 2001.

[33] S. Imamura, M. Tabuchi, H. Kushida et al., "The blood-brain barrier permeability of geissoschizine methyl ether in Uncaria hook, a galenical constituent of the traditional Japanese medicine yokukansan," *Cellular and Molecular Neurobiology*, vol. 31, no. 5, pp. 787–793, 2011.

[34] Y.-N. Zhang, Y.-F. Yang, W. Xu, and X.-W. Yang, "The blood-brain barrier permeability of six indole alkaloids from uncariae ramulus cum uncis in the MDCK-pHaMDR cell monolayer model," *Molecules*, vol. 22, no. 11, 2017.

Hindawi
Evidence-Based Complementary and Alternative Medicine
Volume 2019, Article ID 3756092, 9 pages
https://doi.org/10.1155/2019/3756092

Research Article

Effect of Propolis Preparations on Transepithelial Electrical Potential, Resistance, and Ion Transport in *In Vitro* Study

Paulina Smyk[1,2], **Iga Hołyńska-Iwan**[2] **and Dorota Olszewska-Słonina**[2]

[1]*Department of Pediatric Nursing, Faculty of Health Sciences, Collegium Medicum in Bydgoszcz Nicolaus Copernicus University in Torun, Poland*
[2]*Department of Pathobiochemistry and Clinical Chemistry, Faculty of Pharmacy, Collegium Medicum in Bydgoszcz Nicolaus Copernicus University in Torun, Poland*

Correspondence should be addressed to Paulina Smyk; paulina.smyk@cm.umk.pl

Received 13 August 2018; Revised 1 November 2018; Accepted 1 January 2019; Published 15 January 2019

Guest Editor: Xinguang Liu

Background. Propolis and its ethanol extract show positive germicidal, bacteriostatic, and anti-inflammatory antioxidants and regenerative properties after use on the surface of the skin. Propolis is in common use in production of cosmetics and in folk medicine. The influence of this resinous mixture on ion channels, channels located in skin cells membranes and skin electrical resistance, was not explained. *Objective*. The main aim of the study was the evaluation of electrophysiological skin parameters during mechanical and chemical-mechanical stimulation after use of ethanol extract of propolis and propolis ointment in comparison with iso-osmotic Ringer solution. *Methods*. Skin fragments were taken from white New Zealand rabbits and distributed into three experimental groups which were incubated in ethanol extract of propolis (EEP), propolis ointment, and Ringer solution. Then they were placed in a Ussing chamber to measure electrophysiological parameters values. *Results*. In this study the influence of EEP on changes in value of electrical potential during block of chloride ions transport at the same time was observed. Ethanol propolis extract dissolved in water increases the transepidermal sodium ions transport in contrast to propolis ointment. *Conclusion*. The way of preparation cosmetics, which contain propolis, has effects on transepidermal ions transport in the rabbit's skin. The value of skin electrical resistance is changing with penetration depth of active propolis substances contained in cosmetics.

1. Introduction

Propolis has been used in medicine and cosmetology for centuries. The name of propolis comes from the Greek language, from the words pro- and polis-, which means the city's rampart. The propolis is a complex material collected by honeybees from buds, leaves, and parts of trees or other plants. This substance is a viscous, sticky, resin-balsamic mass. Bees used the propolis to strengthen the construction of the hive, by sealing its interior for the protection against microorganisms [1–3].

In Poland the propolis is obtained from leafy trees (poplar, birch, alder, oak, willow, and chestnut) and coniferous trees (fir, pine, and spruce). The chemical composition of propolis depends upon geographical origin, plants, and change of climate and upon the species of bees. It has a few colours which depend on its source and age [4]. Propolis activities depend on various compounds which it contains. The most biologically active substances are scarcely soluble in oil, water, or other solvents. Propolis should not be used as a crude material [5]. Ethanol extraction is the most popular technique for the production of propolis extracts. EEP has limited uses in cosmetology [6]. In ethanol extract of propolis there is the greatest in quantity of flavonoids. Besides, aromatic acids and esters of aromatic acids were also found. The content of flavonoid compounds in EEP is 2,72-10,81% according to Kędzia et al. and Ellnain-Wojtaszek et al. The average content of flavonoid compounds in EEP in Polish propolis was 5% [7, 8].

Propolis and its extracts have long been used for the prevention and treatment of a variety of diseases due to its antibacterial [9–13], antiviral [14], antifungal, antioxidant [12,

Table 1: The experimental table taking into account the experimental groups, incubation solutions, type of stimulation, and electrophysiological parameters.

Group	Pre- incubation fluid (30 min)	Incubation fluid (30 min)	Mechanical stimulation fluid	Chemical stimulation fluid (15s)	Electrophysiological parameters
I group: Long-term incubation in 1 ml ethanol extract of propolis in 100 ml water *N =22*	1 ml EEP in 100 ml water + RH	RH	RH	B	PDmin
					PDmax
II group: Undisturbed ion transport *N =22*	RH	RH	RH	AB	R
III group: Long- term incubation in propolis ointment *N =18*	propolis ointment + RH	RH	RH		dPD
					PD

Abbreviations. N: number of specimens, RH: Ringer solution, B: bumetanide (0.1mM) in Ringer solution, AB: amiloride in bumetanide (0.1mM) in Ringer solution, PD: transepithelial electrical potential differences in stationary conditions before and after stimulation (mV), dPD: changes of electrical potential differences during stimulation (mV), PDmin: minimal transepithelial electrical potential (mV), PDmax: maximal transepithelial electrical potential (mV), and R: transepithelial resistance (Ohm/cm^2).

15–18], anesthetizing, cytostatic [19, 20], anti-inflammatory [12, 20], immune-strengthening [19], and hepatoprotective properties [19, 21]. Ethanol extract of propolis is widely used in cosmetics. Although propolis is also in use in the treatment of skin diseases caused by microorganisms, such as folliculitis, sweat gland infections, boils, impetigo, nodules, and pyodermas, as well as the treatment of fungal and viral diseases [22].

Propolis is quite safe specimen, but it also causes allergic reactions. Persons with a tendency to be allergic to other bee products (honey/bee pollen) should be especially attentive. After topical application of propolis, indicated by the following symptoms: redness, swelling, and itching of the skin [23], hypersensitivity reactions may occur. In medical literature many publications have centred on the transepithelial ion transport in various tissues (trachea, caecum) [24–28], skin of amphibians [29], and propolis properties, but there are no publications about effect of propolis on ion channels located in the skin cell membranes. Modified Ussing's method used in this experience facilitated the analysis of the interaction of propolis preparations with transepithelial ion transport, value of electrical potential of epithelial tissue and its changes before and during stimulation, and integrity and viability of epithelial tissue.

2. Materials and Methods

The 62 skin fragments taken from 4 experimental animals of both sex were located in the modified Ussing chamber.

Experimental material was divided into three groups, only special rules:

I group: Long-term incubation in 1 ml ethanol extract of propolis dissolved in 100 ml water (N =22)

II group: Undisturbed ion transport (N = 22)

III group: Long-term incubation in propolis ointment (N = 18)

The amount of experimental material (fragments of the rabbit's skin) from females was equal to the material from males in each group.

The Ussing method used in this experiment allows evaluating

(i) transepithelial electrical potential differences in stationary conditions before and after stimulation (PD, mV);

(ii) changes of electrical potential differences during stimulation (dPD, mV);

(iii) minimal transepithelial electrical potential (PDmin, mV);

(iv) maximal transepithelial electrical potential (PDmax, mV)

(v) transepithelial resistance (R, Ohm/cm^2).

The procedure protocol for three experimental groups during preincubation (30 minutes) and short-term mechanical and chemical stimulation was presented in Table 1.

2.1. Animals. Skin samples were taken from experimental animals (adult, New Zealand rabbits of both sexes, two males and two females, from animal husbandry in Medical University of Silesia in Katowice, weighting between 3.5 and 4.0 kilograms, three to four months old). The animals were maintained on a standard light/dark cycle: 12 hours light and 12 hours night schedule. The rabbits were anesthetized with high concentration of isoflurane in carbon (IV) dioxide (about 60% in the inhaled air). This gas mixture provides painless death. After incision of the abdominal wall and removing the subcutaneous fatty tissue and the abdominal wall muscle layers, fragments of abdominal skin of the animal have been collected. The remaining part of skin was subdivided into 2 cm^2 pieces, which were submerged and incubated in the appropriate solution, according to the experimental protocol (see Table 1).

2.2. Chemicals. The following chemicals were used for the experiment:

(i) RH: Ringer solution: basic solution with iso-osmotic properties (K^+ 4.0 mM; Na^+ 147.2 mM; Ca^{2+} 2.2 mM;

Mg^{2+} 2.6 mM; Cl^- 160.8 mM; Hepes 10.0 mM), which was adjusted to pH 7.4 under the control of a pH-meter

(ii) Amiloride hydrochloride hydrate: an inhibitor of transepithelial sodium ions transport; amidynoamid acid, 3,5-diamino-6-chloro-2-carboxylic acid; 266.09 g/mol (Sigma-Aldrich),

(iii) AMI: amiloride (0.1 mM) dissolved and diluted in Ringer solution,

(iv) Bumetanide: an inhibitor of transepithelial chloride ions transport; 3-aminosulfonyl-5-butylamino-4-phenoxybenzoic acid (Sigma-Aldrich),

(v) B: bumetanide (0.1 mM) dissolved in DMSO (dimethylsulfoxide) and diluted in Ringer solution,

(vi) Amiloride in bumetanide (0.1 mM) dissolved in Ringer solution. It is an inhibitor of transepithelial sodium and chloride ions transport.

Mineral compounds (KCl, NaCl, $CaCl_2$, and $MgCl_2$) were purchased from POCH, Poland.

2.3. Preparation of Ethanol Extract of Propolis. The material for research was ethanol extract of propolis (EEP). Propolis was produced by honeybees from the apiary in Białośliwie (Wielkopolska, Great Poland). Hand-collected propolis came from the collection of 2016 year and was desiccated and kept in dark before processing. The portion of 50 g of propolis was put into black bottle. Next 350 cm^3 of 95% ethanol-Grain Luxury Spirit (CEDC International, made by its branch Polmos Białystok, Poland) and 150 cm^3 water were added. Propolis was submitted to 21 days of extraction in order to obtain its ethanol extract. The black bottle was placed in laboratory at room temperature and its content was mixed two times a day for 21 days. After that time brown, rough particles were removed from propolis extract by filtering (sterile bandage MATOCOMP, Dressing Material Factories, Toruń, Poland).

2.4. Preparation of Propolis Ointment. The vessel has been instilling a portion of 100 ml ethanol extract of propolis and placed into hot water bath until dense liquid was obtained. Next, the dark, brown, dense liquid was added to 100 g colourless cosmetic white petrolatum-*Vaselinum album* (Pharmaceutical Laboratory by AVENA, Osielsko, Poland). Having mixed white petrolatum with evaporated propolis extract, the yellow ointment was formed.

2.5. Experimental Procedure. The skin fragments were taken from laboratory animals. After cutting, the animal skin fragments were incubated for 30 minutes (1 ml ethanol extract of propolis, Ringer solution, propolis ointment) and placed in the adapter. This apparatus has two rubber gaskets lubricated with silicone grease, to prevent tissue damage. The adapter was placed in an Ussing chamber composed of two half cells between which the examined tissue has been put. After replenishing chambers with proper liquid, water hoses were shut down with metal snaps. Two pairs of chloride-silver electrodes, connected to measuring set (linked with computer), were used to check voltage and current, to measure the resistance. Electrophysiological parameters were tested using epidermal tissue under mechanical and mechanical-chemical stimulation (Table 1.) These parameters were checked with the presence of chloride ions transport blockers (bumetanide) and blockers of Na^+ ions and Cl^- ions by using both substances (amiloride and bumetanide). Isolated tissue was rinsed with reagents by the use of peristaltic pump to maintain a constant flow rate of 3 ml per 15 seconds. The experimental procedure, conducted at the temperature 23±2°C, lasted about 1 hour. This time was provided for a single tissue fragment.

2.6. Data Analysis. The experimental data were recorded using the experimental protocol. EVC 4000 (WPI, USA) apparatus was used to measure voltage and resistance. It was connected to a computer data acquisition experimental system MP 150 (Biopac, USA) and translated using AcqKnowledge 3.8.1. (WPI, USA) software. Electrophysiological parameters were compared in Microsoft Excel 2016 (Microsoft, Poland). The statistical data relationship was performed using STATISTICA 13.1 (Statsoft, Poland). Shapiro-Wilk's test was applied for the compatibility estimation of the assessed parameters distribution with normal distribution. All results were expressed as mean ± SD/median/interquartile range. All measurements were interpreted in the three groups using a nonparametric Wilcoxon signed-rang test and Mann Whitney U test. Two-tailed P value of < 0.05 was considered statistically significant.

3. Results

3.1. The Comparison of Electrophysiological Parameters of 1ml EEP in 100 ml Water (Group I), Ringer's Solution (Group II), and Ringer's Solution with Propolis Ointment (Group III). The values of electric potential of experimental group I and II before mechanical stimulation RH_1 ($p<0.001$), RH_2 ($p<0.001$), bumetanide ($p=0.004$), and amiloride with bumetanide ($p=0.018$) were different with statistical significance. Between experimental groups II and III this difference is either visible for stimulation with RH_1 solution ($p<0.001$) (Figure 1).

The difference of stationary potential during the stimulation by RH_1 solution (Figure 2) and RH_2 solution (Figure 3) for experimental groups I and II was as observable ($p<0.001$) as during RH_2 (Figure 3) stimulation in experimental groups II and III ($p<0.001$).

Maximal value of transepidermal electric potential was changing in groups I and II during the stimulation by RH_1 solution ($p=0.002$) (Figure 2) and bumetanide ($p<0.001$) (Figure 4).

During the experiment no statistically significant differences of minimal and maximal value of electric potential occurred and neither did the differences in value of electric potential during amiloride with bumetanide (Figure 5) stimulation between experimental groups I and II and II and III.

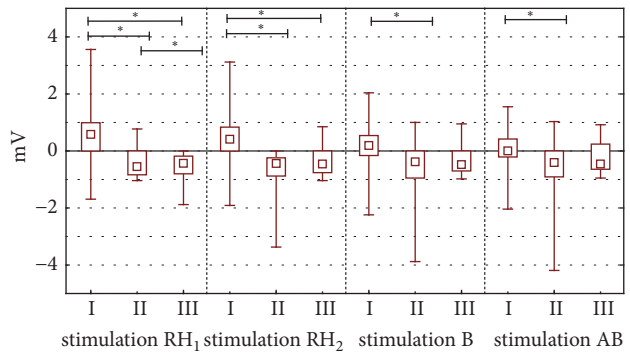

Figure 1: The electrical potential in stationary conditions before stimulation. The figure shows arrangement the electrical potential value before individual stimulation. The experiment were performed according to scheme stimulations by Ringer solution (RH), bumetanide (B), amiloride (AMI) and amiloride with bumetanide (AB). The time of each stimulation was 15 seconds. The figure shows also first and second simulation by Ringer solution (stimulation RH_1 and stimulation RH_2) and stimulation by bumetanide (stimulation B) stimulation by amiloride in bumetanide (stimulation AB). *Abbreviations.* $*p < 0.001$, RH: Ringer fluid, stimulations 1 and 2, B: bumetanide solution (0.1 mM), AB: a mixture of amiloride and bumetanide solutions (0.1 mM). I: long-term incubation in 1 ml ethanol extract of propolis dissolved in 100 ml water, II: undisturbed ion transport, and III: long-term incubation in propolis ointment;

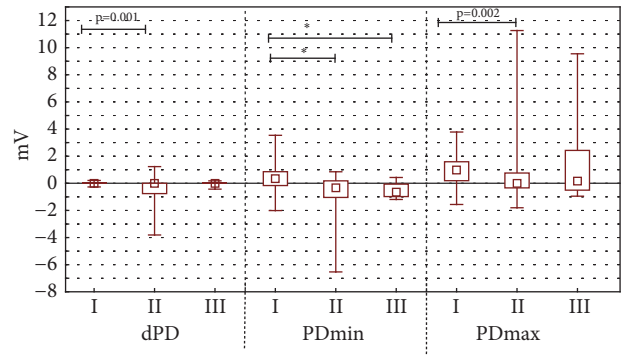

Figure 2: The mean, minimal and maximal transepithelial potential difference value for mechanical stimulation RH_1. The figure shows arrangement the difference of electrical potential, its minimal and maximal value during first stimulation by Ringer solution (stimulation RH_1). The time of stimulation was 15 seconds. *Abbreviations.* $*p < 0.001$. I: long-term incubation in 1 ml ethanol extract of propolis dissolved in 100 ml water, II: undisturbed ion transport, III: long-term incubation in propolis ointment, dPD: difference of electrical potential values during RH_1 stimulation (mV), PD_{min}: minimal transepithelial electrical potential during RH_1 stimulation (mV), and PD_{max}: maximal transepithelial electrical potential during RH_1 stimulation (mV).

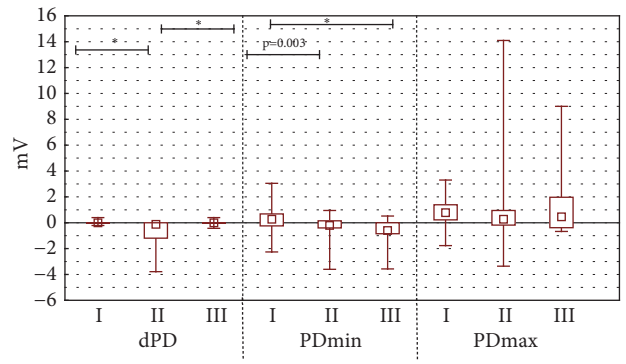

Figure 3: The mean, minimal, maximal transepithelial potential difference value for mechanical stimulation RH_2. The figure shows arrangement the difference of electrical potential, its minimal and maximal value during second stimulation by Ringer solution (stimulation RH_2). The time of stimulation was 15 seconds. *Abbreviations.* $*p < 0.001$. I: long-term incubation in 1 ml ethanol extract of propolis dissolved in 100 ml water, II: undisturbed ion transport, III: long-term incubation in propolis ointment, dPD - difference of electrical potential values during RH_2 stimulation (mV), PD_{min}: minimal transepithelial electrical potential during RH_2 stimulation (mV), and PD_{max}: maximal transepithelial electrical potential during RH_2 stimulation (mV).

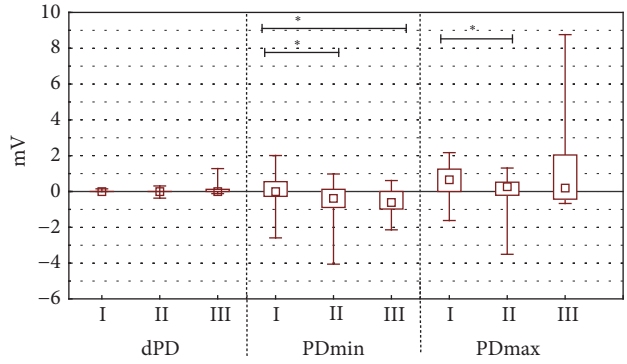

Figure 4: The mean, minimal, maximal transepithelial potential difference value for chemical stimulation B. The figure shows arrangement the difference of electrical potential, its minimal and maximal value during stimulation by bumetanide (stimulation B). The time of stimulation was 15 seconds. Statistical significance between groups was marked as $*p < 0.001$. *Abbreviations.* $*p < 0.001$. I: long-term incubation in 1 ml ethanol extract of propolis dissolved in 100 ml water, II: undisturbed ion transport, III: long-term incubation in propolis ointment, dPD: difference of electrical potential values during bumetanide stimulation (mV), PD_{min}: minimal transepithelial electrical potential during bumetanide stimulation (mV), and PD_{max}: maximal transepithelial electrical potential during bumetanide stimulation (mV).

3.2. The Comparison of Electrophysiological Parameters between Group I (1ml EEP in 100ml Water) and Group III (Propolis Ointment). During the stimulation with RH_1 and RH_2 the solution, propolis ointment and 1ml of EEP in 100 ml of water were showing different stationary potentials (PDbefore) (Figure 1) and minimal values of transepidermal electric potential (PDmin). These differences were statistically significant (value $p<0.001$ for all measured parameters (Figures 2 and 3). Statistically significant difference of electric resistance (R) values between groups I and III for RH_1, RH_2, bumetanide, and amiloride with bumetanide solution stimulations (Figure 6) was noticed (respectively, $p=0.004$, $p<0.001$, and $p<0.001$). Minimal

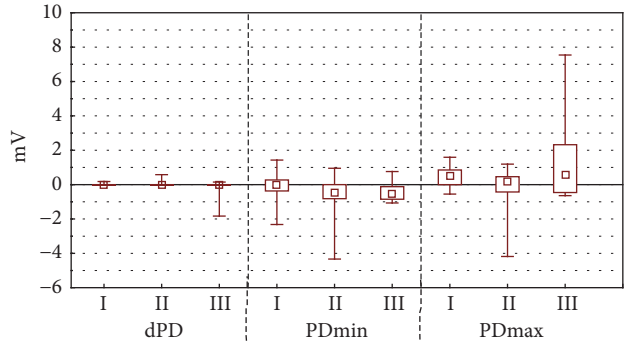

Figure 5: The mean, minimal, maximal transepithelial potential difference value for chemical stimulation AB. The figure shows arrangement the difference of electrical potential, its minimal and maximal value during stimulation by amiloride with bumetanide (stimulation AB). The time of stimulation was 15 seconds. In this experiment no statistically significant changes. *Abbreviations.* $*p < 0.001$. I: long-term incubation in 1 ml ethanol extract of propolis dissolved in 100 ml water, II: undisturbed ion transport, III: long-term incubation in propolis ointment, dPD: difference of electrical potential values during amilloride in bumetanide solution stimulation (mV), PD_{min}: minimal transepithelial electrical potential during amiloride in bumetanide solution stimulation (mV), and PD_{max}: maximal transepithelial electrical potential during amiloride in bumetanide solution stimulation (mV).

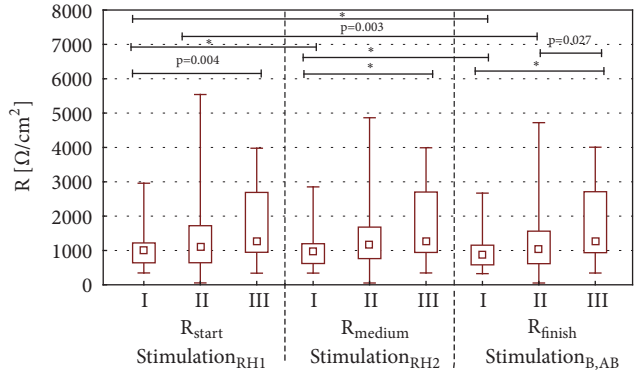

Figure 6: The resistance for I, II, and III group during RH_1, RH_2, B, and AB stimulation. This figure shows arrangement the electrical resistance for first and second simulation by Ringer solution (stimulation RH_1, stimulation RH_2), stimulation by bumetanide (stimulation B), and stimulation by amiloride with bumetanide (stimulation AB). *Abbreviations.* $*p < 0.001$. I: long-term incubation in 1 ml ethanol extract of propolis dissolved in 100 ml water, II: undisturbed ion transport, III: long-term incubation in propolis ointment, R_{start} (RH_1): transepithelial resistance for first Ringer solution stimulation, R_{medium} (RH_2): transepithelial resistance for second Ringer solution stimulation, and R_{finish} (B, AB): transepithelial resistance for bumetanide solution and mixture of amiloride with bumetanide solution stimulations.

potential during bumetanide solution stimulation showed statistically significant difference for both propolis solutions (respectively, $p<0.001$ and $p<0.001$) (Figure 4). There were no differences of electrical potential (dPD) values during stimulation as well as maximal and minimal potential values during amiloride with bumetanide solution (Figure 5) stimulation between experimental groups I and III.

3.3. Value of Electrical Resistance between Experimental Groups. Difference between initial value of electrical resistance (after RH1 stimulation) and final value of electrical resistance (after B, AB stimulation) for Ringer solution ($p=0.003$) and 1ml of EEP in 100ml of water ($p<0.001$) was statistically significant (Figure 6). Changes of electrical value were essentially different for propolis tincture (1ml of EEP in 100ml of water) during each stage of experiment ($p<0.001$). During the experiment described above no statistically significant differences of electrical resistance for propolis ointment were found as well as between Ringer solution and 1ml of EEP in 100 ml of water. However, the differences of electrical resistance were important between propolis ointment and propolis tincture ($p<0.001$ for medium and finish value of resistance and $p=0.004$ start value of resistance). The value of final resistance differs significantly for Ringer solution and propolis ointment ($p = 0.027$, Table 2).

4. Discussion

Ion transport in epidermal cells is taking place through ion channels, ion pumps and transporters localized on apical and basolateral surface of cell membrane. In research, the modification of ion channels permeability is achieved by mechanical and chemomechanical surface stimulation. Transport protein system permits the changes in ions layout in both sides of tested epidermal tissue and thereby generates and keeps transepidermal electrical potentials difference on epidermal surface. Difference of electrical potential shows functioning of electric field on the surface of epidermis and its protective properties [30, 31].

Our research shows the influence of long-term incubation with substances containing propolis and short-term stimulation using the Ringer solution, bumetanide, amiloride with bumetanide. In order to check the effect of substances contained in propolis on sodium and chloride ion transport located in the skin, we used bumetanide and amiloride with bumetanide. Bumetanide stimulation was made to prevent transepidermal chloride ion transport through blocking basolateral cotransport mechanism. During the stimulation with bumetanide, the differences of electrical parameters value between group with propolis tincture and Ringer solution group were observed. Skin incubation with 1ml of EEP contained in 100ml of H_2O and blockage of chloride channels after use of bumetanide were influencing better hydration of skin cells and having positive effect on skin layers hydration. The value of the electrical resistance of the skin is affected by skin hydration, its thickness, damage to continuity, the presence of inflammation, and the degree of blood supply to the dermis [32]. As a result of stratum corneum damage, a decrease of electrical skin resistance was observed. The resistance was reduced by direct contact of electric current with the lower layers of the epidermis and a rapid increase in the flow of electric current occurred [32, 33]. During the experiment with the use of 1 ml ethanol extract of propolis dissolved in 100 ml water, a decrease in

Table 2: The comparison of transepithelial electrical resistance between RH solution, 1 ml ethanol extract of propolis in 100 ml of water, and propolis ointment.

Stimulation	($R\ \Omega/cm^2$) median value			U Mann Whitney test (p value)		
	RH	Propolis ointment	1 ml EEP in 100 ml water	RH comparison with propolis ointment	RH comparison with 1 ml EEP in 100 ml water	Propolis ointment comparison with 1 ml EEP in 100 ml water
R_{start} (stimulation RH_1)	1119	1269	1018	0.064	0.211	0.004
R_{medium} (stimulation RH_2)	1184	1273	966	0.055	0.082	< 0.001
R_{finish} (stimulation B, AB)	1049	1257	883	0.027	0.175	< 0.001
Wilcoxon test (p value)						
	RH	Propolis ointment	1 ml EEP in 100 ml water			
R_{start} -R_{medium}	0.345	0.806	< 0.001			
R_{start} - R_{finish}	0.003	0.507	< 0.001			
R_{medium}-R_{finish}	0.085	0.148	< 0.001			

Abbreviations. R_{start} (stimulation RH_1): the value of electrical resistance after the first stimulation by Ringer solution; R_{medium} (stimulation RH_2): the value of electrical resistance after the second stimulation by Ringer solution; R_{finish} (stimulation B, AB): the value of electrical resistance after stimulation by bumetanide and amiloride in bumetanide; R_{start} - R_{medium}: the comparison of the value of the electrical resistance after first stimulation by Ringer solution with the value of electrical resistance second stimulation by Ringer solution; R_{start} - R_{finish}: the comparison of the value of the electrical resistance after first stimulation by Ringer solution with the value of electrical resistance second stimulation by bumetanide and amiloride in bumetanide; R_{medium}-R_{finish}: the comparison of the value of the electrical resistance after first stimulation by Ringer solution with the value of electrical resistance second stimulation by bumetanide and amiloride in bumetanide.

electrical resistance was observed, which occurred as the result of damage to the skin surface. Damage to the skin surface causes a greater impact of irritants and an increased transepidermal water escape from its surface. In dehydrated skin, a decrease in electrical capacity and increase of electrical resistance was observed. The skin is subject to reversed proportions, and the skin's electrical capacity decreases, while its electrical resistance increases [33]. There was no subsequent increase in electrical resistance in the experiment, while a further decreasing electrical resistance was observed. Good skin hydration is characterized by increasing skin electrical capacity and decreasing electrical resistance. In our research bumetanide, which is an inhibitor of transepithelial chloride ions transport, was used. In the same moment when chloride ions transport was inhibited, an increased influx of sodium ions to skin cells and inflow of water into skin cells occurred in the experiment. As a result of the inflow of water, an increased level of skin hydration was observed. The decreasing electrical resistance in the course of the test indicates properly skin hydration. In the scientific literature there are no publications about effects of cosmetic preparations on ions transport in human skin or rabbit skin. On the other hand there are a lot of publications about ions transport in isolated rabbit trachea, respiratory epithelium, large intestine or frog skin. Effect of irritant substance such us capsaicin and its influence on ion transport was described in the publication of Hołyńska-Iwan et al. (2018) [34]. Similarly to the results of the obtained experiment, capsaicin causes some modification of the sodium ions transport, which in turn causes their inflow into the skin cells can improve skin hydration. In addition, capsaicin may modify the action of epithelial sodium channels. Due to the different nature of the tested substances and another experimental procedure, their results are incomparable.

The use of propolis tincture on skin surface influenced sodium ions transport. During amiloride solution and bumetanide solution stimulations, the changes in values of electrophysiological skin parameters did not occur. Propolis ointment did not influence both sodium and chloride ions transport in tested rabbit's skin fragments. The changes of electrophysiological parameters of rabbit's skin during experiments proved that tested epidermal tissue, derived from laboratory animals, was reactive. The skin, thanks to multilevel, bipolar structure, tight intracellular connections, abundant amount of lipids, and keratin, was showing high value of electrical resistance [33]. The values of electrical resistance observed during the study were higher than values obtained for other tissues incubated with the use of Ussing chamber. Data presented in the article written by Wolska et al. [35] illustrate lower values of electrical resistance of experimental rabbits tissues after Ringer solution stimulation in comparison to the results obtained in our study. The value of electrical resistance in Wolska et al. study for rabbits trachea was 129.0 Ohm/cm^2 and for intestine 273 Ohm/cm^2 [35].

The analysis of influence of propolis preparations on value of electrical resistance during our study was proving discrepancy of results between control group (Ringer

solution) and group with propolis ointment and 1ml of ethanol extract of propolis. Propolis ointment and ethanol extract of propolis dissolved in water was showing statistically important difference of electrical resistance. In our study, the use of 1 ml ethanol extract of propolis dissolved in 100 ml water causes a decrease in electrical resistance during the experiment. The use of an propolis ointment did not cause changes in electrical resistance, as well as the use of Ringer solution.

Differences between these values result from different effect of both preparations on skin surface and have influence on their usage. Petrolatum, through occlusive properties, prevents transepidermal water loss and reduces vaporization from skin surface that help to keep water inside its cells. This substance is hydrophobic, insoluble in water. It does not create unpassable barrier and penetrate through cortex layer of epidermis and makes the regeneration after the damage possible despite of occlusive properties [36, 37]. The occlusive properties of petrolatum prevented damage to the skin surface. Long-term application of petrolatum is not recommended because of forming a film on the skin, slowing down gas exchanges and metabolism of skin, and also decreasing water evaporation and increasing tendency to keep filth and pollution on the skin surface [38]. The result of its occlusive influence is an increase of cortex layer hydration level and reduction of transepidermal water loss by 43%.

The occlusive effect induces comedogenic properties. There are the differences between humans and animal examples. The rabbit skin is much more prone to comedogenicity in comparison to the human skin. Vaseline is safe to use in cosmetics thanks to their limited penetration. It improves the skins softness, but works only on superficial epidermis layers. Petroleum jelly prevents penetration of hydrophilic substances through skin [39]. In our study, petrolatum with ethanol extract of propolis was used to obtain propolis ointment. Ethanol extract is a hydrophilic substance. Petrolatum, through its properties of unable penetration of hydrophilic substances, affects the surface of epidermis. Propolis does not penetrate reaching the depths of skin, so it affects only the skin surface. Ethanol, a substrate of second propolis preparation used in our study, strengthens influence of ethanol on transepidermal ion transport and enables the penetration of propolis in skin depths. Ethanol causes an increase of concentration gradient through enhancement of active compound solubility, as a main driving strength transepidermal transport processes. Important element of chemical composition of cosmetics and their later influence on skin surface are the so-called promotors of transepidermal transport. Ethanol is one of the most commonly used sorption promotors. Sorption promotors, through their influence on lipid matrix of epidermis, speed up and facilitating the diffusion through stratum corneum layer of epidermis. Ethanol extract of propolis dissolved in water penetrates deeper in comparison to propolis ointment [40]. Additional factor, which influences the electrical resistance difference between experimental groups I and II, is a manner of preparation of propolis ointment, which is created through propolis extract evaporation in water bath.

The difference in the effect of these substances on electrical resistance is due to the use and cosmetic properties of petrolatum. It is the only cosmetic ingredient which is different in research groups—1 ml ethanol extract of propolis dissolved in 100 ml water and propolis ointment.

Important differences in value of electrical resistance occur in our study during each 15-second stimulation by RH, AMI, B, and AB solutions. Initial raise of electrical resistance for Ringer solution and propolis ointment in above described study can be caused by reduced water loss. Propolis tincture causes reduction of electrical resistance value through deeper skin penetration and progressive changes in hydration and adhesiveness of skin cells.

It seems that the rabbit skin, which was used in experimental model, is appropriate skin equivalent to study the effects of various substances on epidermal tissue properties in comparison to the human skin [41, 42]. Experimental model in reference to the human skin is not perfect. Differences are the result of interspecific variety. The study of Jirova et al. [42] confirms that rabbit skin is more sensitive than human skin. From 16 chemical substances classified as irritant for rabbits' skin, five were significantly irritant for the same human tissue. Reinferath et al. [43] suggest that with hair density growth in animals, permeability of tissues also increases. Our study suggests that human skin has lower transepidermal permeability for xenobiotics in comparison to skin fragments excised from abdominal surface of experimental animals [43]. Influence of preparation containing propolis on electrophysiological parameters rabbit skin is a referential model to specify the influence on electrophysiological parameters of human skin considering existing interspecific differences. Studies show that the manner of substance preparation and its penetration depth influence the ion transport in the skin and the value of electrical resistant. This research is a preliminary, pioneering study demonstrating the effect of propolis on ion transport. There is a need for further research in which propolis component affects the transport of ions.

5. Conclusions

(1) Model skin study in Ussing chamber allows valueing fast, several-second changes of transepidermal ion transport, which are important for transport of various substances into skin and their positive effects.

(2) The studies of transepidermal electrical potential difference in connection to the use of sodium and chloride ions transport inhibitors allow checking the influence of propolis containing substances on the chosen transport of ions.

(3) Ethanol propolis extract dissolved in water influences transepidermal sodium ions transport.

(4) Propolis ointment does not influence transepidermal sodium ions transport.

(5) The way of preparation cosmetics, which contain propolis, has effects on transepidermal ions transport in the rabbit's skin.

(6) The value of skin electrical resistance is changing with penetration depth of active propolis substances contained in cosmetics.

Data Availability

The data used to support the findings of this study are included within the article.

Ethical Approval

The Local Ethical Committee for Animal Experiments at the Faculty of Animal Breeding and Biology of the University of Technology and Life Sciences in Bydgoszcz has given its consent to the research.

Disclosure

This research was performed as part of the employment of the authors in Collegium Medicum in Bydgoszcz, Nicolaus Copernicus University in Torun, Poland.

Conflicts of Interest

The authors have no conflicts of interest to declare.

References

[1] B. Kedzia, "Pochodzenie propolisu w swietle teorii i badan naukowych," *Herba Polonica*, vol. 54, pp. 179–186, 2008.

[2] N. Oršolić, D. Sirovina, M. Z. Končić, G. Lacković, and G. Gregorović, "Effect of Croatian propolis on diabetic nephropathy and liver toxicity in mice," *BMC Complementary and Alternative Medicine*, vol. 12, no. 1, article 117, pp. 117–132, 2012.

[3] S. L. De Castro, "Propolis: Biological and pharmacological activities. Therapeutic uses of this bee-product," *Annual Review of Biomedical Sciences*, vol. 3, pp. 49–83, 2001.

[4] R. Kubina, A. Kabala-Dzik, J. K. Bulda et al., "Ocena wlasciwosci proapoptotycznych etanolowego ekstraktu propolisu w badaniach in vitro," *Postępy Fitoterapii*, vol. 4, pp. 232–237, 2011.

[5] K. Wolska, A. Górska, and A. Adamiak, "Wlasciwosci przeciwbakteryjne propolisu," *Postepy Mikrobiologii*, vol. 55, pp. 343–350, 2016.

[6] L. Kubiliene, V. Laugaliene, A. Pavilonis et al., "Alternative preparation of propolis extracts: Comparison of their composition and biological activities," *BMC Complementary and Alternative Medicine*, vol. 15, no. 1, pp. 156–162, 2015.

[7] B. Kedzia, "Sklad chemiczny i aktywnosc biologiczna propolisu pochodzacego z róznych rejonów swiata," *Postepy Fitoterapii*, vol. 1, pp. 23–35, 2006.

[8] M. Ellnain-Wojtaszek, A. Marcinek, Z. Kowalewski et al., "Standaryzacja wyciągów z propolisu za pomocą ilościowego oznaczania flawonoidów," *Herba Polonica*, vol. 36, pp. 145–153, 1990.

[9] A. Dziedzic, R. Kubina, R. D. Wojtyczka, A. Kabała-Dzik, M. Tanasiewicz, and T. Morawiec, "The antibacterial effect of ethanol extract of polish propolis on mutans streptococci and lactobacilli isolated from saliva," *Evidence-Based Complementary and Alternative Medicine*, vol. 2013, Article ID 681891, 12 pages, 2013.

[10] J. M. Sforcin, A. Fernandes Jr., C. A. M. Lopes, V. Bankova, and S. R. C. Funari, "Seasonal effect on Brazilian propolis antibacterial activity," *Journal of Ethnopharmacology*, vol. 73, no. 1-2, pp. 243–249, 2000.

[11] R. D. Wojtyczka, M. Kępa, D. Idzik et al., "In vitro antimicrobial activity of ethanolic extract of polish propolis against biofilm forming staphylococcus epidermidis strains," *Evidence-Based Complementary and Alternative Medicine*, vol. 2013, Article ID 590703, 11 pages, 2013.

[12] S. Osés, A. Pascual-Maté, M. Fernández-Muiño, T. López-Diaz, and M. Sancho, "Corrigendum to "Bioactive properties of honey with propolis"," *Food Chemistry*, vol. 196, pp. 1215–1223, 2016.

[13] H. Koo, B. P. F. A. Gomes, P. L. Rosalen, G. M. B. Ambrosano, Y. K. Park, and J. A. Cury, "In vitro antimicrobial activity of propolis and Arnica montana against oral pathogens," *Archives of Oral Biolog*, vol. 45, no. 2, pp. 141–148, 2000.

[14] P. Schnitzler, A. Neuner, S. Nolkemper et al., "Antiviral activity and mode of action of propolis extracts and selected compounds," *Phytotherapy Research*, vol. 24, no. 1, pp. 20–28, 2010.

[15] R. Socha, L. Juszczak, S. Pietrzyk, D. Gałkowska, T. Fortuna, and T. Witczak, "Phenolic profile and antioxidant properties of Polish honeys," *International Journal of Food Science & Technology*, vol. 46, no. 3, pp. 528–534, 2011.

[16] P. Olczyk, P. Ramos, K. Komosinska-Vassev, J. Stojko, and B. Pilawa, "Positive effect of propolis on free radicals in burn wounds," *Evidence-Based Complementary and Alternative Medicine*, vol. 2013, Article ID 356737, 12 pages, 2013.

[17] A. M. Kurek-Górecka, A. Sobczak, A. Rzepecka-Stojko, M. T. Górecki, M. Wardas, and K. Pawłowska-Góral, "Antioxidant activity of ethanolic fractions of Polish propolis," *Zeitschrift für Naturforschung C*, vol. 67, no. 11-12, pp. 545–550, 2012.

[18] M. Leja, A. Mareczek, G. Wyzgolik, J. Klepacz-Baniak, and K. Czekońska, "Antioxidative properties of bee pollen in selected plant species," *Food Chemistry*, vol. 100, no. 1, pp. 237–240, 2007.

[19] N. Zabaiou, A. Fouache, A. Trousson et al., "Biological properties of propolis extracts: Something new from an ancient product," *Chemistry and Physics of Lipids*, vol. 207, pp. 214–222, 2017.

[20] M. Viuda-Martos, Y. Ruiz-Navajas, J. Fernández-López, and J. A. Pérez-Álvarez, "Functional properties of honey, propolis, and royal jelly," *Journal of Food Science*, vol. 73, no. 9, pp. R117–R124, 2008.

[21] A. H. Banskota, Y. Tezuka, I. K. Adnyana et al., "Cytotoxic, hepatoprotective and free radical scavenging effects of propolis from Brazil, Peru, the Netherlands and China," *Journal of Ethnopharmacology*, vol. 72, no. 1-2, pp. 239–246, 2000.

[22] S. E. Walgrave, E. M. Warshaw, and L. A. Glesne, "Allergic contact dermatitis from propolis," *Dermatitis*, vol. 16, no. 4, pp. 209–215, 2005.

[23] A. C. De Groot, "Propolis: a review of properties, applications, chemical composition, contact allergy, and other adverse effects," *Dermatitis*, vol. 24, no. 6, pp. 263–282, 2013.

[24] B. Banach, "Elektrofizjologiczna charakterystyka transport jonów w izolowanej scianie tchawicy po dzialaniu bodzców mechanicznych i hamowaniu transportu sodu," *Roczniki Pomorskiej Akademii Medycznej w Szczecinie*, vol. 53, pp. 56–67, 2007.

[25] S. K. Inglis, R. E. Olver, and S. M. Wilson, "Differential effects of UTP and ATP on ion transport in porcine tracheal epithelium," *British Journal of Pharmacology*, vol. 130, no. 2, pp. 367–374, 2000.

[26] T. Tyrakowski, I. Greczko, A. Sedlaczek et al., "Electrophysiological investigation of the effects of ambroxol on the transepithelial Na+ ion transport pathway in airways," *Polish Journal of Pharmacology*, vol. 50, no. 1, pp. 31–38, 1998.

[27] E. Piskorska, I. Hołyńska-Iwan, P. Kaczorowski et al., "Toluene diisocyanate caused electrophysiological disturbances in the upper airways wall," *International Journal of Occupational Medicine and Environmental Health*, vol. 22, no. 2, pp. 125–134, 2009.

[28] D. Kosik-Bogacka and T. Tyrakowski, "Ion transport in rabbit caecum at 12 and 36 months of age.," *Journal of Physiology and Pharmacology*, vol. 55, pp. 117–128, 2004.

[29] S. R. Jared and J. P. Rao, "Transepithelial sodium transport across frog skin," *Advances in Physiology Education*, vol. 41, no. 3, pp. 444–447, 2017.

[30] E. Wolska, N. Młodzik, and K. Sliwka, *Teoretyczne podstawy zjawisk elektrycznych zachodzących w tkankach nabłonkowych*, 2003, http://www.amsik.pl/index.php?option=com_content&task=view&id=235.

[31] I. Holynska-Iwan, P. Panek, and E. Piskorska, "Przeznabłonkowy transport jonów oraz wody w nabłonku oddechowym," in *Postęp medycyny w leczeniu i ochronie zdrowia*, P. Kicinski and B. Drop, Eds., pp. 235–244, Tom I, Lublin, Poland, 2016.

[32] J. Maimivuo and R. Pionsey, "The electrodermal response," in *Bioelectro Magnetism*, J. Maimivuo and R. Pionsey, Eds., pp. 428–434, Oxford University Press, Nowy Jork, NY, USA, 1995.

[33] K. Chabowski and A. Reich, "Badanie zmian rezystancji skóry w trakcie przepływu prądu elektrycznego," *Dermatologia Kliniczna*, vol. 12, no. 2, pp. 91–94, 2010.

[34] I. Hołyńska-Iwan, I. Dziembowska, P. Smyk, M. Lampka, and D. Olszewska-Słonina, "Capsaicin Used on Skin Influences Ion Transport Pathways: An in vitro Study," *Skin Pharmacology and Physiology*, vol. 31, no. 1, pp. 19–27, 2018.

[35] E. Wolska, N. Mlodzik-Danielewicz, B. Banach, and T. Tyrakowski, "Effect of amiloride and bumetanide on transepithelial ion transport in isolated rabbit cecal and colonic wall," *Postepy Higieny i Medycyny Doswiadczalnej*, vol. 59, pp. 229–235, 2005.

[36] R. Ghadially, L. Halkier-Sorensen, and P. M. Elias, "Effects of petrolatum on stratum corneum structure and function," *Journal of the American Academy of Dermatology*, vol. 26, no. 3, pp. 387–396, 1992.

[37] Cosmetics INFO, 2018, http://www.cosmeticsinfo.org/ingredient/petrolatum-0.

[38] K. Tobiś, "Negatywny wpływ wybranych składników preparatów kosmetycznych na skórę a świadomość klientek gabinetów kosmetycznych," in *Kosmetologia*, A. Wolska, Ed., 71, p. 47, Studenckie Zeszyty Naukowe, E-Publishing Inc., Warszawa, Poland, 2016.

[39] A. V. Rawlings and K. J. Lombard, "A review on the extensive skin benefits of mineral oil," *International Journal of Cosmetic Science*, vol. 34, no. 6, pp. 511–518, 2012.

[40] M. Jaworska, E. Sikora, and J. Ogonowski, "Czynniki wpływające na penetrację składników aktywnych przez skórę," *Wiadomości Chemiczne*, vol. 65, pp. 3-4, 2011.

[41] J. Olejnik, I. Gościańska, and Nowak., "Zastosowanie modeli sztucznej skóry do badan kosmetyków innowacyjnych," *Chemik*, vol. 65, pp. 76–81, 2011.

[42] D. Jírová, D. Basketter, M. Liebsch et al., "Comparison of human skin irritation patch test data with in vitro skin irritation assays and animal data," *Contact Dermatitis*, vol. 62, no. 2, pp. 109–116, 2010.

[43] W. G. Reifenrath, "Enhanced skin absorption and fly toxicity of permethrin in emulsion formulation," *Bulletin of Environmental Contamination and Toxicology*, vol. 78, no. 5, pp. 299–303, 2007.

Hindawi
Evidence-Based Complementary and Alternative Medicine
Volume 2018, Article ID 4181084, 14 pages
https://doi.org/10.1155/2018/4181084

Research Article

Pharmacokinetics and Tissue Distribution Study of Pinosylvin in Rats by Ultra-High-Performance Liquid Chromatography Coupled with Linear Trap Quadrupole Orbitrap Mass Spectrometry

Yuhang Fu,[1,2] Xiaoya Sun,[1,2] Lili Wang,[1,2] and Suiqing Chen [1,2]

[1]*School of Pharmacy, Henan University of Chinese Medicine, No. 156, East Jinshui Road, Zhengzhou, 450046, China*
[2]*Collaborative Innovation Center for Respiratory Disease Diagnosis and Treatment & Chinese Medicine Development of Henan Province, Henan University of Chinese Medicine, No. 156, East Jinshui Road, Zhengzhou, 450046, China*

Correspondence should be addressed to Suiqing Chen; suiqingchen0371@163.com

Received 14 September 2018; Revised 27 October 2018; Accepted 7 November 2018; Published 21 November 2018

Guest Editor: Jiang Ma

Pinosylvin is a potential anti-inflammatory and antioxidant compound and the major effective medicinal ingredient in the root of *Lindera reflexa* Hemsl. However, few investigations have been conducted regarding the pharmacokinetics, excretion, characteristics of tissue distribution, and major metabolites of pinosylvin in rats after oral administration. To better understand the behavior and mechanisms of action underlying the activity of pinosylvin *in vivo*, we established a simple, sensitive, and reliable ultra-high-performance liquid chromatography tandem mass spectrometry (UPLC-MS/MS) method for quantifying pinosylvin in rat plasma, urine, feces, and various tissues (including heart, liver, spleen, lung, kidneys, large intestine, small intestine, and stomach). Noncompartmental pharmacokinetic parameters indicated that pinosylvin is rapidly distributed and taken up by tissues. The time to peak (maximum) concentration (T_{max}) was 0.137 h, and the apparent elimination half-life ($t_{1/2}$) was 1.347±0.01 h. The results of the tissue distribution study suggest that pinosylvin is widely distributed to various tissues; the highest concentration was observed after 10 min in the stomach, followed by the heart, lung, spleen, and kidneys. Results of the excretion study suggest that a small amount of pinosylvin is excreted from the urine and feces in the parent form; the 73 h accumulative excretion ratios of urine and feces were 0.82% and 0.11%, respectively. It is likely that pinosylvin is mostly metabolized *in vivo*. Nine metabolites were found, and the main metabolic pathways of pinosylvin in rats included glucuronidation, hydroxylation, and methylation. Four metabolites had higher concentrations in the stomach, suggesting that the stomach is a potential target organ of pinosylvin. In conclusion, the present study may provide a material basis for studying the pharmacological action of pinosylvin and provides meaningful information for the clinical treatment of chronic gastritis and gastric ulcers using Radix Linderae Reflexae.

1. Introduction

Pinosylvin (3,5-dihydroxy-trans-stilbene) is a naturally occurring stilbenoid mainly found in the leaves or wood of various *Pinus* species [1, 2] and Lauraceae plants [3, 4]; it is structurally similar to the polyphenol resveratrol. Studies have shown that pinosylvin improves resistance to decay in heartwood. Further, pinosylvin has been shown to have various biological activities, including antifungal and antibacterial [5], cancer chemopreventive/anti-inflammatory [6], cell proliferative, antioxidant [7, 8], vasculo-protective [9], and antiproliferative effects in various cancer cells [10, 11]. Pinosylvin promotes cell proliferation in bovine aortic endothelial cells [7, 12] but inhibits proliferation in human lymphoblastoid cell lines [13].

Radix Linderae Reflexae originates from the root of *Lindera reflexa* Hemsl, which is a new herbal drug listed in the *Dictionary of Chinese Medicine* and has recently been prescribed for the treatment of gastritis and peptic ulcers [14, 15]. Screening experiments for the effective components

of Radix Linderae Reflexae showed that the n-butyl alcohol groups significantly improve gastric ulcers. Pinosylvin is included in the n-butyl alcohol groups of Radix Linderae Reflexae [3, 16].

It is well known that pharmacokinetics and characteristics of tissue distribution are vital to understanding *in vivo* behavior and mechanisms of action. To date, a novel and simple high-performance liquid chromatographic method was used for simultaneous determination of pinosylvin in rat serum, and it has been confirmed that plasma levels of pinosylvin decline rapidly after intravenous administration, attributable to a short half-life [17, 18]. However, there are few reports on the pharmacokinetics, excretion, characteristics of tissue distribution, and identification of major metabolites of pinosylvin in rats after oral administration as a single compound.

The goal of this study was to evaluate the metabolic processes associated with pinosylvin in rats and determine target organs by exploring the pharmacokinetics, excretion, characteristics of tissue distribution, and major metabolites after oral administration. This study provides helpful information regarding the clinical study of pinosylvin, as well as traditional Chinese medicines containing pinosylvin.

2. Materials and Methods

2.1. Chemicals and Reagents. Pinosylvin was isolated in our laboratory from the root of *Lindera reflexa* Hemsl and identified using nuclear magnetic resonance (NMR), mass spectrometry (MS), ultraviolet (UV), and infrared (IR) analyses. Isoliquiritigenin (high-performance liquid chromatography [HPLC] ≥ 98%) was used as the internal standard and purchased from Shanghai Yuanye Bio-Technology Co. Ltd. Heparin sodium was purchased from Beijing Dingguo Changsheng Bio-Technology Co. Ltd. Methanol, acetonitrile, and formic acid were HPLC-grade reagents from Fisher Scientific (Fairlawn, NJ, USA). Deionized water was prepared by passing distilled water through a Milli-Q water purification system (Millipore, Milford, MA, USA).

2.2. Instrumentation and Ultra-High-Performance Liquid Chromatography Tandem Mass Spectrometry (UPLC-MS/MS) Conditions. The UPLC-MS/MS system consisted of a Dionex Ultimate 3000 UHPLC system (Thermo Scientific, Germering, Bavaria, Germany) equipped with a binary pump, a thermostatted autosampler, a thermostatically controlled column compartment, a diode array detector (DAD), and a Thermo Fisher LTQ-Orbitrap XL Hybrid Mass Spectrometer with an electrospray ionization (ESI) source. The system control and data analysis were performed using Xcalibur 3.0 software (Thermo Fisher Scientific).

Chromatographic separation was carried out on a reverse-phase Hypersil GOLD C18 column (2.1×50 mm, 1.9 μm) with a UPLC filter (2.1 mm × 0.2 μm) guard column (Thermo Fisher Scientific). The UPLC was operated with a gradient mobile phase system comprising water containing 0.1% formic acid (phase A) and acetonitrile (phase B) at a flow rate of 0.3 ml/min and maintained at 30°C [19]. The pump was programmed as follows: 0.0–1 min, 30% B; 1.0–12.0 min, 30.0–50% B; 12.0–15 min, 50.0–100% B; 15.0–15.1 min, 100.0–30.0% B; 15.1–18.0 min, 30.0%. A 5-μl sample was injected into the system with the autosampler conditioned at 7°C.

The mass spectrometer was operated in positive ion mode. Selected ion monitoring (SIM) was used, and the fragmentation transitions were m/z 213.09 for pinosylvin and m/z 257.08 for isoliquiritigenin (Figure 1). The ESI source parameters were set as follows: ion spray voltage, 4200 V; capillary temperature, 350°C; capillary voltage, 23 V; and tube lens voltage, 90 V. The flow rates of sheath (N_2) and auxiliary gas (He) were 40 and 10 arbitrary units, respectively.

2.3. Collection and Treatment of the Plasma, Urine, Feces, and Tissues. Sprague-Dawley (SD) male rats weighing 180–220 g were provided by Henan Experimental Animal Center (Zhengzhou, China). All rats were kept in an environmentally controlled breeding room maintained at a temperature of 22 ± 2°C with relative humidity of 50% and were fed standard laboratory food and water for one week prior to the experiments. All rats were fasted overnight with access to water only before experiments.

Blood samples were obtained from the rat orbital vein and placed into centrifuge tubes containing heparin sodium (20 μl, 1%). The blood samples were immediately centrifuged at 10000 rpm for 10 min (4°C), and the supernatant was gathered as the plasma. Urine and feces were collected in metabolic cages and packed separately with centrifuge tubes as samples [20]. Various tissues (including heart, liver, spleen, lung, kidney, large intestine, small intestine, and stomach) were harvested and rinsed with ice-cold 0.9% NaCl to remove the superficial blood and contents. After being blotted dry with filter paper, certain equal amounts of tissues were accurately weighed and homogenized in 0.9% NaCl to prepare the homogenates (1:2, m/v) [21].

2.4. Standard and Sample Preparation

2.4.1. Preparation of Stock and Working Solutions. The stock solutions were prepared by dissolving pinosylvin and isoliquiritigenin in methanol to reach a final concentration of 5.40 mg/mL and 0.55 mg/mL, respectively. The stock working solution of pinosylvin was serially diluted with methanol to a linear concentration of 0.0027–1728.0000 μg/ml. An isoliquiritigenin solution (IS, 100 ng/ml) was prepared in methanol. All solutions were stored at 4°C in the dark.

2.4.2. Preparation of Calibration Standards and Quality Control (QC) Samples. Calibration curves were prepared by spiking the standard working stock solutions with 10 μl of the different concentrations, 20 μl IS (110 ng/ml), and 90 μl blank rat plasma, urine, feces, or tissue homogenate sample in a 1.5-ml centrifuge tube on the analysis day. The calibration standards were prepared at concentrations of 0.0027, 0.0054, 0.1080, 0.1350, 0.2700, and 0.5400 μg/ml for the plasma; 0.0027, 0.5400, 1.3500, 2.7000, 5.4000, 13.5000, 27.0000, and 54.0000 μg/ml for urine; 0.1350, 0.2700, 1.3500, 2.7000, 5.4000, and 27.0000 μg/ml for the feces, spleen, and kidney; 0.2700, 0.5400, 1.3500, 2.7000, 5.4000, 13.5000, 27.0000, and

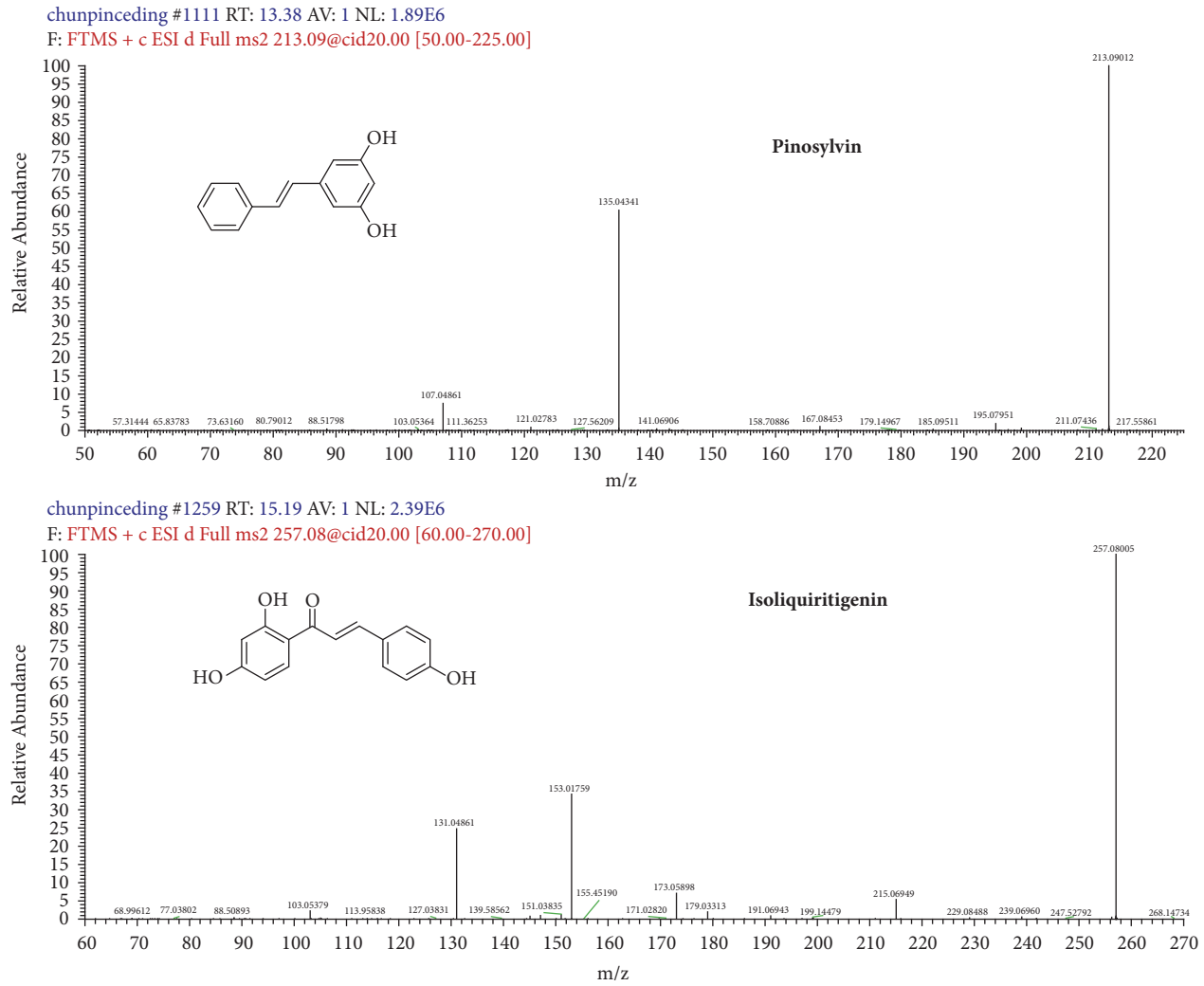

Figure 1: Chemical structures and mass spectra of pinosylvin and isoliquiritigenin (IS).

54.0000 μg/ml for the heart; 1.3500, 2.7000, 13.5000, 27.0000, 54.0000, and 108.0000 μg/ml for the liver and large intestine; 0.5400, 1.3500, 2.7000, 5.4000, 13.5000, and 27.0000 μg/ml for the lung; 2.7000, 5.4000, 13.5000, 27.0000, 54.0000, 108.0000, 216.0000, and 432.0000 μg/ml for the small intestine; 1.3500, 2.7000, 5.4000, 13.5000, 27.0000, 54.0000, 108.0000, 216.0000, 432.0000, 864.0000, and 1728.0000 μg/ml for the stomach. Quality control (QC) samples were prepared in the same way with blank plasma, urine, feces, or tissue homogenates at concentrations of 0.0054, 0.1350, and 0.5400 μg/ml for the plasma; 0.2700, 2.7000, and 5.4000 μg/ml for the feces; 1.3500, 5.4000, and 54.0000 μg/ml for the urine; 0.5400, 5.4000, and 27.0000 μg/ml for the heart; 2.7000, 13.5000, and 54.0000 μg/ml for the liver and large intestine; 0.2700, 5.4000, and 13.5000 μg/ml for the spleen; 0.5400, 2.7000, and 13.5000 μg/ml for the lung; 0.5400, 5.4000, and 13.5000 μg/ml for the kidney; 5.4000, 108.0000, and 216.0000 μg/ml for the small intestine; 13.5000, 216.0000, and 864.0000 μg/ml for the stomach. Moreover, the concentration of IS in all samples was 110.0000 ng/ml.

2.4.3. Sample Treatment. A simple liquid-liquid extraction (LLE) method was used to extract pinosylvin from QC samples, calibration standards, and all biosamples (including plasma samples, urine samples, fecal samples, and tissue homogenate samples). After biosamples were thawed at room temperature, 100-μl aliquots were transferred to 1.5-ml tubes. The samples were first vortex-mixed with IS (10 μl, 110 ng/ml) and then with a solution of methanol-acetonitrile (0.9 ml, 5:95, v/v) for extraction. After vortexing for 5 min and centrifuging at 10000 rpm, 4°C for 10 min. The supernatant (900 μl) was transferred to a new 1.5-ml centrifuge tube and evaporated to dryness under vacuum. The dried residue was reconstituted with 50 μl methanol, vortex-mixed at 2000 k for 5 min, and centrifuged at 16000 rcf (4°C for 10 min). Finally, the supernatant liquid (5 μl) was injected into the UPLC-ESI-MS/MS system.

2.5. Method Validation. The developed method was validated according to the China Food and Drug Administration

(CFDA) technical guidelines for the study of nonclinical pharmacokinetics.

2.5.1. Specificity. Specificity of the method was assessed by analyzing blank biological samples from at least six different sources (plasma, urine, feces, and various tissue homogenate samples), blank biological matrix samples spiked with pinosylvin and IS, and actual biosamples after oral administration of pinosylvin and spiking with IS.

2.5.2. Linearity and Sensitivity. The calibration standards of pinosylvin were in the concentration range of 0.0027–0.5400 μg/ml for plasma samples; 0.0027–54.0000 μg/ml for urine samples; 0.1350–27.0000 μg/ml for feces, and 0.1350–1728.0000 μg/ml for tissue samples. Calibration curves were established by plotting the peak area ratios of the analytes to IS (Y-axis) versus the nominal concentration of pinosylvin (X-axis) using weighted least-squares linear regression analysis.

The lowest concentration on the calibration curve was set as the lower limit of quantification (LLOQ), and we determined the drug concentration in the sample for at least 3–5 half-lives as required. The precision and accuracy of LLOQ should not exceed 20%.

2.5.3. Precision and Accuracy. Precision and accuracy were assessed with the QC samples (low, middle, and high concentration) in five replicates prepared and analyzed on three consecutive days. Intraday and interday precision was evaluated with relative standard deviation (RSD%) values. To assess the accuracy, the relative error (RE%) was calculated according to the following formula: RE% = [(assayed value - normal value)/normal value]×100%. An accuracy within ±15% of the RE and a precision ≤ 15% of the RSD (all of them near the lower limit and should be less than 20%) were deemed acceptable.

2.5.4. Extraction Recovery and Matrix Effects. The extraction recoveries in rat sample matrices for pinosylvin and the IS were calculated as the peak area ratios of the rat sample matrix spiked with a standard solution to the blank matrix spiked with an equivalent standard solution. The recovery of pinosylvin was determined at low, medium, and high concentrations, while the recovery of the IS was determined at a single concentration of 110 ng/ml.

The matrix effect of extraction on pinosylvin was evaluated by comparing the peak areas of the methanol-acetonitrile (5:95, v/v) extracted blank samples spiked with pinosylvin at three QC concentrations with those of the pinosylvin standard solution at equivalent concentrations.

2.5.5. Stability. Stability was investigated by analyzing five replicates of the samples at three QC levels under different conditions, including storage for 24 h in the autosampler, three freeze/thaw cycles, storage for 12 h at ambient temperatures (25°C), and storage at -80°C for 30 days. The samples were considered stable if the average percentage concentration deviation was within 15% of the actual value.

2.6. Pharmacokinetic Study. For the pharmacokinetic study, blank blood samples were collected from the orbital vein of rats using sterile capillary tubes. After oral administration of pinosylvin (49.44 mg/kg dissolved in 0.1% sodium carboxymethyl cellulose) to SD rats (n=6), approximately 200 μl blood was collected into heparinized tubes at 8 min, 10 min, 20 min, 30 min, 45 min, 60 min, 80 min, 100 min, 2 h, 4 h, 6 h, 12 h, and 24 h. The samples were immediately centrifuged at 10000 rpm for 10 min and 4°C, and the supernatant plasma layer (100 μl) was transferred to a new 1.5-ml centrifuge tube and stored at -80°C until analysis.

2.7. Excretion Study. For the excretion study, blank urine samples and fecal samples were collected using metabolic cages. After oral administration of pinosylvin (49.44 mg/kg dissolved in 0.1% sodium carboxymethyl cellulose) to SD rats (n=6), urine and feces were collected at 0–2 h, 2–4 h, 4–8 h, 8–10 h, 10–12 h, 12–24 h, 24–36 h, 36–48 h, 48–60 h, and 60–73 h. Urine volumes were recorded, and 100 μl was transferred to centrifuge tubes for use as the urine samples. Fecal weights were recorded after drying in a dark environment; the resulting powders (0.05 g) were added to centrifuge tubes and then mixed with NaCl (200 μl, 0.9% solution) for use as the fecal samples. All the samples were stored at -80°C until analysis.

2.8. Tissue Distribution Study. For the tissue distribution study, 36 rats were randomly assigned to six groups (6 rats/group) and sacrificed at 10 min, 20 min, 1 h, 2 h, 6 h, and 8 h after orally administering pinosylvin (49.44 mg/kg dissolved in 0.1% sodium carboxymethyl cellulose). Subsequently, the heart, liver, spleen, lungs, kidneys, large intestine, small intestine, and stomach were immediately removed, washed in normal saline, and blotted dry with filter paper. An accurately weighed amount of fresh tissue sample (0.25 g) was individually homogenized with normal saline (0.5 ml) and transferred (100 μl) as a tissue homogenate to 1.5-ml centrifuge tubes for use as the tissue samples. All tissue samples were stored at -80°C until analysis.

2.9. Analysis of Metabolites. We used MetWorks™ 1.3 SP4 software (Henan University of Chinese Medicine, Zhengzhou, China) to analyze the metabolite and biosample data collected via Xcalibur 3.0 software (Thermo Fisher Scientific); the aim was to further describe the metabolite profiles of pinosylvin in rat plasma and tissue.

2.10. Data Analysis. DAS 3.2.8 software (Henan University of Chinese Medicine, Zhengzhou, China) was used to calculate the pharmacokinetic parameters using a noncompartmental model, including half-life ($t_{1/2}$), area under the curve (AUC), apparent central volume of mean residual time (MRT), and clearance rate (CL). All other results are expressed as means ± SD. Concentrations of pinosylvin in rat urine and feces were calculated according to their respective calibration curves using the ratio of their peak area to that of the IS using the following equation: excretion ratio = [measured concentration × volume (weight)/dosage]×100%.

Table 1: Calibration curve, correlation coefficients, and linear ranges of pinosylvin in different biosamples.

Samples	Calibration Curve	Correlation Coefficient (r)	Linear range (μg/ml)
Plasma	Y=0.9749X+0.1711	0.9997	0.0027-0.5400
Urine	Y=1.4788X+1.1261	0.9936	0.0027-54.0000
Feces	Y=0.6249X-0.3637	0.9995	0.1350-27.0000
Heart	Y=2.8938X+0.3503	0.9964	0.2700-54.0000
Liver	Y=4.3646X-0.3492	0.9974	1.3500-108.0000
Spleen	Y=2.2020X+0.2676	0.998	0.1350-27.0000
Lung	Y=1.6875X+0.3068	0.9995	0.5400-27.0000
Kidney	Y=1.5383X+0.1088	0.9987	0.1350-27.0000
Large intestine	Y=0.9523X+1.0799	0.9916	1.3500-108.0000
Small intestine	Y=2.3900X+15.9520	0.9932	2.7000-432.0000
Stomach	Y=3.3719X-7.1728	0.9968	1.3500-1728.0000

3. Results and Discussion

3.1. Optimization of UPLC-MS/MS Conditions and Extraction Method. The LTQ-Orbitrap conditions were systematically optimized; full scan was used in the positive and negative detection mode after individually injecting approximately 540 ng/ml pinosylvin in methanol and 110 ng/ml IS in methanol. The results show that sensitivity was higher for pinosylvin and IS when analyzed in the positive ion mode. Pinosylvin and isoliquiritigenin predominantly gave a singly charged protonated precursor $[M+H]^+$ at m/z 213.09 and 257.08 in Q1 full scan mode, respectively. Therefore, selected ion monitoring (SIM) was used, and the fragmentation transitions were m/z 213.09 for pinosylvin and m/z 257.08 for isoliquiritigenin.

The UPLC conditions, including the mobile phase systems and the type of chromatographic columns. The results show that acetonitrile gave a better peak shape and lower background noise than methanol as the organic phase. Further, pinosylvin and IS had a higher response when the water phase contained 0.1% formic acid. Retention times for both pinosylvin and IS were less than 5 min when using the Hypersil GOLD C18 column with a shorter length (50 mm) when the mobile phase was set at a flow rate of 0.3 ml/min. These parameters improved the speed of sample analysis.

The solid phase extraction column was first considered for use in sample preparation; however, the extraction recovery did not meet the analytical requirements. Therefore, a liquid-liquid extraction (LLE) method was chosen for sample preparation. We found that methanol-acetonitrile (5:95, v/v) was the best choice as an extraction solvent, yielding a higher extraction ratio and lower background interference.

3.2. Method Validation

3.2.1. Selectivity. Due to the high selectivity and specificity of SIM mode by the linear trap Quadrupole Orbitrap Mass Spectrometer, no endogenous interference was observed at retention times of 4.70 min (pinosylvin) or 3.46 min (IS). Typical chromatograms of blank plasma, urine, feces, and stomach homogenates; blank plasma, urine, feces, stomach, and liver spiked with pinosylvin and IS; and all biosamples after oral administration of pinosylvin are presented in Figure 2.

3.2.2. Calibration Curves and LLOQ. Calibration curves used to determine coefficients and linear ranges of pinosylvin in plasma, urine, feces, and each tissue are listed in Table 1. Further, calibration curves for all matrices showed good linearity (r>0.9916) over the concentration ranges. LLOQs were 0.0027 μg/ml (S/N>10) for plasma and urine; 0.2700 μg/ml for heart; 0.1350 μg/ml for feces, spleen, and kidney; 1.3500 μg/ml for liver, stomach, and large intestine; 0.5400 μg/ml for lung; and 2.7000 μg/ml for small intestine.

3.2.3. Precision and Accuracy. The results for intra- and interday precision and accuracy at three QC concentrations are presented in Table 2. The intra- and interday accuracy were within -10.8 % to 11.6%, respectively, while the intra- and interday precision were less than 14.7% and within the acceptable criteria of ±15%, indicating that the precision and accuracy of this assay were within acceptable ranges for analysis.

3.2.4. Extraction Recovery and Matrix Effect. The extraction recovery and matrix effect for pinosylvin are shown in Table 3. All extraction recoveries of pinosylvin (at three concentration levels) and IS (at 110 ng/ml) in biosamples ranged from 83.3% to 108.5% with a RSD% less than 13.3%, demonstrating that the extraction method was acceptable and met the requirements of analysis. The absolute matrix effect values of pinosylvin ranged from 81.3% to 114.8%, with a RSD% less than 13.5%. These results indicate that, for this UPLC-MS/MS determination, there were no significant matrix effects for pinosylvin in the plasma, urine, feces, or tissue samples.

3.2.5. Stability. Stability was tested under various conditions that might occur during sample preparation. The results shown in Table 4 demonstrate that pinosylvin was stable in rat plasma, urine, feces, and tissue homogenates after storage

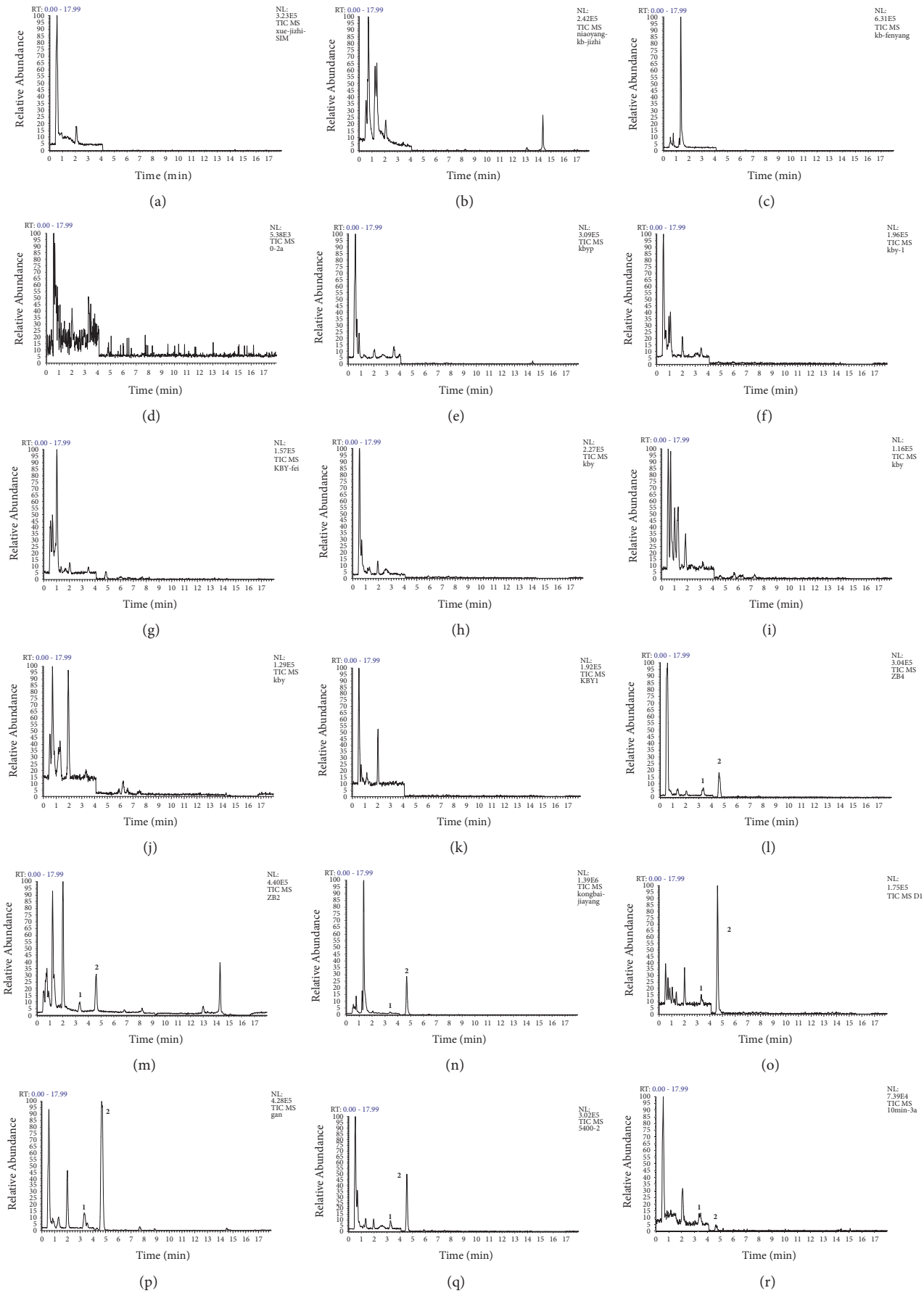

Figure 2: Continued.

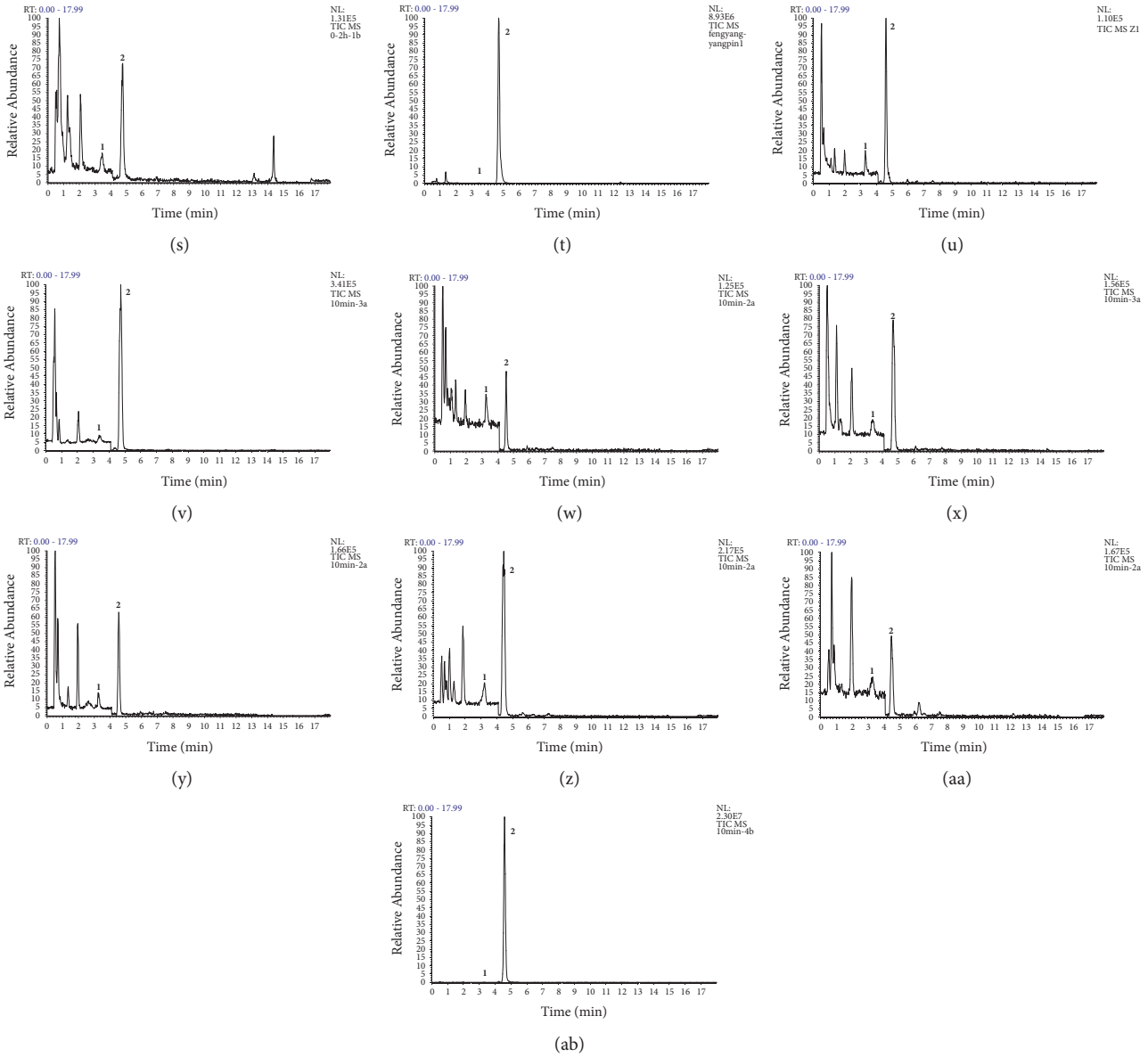

Figure 2: Representative selected ion monitoring (SIM) chromatograms of blank plasma (a), blank urine (b), blank feces (c), blank heart (d), blank liver (e), blank spleen (f), blank lung (g), blank kidney (h), blank large intestine (i), blank small intestine (j), blank stomach (k), plasma spiked with pinosylvin and isoliquiritigenin solution (IS) (l), urine spiked with pinosylvin and IS (m), feces spiked with pinosylvin and IS (n), stomach spiked with pinosylvin and IS (o), liver spiked with pinosylvin and IS (p), kidney spiked with pinosylvin and IS (q), plasma sample (r) obtained 10 min after oral administration of 49.44 mg/kg pinosylvin, urine sample (s) obtained 0–2 h after oral administration of 49.44 mg/kg pinosylvin, feces sample (t) obtained 4–6 h after oral administration of 49.44 mg/kg pinosylvin, and heart sample (u), liver sample (v), spleen sample (w), lung sample (x), kidney sample (y), large intestine sample (z), small intestine sample (aa), stomach sample (ab) obtained 10 min after oral administration of 49.44 mg/kg pinosylvin. Peak 1 reflects IS, and peak 2 reflects pinosylvin.

for 24 h in the autosampler, three freeze/thaw cycles, storage for 12 h at ambient temperature, and storage at -80°C for 30 days.

3.3. Pharmacokinetic Study. The validated UPLC-MS/MS method was successfully used to investigate the pharmacokinetics of pinosylvin after oral administration at a dose of 49.44 mg/kg. The mean plasma concentration-time curves are shown in Figure 3. The corresponding pharmacokinetic parameters calculated with noncompartmental analysis are listed as means ± SD and shown in Table 5.

The results show that the time to peak (maximum) concentration (T_{max}) was 0.137 h after oral administration in rats, and the peak (maximum) plasma concentration

Table 2: Intra- and interassay precision and accuracy for determining pinosylvin in rat plasma, urine, feces, and various tissue homogenates (n=3 days, 5 replicates per day).

Bio-sample	Nominal concentration (ng/mL)	Inter-day (n=5)		Intra-day (n=15)	
		Precision RSD (%)	Accuracy R.E (%)	Precision R.S.D (%)	Accuracy R.E (%)
Plasma	5.4	2.7	7.5	3.7	9.4
	135	10	-6.1	10.1	-7.4
	540	4.8	0.2	9.4	6.5
Urine	1350	0.7	9.5	1.7	9.9
	5400	8.6	-7.4	8	-7.8
	54000	6.4	-6.3	4.5	-2.9
Feces	270	8.6	-5.4	9.8	2.4
	2700	8.3	-3.6	9.6	-1.1
	5400	9.3	-3.5	9.5	-5.9
Heart	540	9.1	-4.7	9.8	6.4
	5400	4.4	2.1	7.3	4.1
	27000	3	10	3	9.6
Liver	2700	6.6	-4.8	9	-5.3
	13500	0.8	0.09	9.5	7
	54000	4.6	8.4	5.1	9.7
Spleen	270	1.2	9.9	1.7	11.6
	5400	7.9	0.2	8.9	4.8
	13500	9.2	-8.7	9.8	-7.3
Lung	540	6.1	9.8	6.4	10.7
	2700	8.6	-2.5	9.6	3
	13500	6.5	9	8.6	11
Kidney	540	6	-7.9	9.5	-8.5
	5400	5.2	-3.1	6.1	-3.9
	13500	7.6	-10.8	9.1	-8.7
Large intestine	2700	12.4	-8.6	11.9	-1.4
	13500	6.5	-9.4	10	-7.5
	54000	4.1	3.4	7.1	2
Small intestine	5400	2.2	9	10.7	8.9
	108000	8.4	1.1	9.7	2.3
	216000	8.6	1.7	7.2	7.3
Stomach	13500	14.3	7.5	13.5	4.6
	216000	13.1	-0.2	14.2	2.4
	864000	12.1	-8.5	14.7	-4.8

(C_{max}) of pinosylvin was 164.231 ± 64.264 ng/ml. The plasma concentration of pinosylvin decreased sharply from 160.929 ng/ml to 22.581 ng/ml after 2 h. The apparent elimination half-life ($t_{1/2}$) was 1.347 ± 0.01 h, indicating pinosylvin was quickly cleared from the rat plasma. The $AUC_{0\text{-}24h}$ and $AUC_{0\text{-}\infty}$ were 711.142 ± 46.885 and 711.195 ± 46.885, respectively. The apparent volume of distribution (V_d) results imply that pinosylvin is taken up by the tissues after oral administration [18, 22, 23].

To our knowledge, there are no reports regarding the pharmacokinetics of pinosylvin administered orally as a single compound. In this study, we investigated the pharmacokinetics of pinosylvin in rats to determine its pharmacokinetic behavior *in vivo*. These results will provide helpful information for the clinical treatment of chronic gastritis and gastric ulcers using Radix Linderae Reflexae.

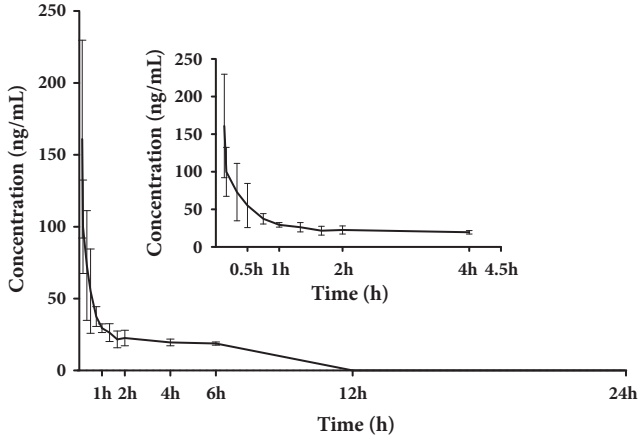

Figure 3: Mean plasma concentration-time curve of pinosylvin after oral administration of 49.44 mg/kg pinosylvin (n=6, mean ± SD).

Table 3: Extraction recovery and matrix effect of pinosylvin in rat plasma, urine, feces, and various tissue homogenates (n=5).

Bio-sample	Nominal concentrations (ng/mL)	Extraction recovery (%)	RSD (%)	Matrix effect (%)	RSD (%)
	5.4	98.8±7.1	8	99.1±8.5	8.6
Plasma	135	95.2±2.5	3	103.3±5.4	5.8
	540	99.5±3.7	4.2	114.8±3.3	3.2
	1350	91.6±8.0	9.8	110.3±10.6	10.8
Urine	5400	108.5±2.5	2.6	81.3±5.3	7.3
	54000	98.3±6.8	7.7	107.2±9.2	9.6
	270	83.3±7.3	9.7	107.8±7.7	8
Feces	2700	99±6.1	7	98.2±6.7	7.6
	5400	96.4±4.4	5.1	97.8±5.9	6.8
	540	89.8±5.1	6.3	103.7±6.8	7.3
Heart	5400	99.3±5.3	6	94.1±7.1	8.4
	27000	99.8±2.6	2.9	96.9±6.5	7.5
	2700	86.5±4.8	6.3	103.2±4.7	5.1
Liver	13500	83.4±5.5	7.4	88.4±7.9	10
	54000	87.1±3.8	4.9	89.3±5.5	6.9
	270	91.1±7.3	9	89.7±7.9	9.8
Spleen	5400	93.5±7.3	8.7	94.8±7.3	8.7
	13500	93.7±5.2	6.2	93.7±8	9.6
	540	98.4±6.4	7.3	88.5±5.3	6.8
Lung	2700	91.5±6.7	8.2	91.6±7.8	9.4
	13500	86±4	5.2	90.5±6.9	8.5
	540	86.5±6.1	7	98.4±8	8.2
Kidney	5400	99.6±4.8	4.9	101.8±6.2	6.1
	13500	90.5±6.4	7	92.6±9.2	9.9
	2700	96.5±8.3	9.6	107.1±9.4	9.8
Large intestine	13500	98.6±5	5.7	99±6.8	7.7
	54000	98.9±5	5.6	93.0±7.6	9.1
	5400	89.4±10.7	13.3	88.7±7.7	9.7
Small intestine	108000	88.6±6	7.5	89.4±8	10
	216000	92.9±7.5	9.1	83.2±1.3	1.7
	13500	87.5±10.1	13	90.8±7.1	8.8
Stomach	216000	89.9±7.7	9.6	94±11.4	13.5
	864000	86.3±9.2	12	92.6±9	10.8

3.4. Tissue Distribution Study. Pinosylvin distributions to the heart, liver, spleen, lungs, kidneys, large intestine, small intestine, and stomach are listed in Figure 4. Pinosylvin was widely distributed in various tissues, and the highest concentration was observed at 10 min in the stomach, followed by the heart, lungs, spleen, and kidneys. While the highest concentration was observed in the liver at 20 min, high concentrations remained in the small intestine from 20 min to 6 h after oral administration. These results demonstrate enterohepatic circulation of pinosylvin in rats. Pinosylvin was more concentrated in the tissue than the plasma, suggesting that pinosylvin is rapidly divided into various target organs after oral administration.

To date, there have been few pharmacokinetic or tissue distribution studies of pinosylvin after oral administration. In contrast, there have been many reports regarding resveratrol, which has a similar structure to that of pinosylvin; these reports mainly focus on cellular aspects. As a potential anti-inflammatory compound [24, 25], pinosylvin is rapidly distributed to the stomach where it persists over time, suggesting that it may be an effective component of Radix Linderae

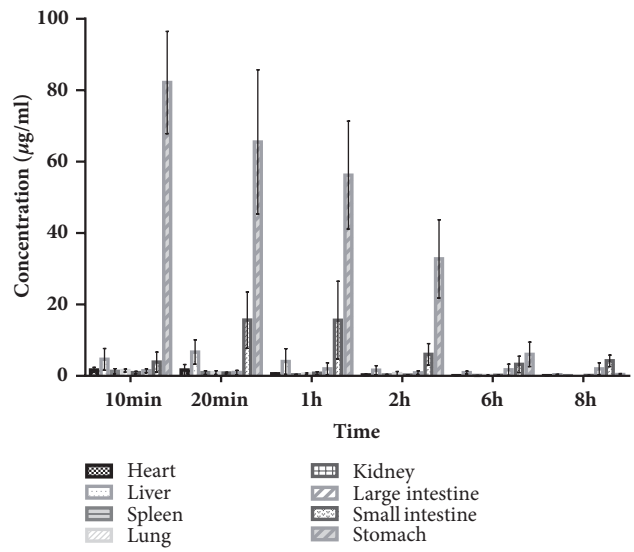

Figure 4: Mean concentration of pinosylvin in various tissues (including heart, liver, spleen, lungs, kidneys, large intestine, small intestine, and stomach) 10 min, 20 min, 1 h, 2 h, 6 h, and 8 h after oral administration of 49.44 mg/kg pinosylvin (n=6, mean ± SD).

Table 4: Stability of pinosylvin in rat plasma, urine, feces, and various tissue homogenates (n=5).

Bio-sample	Nominal concentration (ng/mL)	Autosampler (24 h, 7°C)		Three freeze/thaw cycles		Room temperature (12 h)		Long term (30 days,-80°C)	
		Precision (%)	Accuracy (%)	Precision (%)	Accuracy (%)	Precision (%)	Accuracy (%)	Precision (%)	Accuracy (%)
Plasma	5.4	1.2	10.9	4.2	7.9	2.9	9.3	6	10
	135	6.4	-3.3	6.1	4.1	8.9	-3.5	9.5	-4.6
	540	8.4	0.9	9.8	0.8	8.7	4.1	6.2	1.6
Urine	1350	3.6	5	1.3	8	1.4	8.6	0.4	9.9
	5400	9.2	-1.4	5.5	-3.4	0.9	-4.7	3	-2.6
	54000	7.3	-6.8	1.6	-0.7	1.8	-6	7.3	-6.8
Feces	270	6.5	-4.4	7.8	-5.8	9.6	-3.3	12.9	8.5
	2700	2.1	-8.5	3.4	-3.2	2	7.8	2	2.7
	5400	3.8	0.7	4.7	-2.6	8.9	3.1	4.5	-1
Heart	540	1.5	9.2	4	8.3	4.7	7.7	2.6	5.4
	5400	8	-0.3	7.9	2.6	4.7	2.2	4.9	-9.6
	27000	9.6	2.1	9.1	5.7	0.5	8.7	2.3	8.2
Liver	2700	8.4	-9.6	8.4	6.8	9.6	5.2	7.2	2.8
	13500	9.7	-1.6	4	-4.9	8.3	8.7	9.2	4
	54000	6.8	-5.1	5.4	0.6	8.7	-8.1	9.4	-9.4
Spleen	270	2.4	14.7	1.6	15	1.9	17.5	1.8	16.7
	5400	7.7	2.5	4.9	4.2	6.1	-7.1	5.8	2.2
	13500	7.8	-7.5	9.2	-1.7	9.2	-7.7	6.6	-8.8
Lung	540	2.1	14.6	4.2	6	4	10.7	3.2	10.2
	2700	6.5	3.7	7.4	-5.2	4.1	11	9.5	7
	13500	9.8	2.6	6.7	4.9	6.2	5.2	9.5	8
Kidney	540	8.8	-9.1	7.2	-5.4	8.2	-6.5	9.7	1.3
	5400	9	-2.2	10.4	3	4.8	-2.7	10.8	-5.3
	13500	8	-0.3	8	-7	8.7	-1.5	9.4	1.5
Large intestine	2700	7.9	8.3	9.2	6.8	9.3	4.8	10.4	-5.4
	13500	9.5	-8.9	6.8	-8.9	3.9	-10.3	8.4	-9
	54000	8.6	5.7	8.2	8.1	7.1	8.1	7.9	7.6
Small intestine	5400	13	-2.5	8.9	-13	7.9	10.5	13.1	5.1
	108000	6.3	15.1	4.2	6.8	13.9	8.3	1.6	8.3
	216000	5.9	13.3	5	14.5	5	-4.7	4.1	-7.7
Stomach	13500	9.5	14.5	7.8	13.7	14.6	7.7	9.5	10.5
	216000	8.9	-13.7	13.3	-11.5	13.3	0.9	11.4	-0.9
	864000	13.3	-3	11.9	-9.4	11.9	-9.1	13.5	-12.2

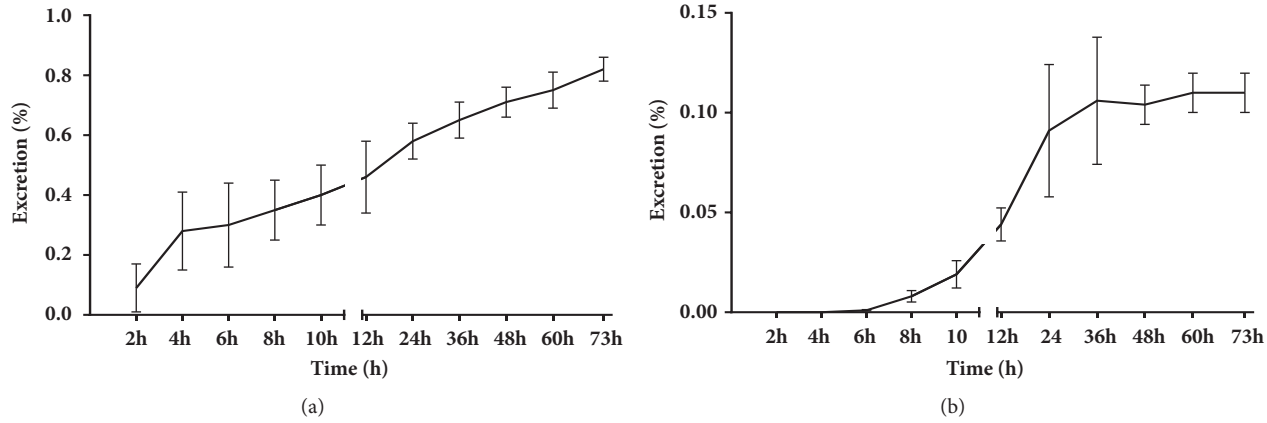

Figure 5: Accumulative excretion ratio of pinosylvin in urine (a) and feces (b) after oral administration of 49.44 mg/kg pinosylvin (n=6, mean ± SD).

Table 5: Noncompartmental pharmacokinetic parameters of pinosylvin in rats after oral administration (n=6, means ± SD).

Pharmacokinetic parameters	Unit	Value
$t_{1/2}$	h	1.347±0.01
T_{max}	h	0.137±0.016
V_d	L/kg	434.716±25.508
CL	L/h/kg	223.635±11.866
C_{max}	ng/ml	164.231±64.264
$MRT_{0\text{-}t}$	h	3.209±0.129
$MRT_{0\text{-}\infty}$	h	3.210±0.129
$AUC_{0\text{-}24h}$	ng/ml h	711.142±46.885
$AUC_{0\text{-}\infty}$	ng/ml h	711.195±46.885

$T_{1/2}$: elimination half-life; T_{max}: time to peak concentration; V_d: volume of distribution; CL: clearance; C_{max}: peak plasma concentration; MRT: mean retention time; AUC: area under the curve.

Reflexae for the treatment of chronic gastritis and gastric ulcers.

3.5. Excretion Study. Results from the excretion study of urine and feces are shown in Figure 5. The 73-h accumulative excretion ratios of urine and feces were 0.82% and 0.11%, respectively. The excretion peak of pinosylvin in urine samples was noted 2–4 h after oral administration. After 24 h, a small amount of pinosylvin was detected in the urine. Similar to the urine excretion data, pinosylvin was rapidly excreted from the feces in the parent form from 6 to 24 h after oral administration. It is likely that pinosylvin is mostly metabolized *in vivo* and plays a role in different organs.

3.6. Metabolite Identification Study. In this study, 9 possible metabolites were found in rats according to the full-scanning mass spectrograms of all biosamples and the characteristics of phase I and phase II, which are shown in Table 6. The metabolic processes in rats are complex. Therefore, it is difficult to determine the exact metabolic pathways of parent compounds into the respective metabolites. As such, metabolic pathways can only be speculated [26, 27]. The proposed metabolic pathways of pinosylvin in rats are shown in Figure 6.

The liver is the main metabolic organ of pinosylvin in rats [18, 28, 29], and all metabolites were detected in the liver except M8. However, M8 was more concentrated in the urine and fecal samples than the other metabolites examined. M9 was the main phase II metabolite and was widely found in all biosamples except urine. The stomach is a potential target organ of pinosylvin, and all measured metabolites were detected in the stomach after oral administration. The main metabolites detected in the heart were M7 and M9, whereas M1, M2, M5, and M9 were detected in samples from the large and small intestines. As a phase I metabolite of pinosylvin, M6 was more concentrated in the kidney than in other organs. These results could provide references for the further development of pinosylvin.

4. Conclusions

In the present study, a simple, sensitive, and reliable UPLC-MS/MS method for the quantification of pinosylvin in rat plasma, urine, feces, and various tissues (including heart, liver, spleen, lungs, kidneys, large intestine, small intestine, and stomach) was established. This method was validated with good specificity, linearity, precision, accuracy, and extraction; therefore, it was successfully used to evaluate the pharmacokinetics, excretion, and tissue distribution of pinosylvin in rats. As a potential anti-inflammatory compound, pinosylvin was cleared quickly from rat plasma within 2 h after a single oral administration of 49.44 mg/kg. Within 6 h after oral administration, the concentration of pinosylvin in the stomach was at the highest level. A small amount of pinosylvin was excreted from the urine and feces, indicating that most of the parent drug (pinosylvin) was metabolized *in vivo*. Nine metabolites were found in the samples, and the main metabolic pathways for pinosylvin in rats included glucuronidation, hydroxylation, and methylation. Four metabolites had higher concentrations in the stomach than other organs, suggesting that the stomach is a potential target organ of pinosylvin.

Table 6: Metabolites (M1-M9) in rats after oral administration of 49.44 mg/kg pinosylvin.

Metabolites	RT (min)	Metabolic Pathway	Mass Shift	Formula Change	Chemical Formula	$[M+H]^+$	ppm
M0					$C_{14}H_{12}O_2$	213.0865	-3.81
M1	1.20	Epoxidation	+15.99	[M+O]	$C_{14}H_{12}O_3$	229.0859	-3.54
M2	3.03	Hydroxylation	+15.99	[M+O]	$C_{14}H_{12}O_3$	229.0859	-2.71
M3	8.78	Methylation	+14.02	$[M+CH_2]$	$C_{15}H_{14}O_2$	227.1067	-2.49
M4	5.51	Methylation	+14.02	$[M+CH_2]$	$C_{15}H_{14}O_2$	227.1067	-1.41
M5	4.39	Double-bond Reduction	+2.02	$[M+H_2]$	$C_{14}H_{14}O_2$	215.1067	-1.98
M6	1.90	Sulfation	+79.96	$[M+SO_3]$	$C_{14}H12O_5S$	293.0478	-1.98
M7	1.63	Acetylation	+42.01	$[M+COCH_2]$	$C_{16}H_{14}O_3$	255.1016	-2.47
M8	1.58	Glycine	+57.02	$[M\text{-}OH+C_2H_4NO_2]$	$C_{16}H_{15}NO_3$	270.1125	-2.63
M9	1.66	Glucuronidation	+176.03	$[M+C_6H_8O_6]$	$C_{20}H_{20}O_8$	389.1231	-1.06

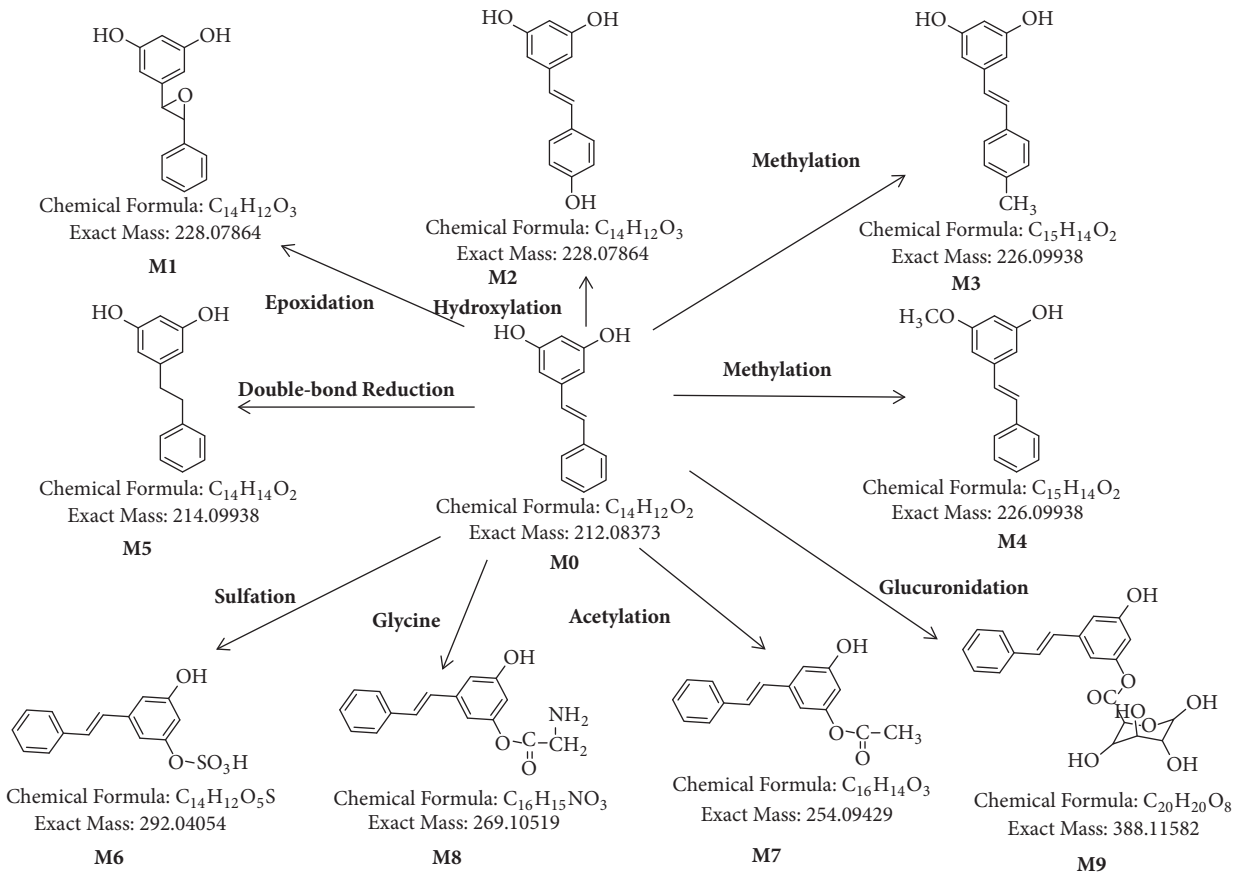

Figure 6: Proposed metabolic pathways in rats after oral administration of 49.44 mg/kg pinosylvin.

Pinosylvin is a main chemical constituent of the effective component of Radix Linderae Reflexae. This study evaluated the metabolic processes of pinosylvin in rats. The results provide valuable information regarding the clinical treatment of chronic gastritis and gastric ulcer with Radix Linderae Reflexae.

Data Availability

No data were used to support this study.

Conflicts of Interest

The authors declare no conflicts of interest.

Authors' Contributions

Yuhang Fu, Xiaoya Sun contributed equally to this work.

Acknowledgments

This work was supported by the National Natural Science Foundation of China [Grant No. 81773859], Overseas Scholars and Experts Service Center of Henan Province [Grant No. [2017]-7], and Henan Provincial Science and Technology Department Foundation and Frontier Technology Research Project [Grant No. 162300410089].

References

[1] S. Bien-Aime, W. Yu, and K. E. Uhrich, "Pinosylvin-based polymers: biodegradable poly(anhydride-esters) for extended release of antibacterial pinosylvin," *Macromolecular Bioscience*, vol. 16, no. 7, pp. 978–983, 2016.

[2] A. Kodan, H. Kuroda, and F. Sakai, "Simultaneous expression of stilbene synthase genes in Japanese red pine (Pinus densiflora) seedlings," *Journal of Wood Science*, vol. 47, no. 1, pp. 58–62, 2001.

[3] S. Chen, L. Wang, W. Zhang, and Y. Wei, "Secondary metabolites from the root of Lindera reflexa Hemsl," *Fitoterapia*, vol. 105, article no. 3222, pp. 222–227, 2015.

[4] M. Jiang, S. Lin, Q.-L. Guo et al., "Chemical constituents from Litsea greenmaniana," *China Journal of Chinese Materia Medica*, vol. 38, no. 7, pp. 1004–1007, 2013.

[5] J. Fliegmann, G. Schröder, S. Schanz, L. Britsch, and J. Schröder, "Molecular analysis of chalcone and dihydropinosylvin synthase from Scots pine (Pinus sylvestris), and differential regulation of these and related enzyme activities in stressed plants," *Plant Molecular Biology*, vol. 18, no. 3, pp. 489–503, 1992.

[6] E.-J. Park, H.-Y. Min, Y.-H. Ahn, C.-M. Bae, J.-H. Pyee, and S. K. Lee, "Synthesis and inhibitory effects of pinosylvin derivatives on prostaglandin E2 production in lipopolysaccharide-induced mouse macrophage cells," *Bioorganic & Medicinal Chemistry Letters*, vol. 14, no. 23, pp. 5895–5898, 2004.

[7] E. Jeong, H.-R. Lee, J. Pyee, and H. Park, "Pinosylvin induces cell survival, migration and anti-adhesiveness of endothelial

cells via nitric oxide production," *Phytotherapy Research*, vol. 27, no. 4, pp. 610–617, 2013.

[8] E.-J. Park, H. J. Park, H.-J. Chung et al., "Antimetastatic activity of pinosylvin, a natural stilbenoid, is associated with the suppression of matrix metalloproteinases," *The Journal of Nutritional Biochemistry*, vol. 23, no. 8, pp. 946–952, 2012.

[9] S. C. M. Yeo, W. Luo, J. Wu, P. C. Ho, and H.-S. Lin, "Quantification of pinosylvin in rat plasma by liquid chromatography-tandem mass spectrometry: application to a pre-clinical pharmacokinetic study," *Journal of Chromatography B*, vol. 931, pp. 68–74, 2013.

[10] A. Ludwiczuk, A. Saha, T. Kuzuhara, and Y. Asakawa, "Bioactivity guided isolation of anticancer constituents from leaves of Alnus sieboldiana (Betulaceae)," *Phytomedicine*, vol. 18, no. 6, pp. 491–498, 2011.

[11] F. Simard, J. Legault, S. Lavoie, V. Mshvildadze, and A. Pichette, "Isolation and identification of cytotoxic compounds from the wood of Pinus resinosa," *Phytotherapy Research*, vol. 22, no. 7, pp. 919–922, 2008.

[12] J. Park, J. Pyee, and H. Park, "Pinosylvin at a high concentration induces AMPK-mediated autophagy for preventing necrosis in bovine aortic endothelial cells," *Canadian Journal of Physiology and Pharmacology*, vol. 92, no. 12, pp. 993–999, 2014.

[13] L. Skinnider and A. Stoessl, "The effect of the phytoalexins, lubimin, (-)-maackiain, pinosylvin, and the related compounds dehydroloroglossol and hordatine M on human lymphoblastoid cell lines," *Experientia*, vol. 42, no. 5, pp. 568–570, 1986.

[14] Jiangsu New Medical College, "Dictionary of Chinese Medicine," Tech. Rep., Shanghai Scientific & Technical Publishers, Shanghai, China, 1975.

[15] L.-L. Wang, Y.-B. Zhang, X.-Y. Sun, and S.-Q. Chen, "Simultaneous quantitative analysis of main components in linderae reflexae radix with one single marker," *Journal of Liquid Chromatography & Related Technologies*, vol. 39, no. 8, pp. 422–427, 2016.

[16] X. Sun, Y. Zhang, S. Chen, and Y. Fu, "Characterization and identification of the chemical constituents in the root of Lindera reflexa Hemsl. using ultra-high performance liquid chromatography coupled with linear trap quadrupole orbitrap mass spectrometry," *Journal of Pharmaceutical and Biomedical Analysis*, vol. 126, pp. 34–47, 2016.

[17] K. Roupe, S. Halls, and N. M. Davies, "Determination and assay validation of pinosylvin in rat serum: application to drug metabolism and pharmacokinetics," *Journal of Pharmaceutical and Biomedical Analysis*, vol. 38, no. 1, pp. 148–154, 2005.

[18] K. A. Roupe, J. A. Yáñez, X. W. Teng, and N. M. Davies, "Pharmacokinetics of selected stilbenes: rhapontigenin, piceatannol and pinosylvin in rats," *Journal of Pharmacy and Pharmacology*, vol. 58, no. 11, pp. 1443–1450, 2006.

[19] S. Gu, G. Zhu, Y. Wang et al., "A sensitive liquid chromatography-tandem mass spectrometry method for pharmacokinetics and tissue distribution of nuciferine in rats," *Journal of Chromatography B*, vol. 961, pp. 20–28, 2014.

[20] D.-J. Chen, H.-G. Hu, S.-F. Xing, Y.-J. Gao, S.-F. Xu, and X.-L. Piao, "Metabolic profiling of Gynostemma pentaphyllum extract in rat serum, urine and faeces after oral administration," *Journal of Chromatography B*, vol. 969, pp. 42–52, 2014.

[21] Y.-Q. Liu, G.-H. He, H.-L. Li et al., "Plasma pharmacokinetics and tissue distribution study of roemerine in rats by liquid chromatography with tandem mass spectrometry (LC-MS/MS)," *Journal of Chromatography B*, vol. 969, pp. 249–255, 2014.

[22] Y. Li, R.-J. Zeng, J.-Z. Chen et al., "Pharmacokinetics and metabolism study of isoboldine, a major bioactive component from Radix Linderae in male rats by UPLC-MS/MS," *Journal of Ethnopharmacology*, vol. 171, pp. 154–160, 2015.

[23] H. Zhu, X. Liu, T. T. Zhu et al., "UHPLC–MS/MS method for the simultaneous quantitation of five anthraquinones and gallic acid in rat plasma after oral administration of prepared rhubarb decoction and its application to a pharmacokinetic study in normal and acute blood stasis rats," *Journal of Separation Science*, vol. 40, no. 11, pp. 2382–2389, 2017.

[24] J. W. Lei, Y. L. Guo, Y. Bai, and S. Q. Chen, "Establish the quantitative model of 3, 5-didroxystilbene in Lindera reflexa Hemsl by near-infrared spectroscopy," *Chinese Journal of Experimental Traditional Medical Formulae*, vol. 17, pp. 75–77, 2011.

[25] E.-J. Park, H.-J. Chung, H. J. Park, G. D. Kim, Y.-H. Ahn, and S. K. Lee, "Suppression of Src/ERK and GSK-3/β-catenin signaling by pinosylvin inhibits the growth of human colorectal cancer cells," *Food and Chemical Toxicology*, vol. 55, pp. 424–433, 2013.

[26] C.-Y. Li, L.-W. Qi, and P. Li, "Correlative analysis of metabolite profiling of Danggui Buxue Tang in rat biological fluids by rapid resolution LC-TOF/MS," *Journal of Pharmaceutical and Biomedical Analysis*, vol. 55, no. 1, pp. 146–160, 2011.

[27] C. Yu, Y. Geun Shin, A. Chow et al., "Human, rat, and mouse metabolism of resveratrol," *Pharmaceutical Research*, vol. 19, no. 12, pp. 1907–1914, 2002.

[28] H. Wang, X. Bai, J. Sun, Y. Kano, T. Makino, and D. Yuan, "Metabolism and excretion of kakkalide and its metabolites in rat urine, bile, and feces as determined by HPLC/UV and LC/MS/MS," *Planta Medica*, vol. 79, no. 16, pp. 1552–1557, 2013.

[29] U. Kim, M. H. Park, D.-H. Kim, and H. H. Yoo, "Metabolite profiling of ginsenoside Re in rat urine and faeces after oral administration," *Food Chemistry*, vol. 136, no. 3-4, pp. 1364–1369, 2013.